IMPACT OF BRIEF ELECTRICAL STIMULATION ON PERIPHERAL NERVE REMYELINATION

A Thesis Submitted to the College of

Graduate Studies and Research

In Partial Fulfillment of the Requirements

For the Degree of Doctor of Philosophy

In the Department of Anatomy & Cell Biology

University of Saskatchewan

Saskatoon

By

NIKKI A M^{C}LEAN

PERMISSION TO USE

In presenting this thesis in partial fulfilment of the requirements for a Postgraduate degree from the University of Saskatchewan, I agree that the Libraries of this University may make it freely available for inspection. I further agree that permission for copying of this thesis in any manner, in whole or in part, for scholarly purposes may be granted by the professor or professors who supervised my thesis work or, in their absence, by the Head of the Department or the Dean of the College in which my thesis work was done. It is understood that any copying or publication or use of this thesis or parts thereof for financial gain shall not be allowed without my written permission. It is also understood that due recognition shall be given to me and to the University of Saskatchewan in any scholarly use which may be made of any material in my thesis.

Requests for permission to copy or to make other use of material in this thesis in whole or part should be addressed to:

Head of the Department of Anatomy & Cell Biology

University of Saskatchewan

Saskatoon, Saskatchewan S7N 5E5

ABSTRACT

Demyelinating diseases such as Guillain-Barré syndrome are characterized by segmental axon demyelination and infiltration by cells of the monocyte lineage. Destruction of the myelin sheath is accompanied by losses of phosphorylated neurofilament proteins and node of Ranvier protein organization, impairing axon function and health. Effective repair depends on clearance of myelin debris, reorganization of the nodal proteins, resolution of the inflammatory response as well as increased expression of a molecule involved in myelination, brain-derived neurotrophic factor (BDNF). Brief electrical stimulation (ES) of transected and repaired peripheral nerves has been shown to enhance remyelination, and also elevate neuronal BDNF expression, the latter raising the question about whether ES might be an effective therapeutic intervention for repair of nerves following a focal demyelinating insult. To examine this, adult male Wistar rat tibial nerves underwent unilateral focal demyelination via injection of 1% lysophosphatidyl choline just distal to the sciatic nerve trifurcation. Five days later, the sciatic nerve in half of the animals underwent 1 hour continuous 20 Hz ES proximal to the injection site. At various time points after ES, animals were euthanized and ipsilateral and contralateral nerves were processed to examine the impact of stimulation on the degree of remyelination, axonal integrity, glial reactivity and the immune response. Stimulated nerves displayed greater remyelination, increased BDNF expression at the lesion site, and a decrease in local Schwann cell reactivity. The stimulated axons also displayed important markers of axonal health - increased phosphorylated neurofilament expression and a re-formation of node of Ranvier Caspr/Kv1.2 protein clusters. The ES procedure had a remarkable impact on the inflammatory/immune response, enhancing debris clearance, decreasing the total number of macrophages present and shifting macrophage phenotype from a pro-inflammatory (M1) to a pro-repair (M2) one. Collectively these results support that ES not only helps to create an environment permissive for early remyelination, but also does so by promoting the protection and preservation of axons and favorably altering the immune response.

ACKNOWLEDGMENTS

I would like to thank my supervisor, Dr. Valerie Verge. Thank you for taking a leap of faith on this immunologist-turned-neuroscientist. I am grateful for all of the support you have given me, for allowing me to grow and to find my own scientific path and passion. Thank you to the members of my advisory committee, both past and present, Dr. Bogdan Popescu, Dr. Helen Nichol, Dr, Katherine Knox, Dr. Patrick Krone, Dr. Ron Doucette, and Dr. Ric Devon for your excellent guidance and mentorship along the long and bumpy road to completing this thesis.

I wish to extend a sincere thank you to Ruiling Zhai, Jayne Johnston, Carter Britz, and Anita Givens for their excellent technical assistance with the surgical procedures, histological staining, and image analysis. Thank you for letting me pick your brains, for sharing your vast knowledge, and for listening to me think out loud while troubleshooting stubborn protocols. To my lab mates, my fellow sufferers, and my partners in crime, thank you for putting up with my nerdy self, thank you for the 2am laughs over data analysis and donairs, and thank you for occasionally talking me down from the proverbial ledge.

Last, but certainly not least, thank you to my family, both biological and chosen. Words cannot express how much each of you means to me. Without your love and support I would not have made it to where I am today.

The funding for this project has been generously provided by the Canadian Institutes of Health Research, as well as the University of Saskatchewan College of Medicine and University of Saskatchewan Graduate Scholarship programs.

"Every question leads to new answers, new discoveries, and new, smarter questions."

- *Bill Nye (the science guy)*

TABLE OF CONTENTS

LIST OF TABLES

LIST OF FIGURES

LIST OF ABBREVIATIONS

AIDP – Acute inflammatory demyelinating polyradiculopathy
AMAN – Acute motor axonal neuropathy
AMSAN – Acute motor & sensory axonal neuropathy
Arg1 – Arginase-1
BDNF – Brain derived neurotrophic factor
Caspr – Contactin-associated protein
CBB – Coomassie brilliant blue
CD206 – Mannose receptor
CNS – Central nervous system
Contra – Contralateral
CTL – Cytotoxic T lymphocyte
DAB – 3,3'-diaminobenzidine
DRG – Dorsal root ganglion
EAE – Experimental autoimmune encephalomyelitis
ED-1 – CD68
ELISA – Enzyme-linked immunosorbent assay
ES – Electical stimulation
FBS – Fetal bovine serum
FG – Fluorogold
FiFr – Fixed, frozen
FrFr – Fresh, frozen
GBS – Guillain-Barré syndrome
GFAP – Glial fibrillary acidic protein
IF – Immunofluorescence
IFN-γ – Interferon-gamma
IL – Interleukin
Ipsi – Ipsilateral
LFB – Luxol fast blue
iNOS – Inducible nitric oxide synthase
IPL – Intraperiod line
LPC – Lysophosphatidyl choline
MBP – Myelin basic protein
M-CSF – Monocyte colony stimulating factor
MDL – Major dense line
MHC – Major histocompatibility complex
MMP – Matrix metalloproteinase
NF – Neurofilament
NFR – Nuclear fast red
NGF – Nerve growth factor
NO – Nitric oxide
NRG – Neuregulin
NT – Neurotrophin
OPC – Oligodendrocyte precursor cell
Par-3 – Partitioning defective-3
PBS – Phosphate buffered saline
PNS – Peripheral nervous system
ROI – Region of interest
SIDP – Subacute inflammatory demyelinating polyradiculoneuropathy
SMI-31 – Phosphorylated neurofilament
TBST – Tris-buffered saline + Tween
TGF-β – Transforming growth factor-beta
TNF-α – Tumor necrosis factor-alpha
Trk – Tropomyosin-related kinase
VEGF – Vascular endothelial growth factor

CHAPTER 1:
INTRODUCTION

1.1 Peripheral Nerves – structure & function

1.1.1 Peripheral Nerve Anatomy

The morphology of a peripheral nerve is not unlike an onion, with layer upon layer of structural organization (Fig 1, (Boron and Boulpaep 2005)). There are three layers of connective tissue that bind the nerve components together into a single unit. The most exterior layer is the epineurium, surrounding the entire nerve structure. Moving inward, the perineurium surrounds the various bundles of nerve fibers, or fascicles. Interspersed among the fascicles are small blood vessels, which run along the longitudinal axis of the nerve, and send radial branches through the perineurium to form the endoneurial capillaries. The innermost layer of connective tissue is the endoneurium, which surrounds the individual myelinated axons, as well as the groups of unmyelinated fibers (Campbell 2008). A key difference between these connective tissue layers is in their orientation. While the epi- and perineurium have a circumferential orientation, the endoneurium is oriented longitudinally along the same axis as the nerve fibers (Sunderland 1990). Within the endoneurium are found the two key cells of the peripheral nervous system (PNS), the axons belonging to the various neurons (i.e. motor and sensory), and their associated glia, the Schwann cells. Of particular interest here are the myelinated axons, which are surrounded by a specialized membrane produced by their associated Schwann cells. If an axon is not covered by a myelin sheath it will still associate with Schwann cells, but in this case the glial cell will surround a number of axons without elaborating the myelin membrane.

1.1.2 Peripheral Nerve Function

Peripheral nerves are the channels through which information is relayed between the environment and the central nervous system (CNS) where the appropriate responses are executed. The particular functions performed by a peripheral nerve are related to the nature of

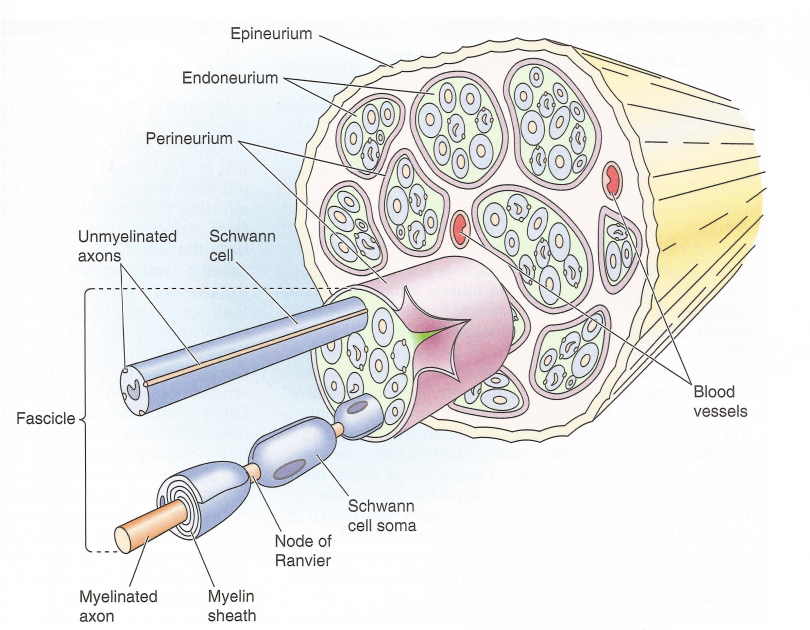

Figure 1: Structural organization of a peripheral nerve. Schematic diagram depicting the structure of a typical peripheral nerve with its associated connective tissue, and internal structures. Individual axon-Schwann cell units are covered by the endoneurium and bundled with several others into fascicles surrounded by the perineurium. The various fascicles and blood vessels supplying the nerve fibers are held together by the outermost connective tissue layer, the epineurium. *Reprinted with permission from Boron & Boulpaep (Boron and Boulpaep 2005).*

the fibers it contains. Information gathered from physical or chemical stimuli from the external environment is relayed to the CNS via the sensory axons, whose cell bodies are found within the dorsal root ganglia (DRG) that lie in the intervertebral spaces. Motor neurons transmit information in the form of an action potential from their cell bodies in the CNS to the target organs (i.e. skeletal muscle) where it is converted into a chemical stimulus at the synapse. Lastly, the autonomic division transmits information to and from the organs, glands and other viscera in order to regulate the body's internal environment (Boron and Boulpaep 2005). Each nerve potentially transmits any or all of these information modalities depending on the nature of the individual fibers that make up that particular nerve. The speed at which these fibers transmit their information is dependent upon two major factors, the diameter of the axon fiber, and whether that fiber is covered by a myelin sheath. The larger the diameter of the axon, the more rapidly it is able to conduct an action potential. Similarly, those fibers that are myelinated conduct action potentials much more efficiently, with the conduction velocity proportional to the

thickness of the myelin covering – the thicker the myelin, the more rapid the conduction (Bear et al. 2007). These anatomical and physiological properties are impacted in a variety of peripheral nerve pathologies. The challenge detailed below, is elucidating the cellular and molecular details to aid in the design of more effective repair strategies.

1.2 Peripheral Nervous System Dysfunction – Injury & Disease

1.2.1 Trauma-Induced Peripheral Neuropathy

The myelin sheath of peripheral nerves can become compromised as a consequence of traumatic nerve injury. These non-immune initiated forms of insult may arise through a number of means such as nerve compression, transection, or ischemia. There is also a much greater incidence of injury to nerves of the upper limb (radial nerve most commonly injured) than to the nerves of the lower limb (sciatic nerve most commonly injured) (Robinson 2000). The Sunderland classification system is used to group nerve injuries according to their severity and the nature of the tissue damage. First-degree nerve injuries are defined as damage to the myelin sheath, which may or may not involve axonal loss, and will typically have the best clinical outcomes, requiring little to no medical intervention with resolution occurring over several weeks to months. Second through fifth degree injuries are all accompanied by axonal loss, with severity escalating as the endoneurium, perineurium and finally epineurium become involved (Sunderland 1978). Trauma to the nerve alters blood vessel permeability, with long duration or high force compression injuries damaging not only the epineurial vessels (Fig 1, (Boron and Boulpaep 2005)), but also those within the endoneurium. This leads to intrafascicular edema, further potentiating injury to the nerve due to swelling as well as the accumulation of inflammatory cells and molecules (Rydevik and Lundborg 1977). In the milder first-degree nerve injuries, the damage to the myelin sheath surrounding the axons results in a loss of motor and/or sensory function (depending on the nature of the fibers that make up the nerve in question), which will remain until the fibers are remyelinated (Campbell 2008). More severe injuries, in which the integrity of the axons has also been compromised, have a demyelination

component, as well as degradation of the distal portion of the injured axon due to Wallerian degeneration. The degeneration of the axons will begin within hours of nerve injury, and is largely complete within 6-8 weeks. In this process, the damaged axon and myelin sheath are broken down and are taken up by inflammatory macrophages that have infiltrated the injury site through the compromised blood vessels (Bruck 1997; Chaudhry et al. 1992). Surgical intervention (e.g. rejoining the severed proximal and distal nerve stumps) is usually required for those injuries classified as third through fifth degree. The prognosis for these injuries is typically grave, as the axons themselves must be regenerated and reconnected with their distal targets in addition to the remyelination of the axons. The recovery process is protracted, and often incomplete, leading to loss of function and permanent disability (Sunderland 1978).

1.2.2 Immune-Associated Peripheral Neuropathy

Demyelination and inflammation are common features of a variety of peripheral nervous system disorders, including Guillain-Barré syndrome and other associated demyelinating neuropathies (Yuki and Hartung 2012). The pathological features of the peripheral demyelinating disorder Guillain-Barré syndrome (GBS) can be organized into at least four different subtypes according to whether the primary insult is axonal or glial in nature (reviewed in (Hiraga et al. 2005)). The most common subtype of this neurological disorder is acute inflammatory demyelinating polyradiculoneuropathy (AIDP), and represents approximately 90% of GBS cases reported in North America and Europe, at an annual incidence of 1-3 per 100 000 (Newswanger and Warren 2004). The second demyelinating form of GBS is referred to as subacute inflammatory demyelinating polyradiculoneuropathy (SIDP), which is similar in features to AIDP but follows a much slower progressive course (Burns 2008). When there is axonal involvement the disease is classified as acute motor axonal neuropathy (AMAN) or acute motor and sensory axonal neuropathy (AMSAN), depending on the nature of axonal involvement (Hughes and Cornblath 2005). Patients with GBS report a variety of symptoms, namely an ascending flaccid paralysis (in which the lower limbs are affected before the upper), numbness,

significant pain, and parasthesia (due to involvement of sensory nerves) (Vucic et al. 2009). The cranial nerves can also become involved, affecting functions such as eye movement, swallowing, and airway maintenance, with up to ~30% of GBS patients requiring assisted ventilation (Newswanger and Warren 2004). The muscle weakness is generally bilateral, accompanied by diminished tendon reflexes and appears to develop over a period of 12 hours to up to four weeks. When compared to patients plagued by central neuropathies, there is an increased capacity for peripheral nerve remyelination in patients with GBS, with studies reporting positive outcomes for ~60-90% of patients (Chio et al. 2003; Winer et al. 1988). However, after recovery from the initial illness a large number of patients (up to 20%) will still have significant residual impairment and overall recovery, even if eventually successful, is slow, with the disease perhaps taking months to resolve and any deficits still present after 2-3 years are likely to be permanent (Chio et al. 2003; Hughes and Cornblath 2005). A classic diagnostic feature of AIDP is a reduction in nerve conduction velocity upon electrophysiological examination, indicative of a demyelinating insult (Burns 2008). Histologically, the AIDP subtype of GBS is characterized by an inflammatory demyelination of the peripheral nerves due to the infiltration of macrophages and lymphocytes, which indicates that the primary target is the Schwann cell or its myelin membrane (Kuwabara 2004). The observed demyelination may be found throughout the entire length of the nerve, including the proximal roots and the distal intramuscular terminals, sites where the blood-nerve barriers are weakest (Olsson 1968; Willison 2005). There are currently two predominant mechanisms believed to responsible for the demyelination. The first is the direct targeting of macrophages to the Schwann cell membranes by activated $CD4^+$ helper T cells, via production of inflammatory mediators which serve as chemoattractants for the infiltrating macrophages, such as the CCL5 chemokine (commonly known as RANTES) (Wu et al. 2000). Alternatively, the phagocytic cells may be targeted to the Schwann cells through the binding of antibodies and activation of the complement cascade (Hughes and Cornblath 2005). Membrane attack complex formation, the terminal step in the complement cascade damages the axonal cytoskeleton and mitochondria (Willison 2005), and in addition to the standard modes of

axonal damage following demyelination, may be an additional mechanism responsible for some of the secondary axonal degeneration observed (Asbury et al. 1969). For patients with GBS, the standard therapies are plasma exchange and intravenous immunoglobulin, which are most effective at shortening disease course, and minimizing disease progression, if given early after onset (Burns 2008). While the traditional routes of therapy (e.g. surgical repair of damaged nerves, the immunomodulatory or immunosuppressive agents currently in use, such as corticosteroids) have played and continue to play important roles in the comprehensive management of demyelinating disorders and injuries to both the PNS and CNS, they unfortunately do not have the ability to reconstruct the damaged myelin sheath.

1.2.3 Improving Patient Outcomes In Peripheral Neuropathies

Perhaps one of the most important issues facing research into nervous system injuries and demyelinating disorders is translating the basic science work into clinical practice. An important aspect of this bench to bedside approach is how to tackle the fundamental problem of remyelination. In demyelinating disease, patients will present with neurological deficits only after the demyelination has occurred, leaving one unable to therapeutically intervene at the initiation of the demyelinating event in order to prevent the damage from occurring. Similarly, a patient with a transected nerve only seeks medical assistance once the injury has already happened. While both the central and peripheral nervous systems display some intrinsic capacity for repair, these repair processes are far from perfect. Development of strategies that are able to target and enhance the already demonstrated intrinsic repair capabilities would prove to be a valuable addition to the arsenal of the clinician, and ultimately would improve patient outcomes. Any therapy that would aid in the reconstruction of the damaged myelin sheath would be a valuable tool, not only for the resolution of current symptoms, but for preventing the permanent disability associated from the secondary axonal loss due to prolonged demyelination. However, before the development of any potential therapeutic interventions may occur, a thorough understanding of all peripheral nerve features, both morphological and molecular, as well as how

each of the cellular components interact must be gathered. Furthermore, the successful development of any potential therapy is predicated upon an understanding how each of these components will be affected by disease or injury.

1.3 Myelin – more than just a membrane

1.3.1 Myelin Composition

The myelin sheath is an elaborate membrane structure found surrounding axons of both the peripheral and central nervous systems. In the PNS, it is the Schwann cell that is responsible for the production and maintenance of the myelin sheath. These cells are the main glial cell type found within the PNS, and during embryonic development are derived from the neural crest. The determination of whether a Schwann cell precursor will go on to form either a myelinating or non-myelinating Schwann cell is controlled by axon-derived signals, including neuregulin (NRG), which inhibits the acquisition of a myelinating phenotype characterized by the expression of the myelin proteins (reviewed in (Zorick and Lemke 1996)). This fate determination is a highly plastic state, as upon axonal injury the myelinating Schwann cells undergo a shift in gene expression that recapitulates that of the immature precursor cells (Mirsky and Jessen 1999). In an injured state, the previously myelinating Schwann cells re-express markers associated with their non-myelinating counterparts, such as the intermediate filament, glial fibrillary acidic protein (GFAP) (Jessen et al. 1990).

Myelin contains a mixture of both lipids and proteins like the typical cell membrane. However, it is distinguished from the average cell membrane through its unusual composition. The myelin sheath is predominantly composed of lipids (70-80%), with the various proteins representing a minority of the myelin components (20-30%) (Garbay et al. 2000), this composition bestows the membrane with its efficient insulating properties. Among the various lipid species present within the myelin sheath, cholesterol represents a significant portion (20-30%) of the total lipid population, and is necessary for proper compaction of the many layers of elaborated myelin (Detering and Wells 1976; Nussbaum et al. 1969). PNS myelin also contains a large proportion of sphingomyelin (10-35% of total lipid content), as well as

galactocerebrosides (14-26%) and sulfatides (2-7%) (reviewed in (Garbay et al. 2000)). PNS myelin proteins fall into three general categories, glycoproteins, basic proteins, and miscellaneous other proteins. The majority of myelin proteins are glycosylated, representing ~60% of the total protein population, with the basic proteins representing 20-30%, and all other types comprising 10-20%. Expression of these myelin-specific proteins is dependent on an intimate interaction between the ensheathing Schwann cell, and the axon that is to be myelinated (Lemke and Chao 1988). This axo-glial interaction induces the expression of the Krox-20 transcription factor, a protein necessary for the expression of myelin basic protein (MBP) and the peripheral nerve myelin specific protein P_0 (Jessen and Rhona 1992; Topilko et al. 1994).

1.3.2. Myelin Structure

Peripheral nerve myelin is formed from the extension of a portion of the Schwann cell plasma membrane, as it spirals around the axon to form concentric layers proportional to the diameter of the contacted axon, with larger diameter axons having more layers. As the Schwann cell membrane wraps itself around the axon it forms a double membrane structure, the mesaxon, which allows for communication with the cell surface (Quarles et al. 2006). In order to form a mature myelin sheath, the layers of membrane must be compacted, squeezing out most of the cytoplasm and associated organelles from between the layers, confining them to the paranodal loops near the external mesaxon and the Schmidt-Lanterman incisures (Webster 1971). The compacted layers of membrane form a series of alternating light and dark bands when viewed under the electron microscope, termed the intraperiod (IPL) and major dense lines (MDL), respectively (Fig 2, (Suter et al. 1993)). The electron-light intraperiod lines are composed of the closely apposed outer leaflets of membrane, while the electron-dark major dense lines represent the fused inner leaflets of membrane (Paz Soldan and Pirko 2012). The proteins that comprise the myelin sheath display a differential distribution to either the electron-light or electron-dark layers. Myelin basic protein is found within the MDL, where its combination of polar and charged amino acids allow for both hydrophobic and hydrophilic interactions between the apposing inner leaflets (Mendell and Whitaker 1978; Omlin et al. 1982), while it plays a crucial

role in the stabilization of CNS myelin, it does not appear to play a significant structural role in the PNS. The PNS-specific protein P_0, localizes to the IPL, where its main function is speculated to be stabilization of the MDL via homophilic interactions. In P_0 knockout animals there is a severe hypomyelination with additional defects in the compaction of the thin myelin layers (Kirshner et al. 2004). The myelin-associated glycoprotein is localized to the membranes of the paranodal loops, Schmidt-Lanterman incisures, and the outer mesaxon. Myelin-associated glycoprotein is believed to thus play a role in the cell-cell interactions between adjacent Schwann cells, as well as between axons and Schwann cells (Georgiou et al. 2004; Quarles 2002).

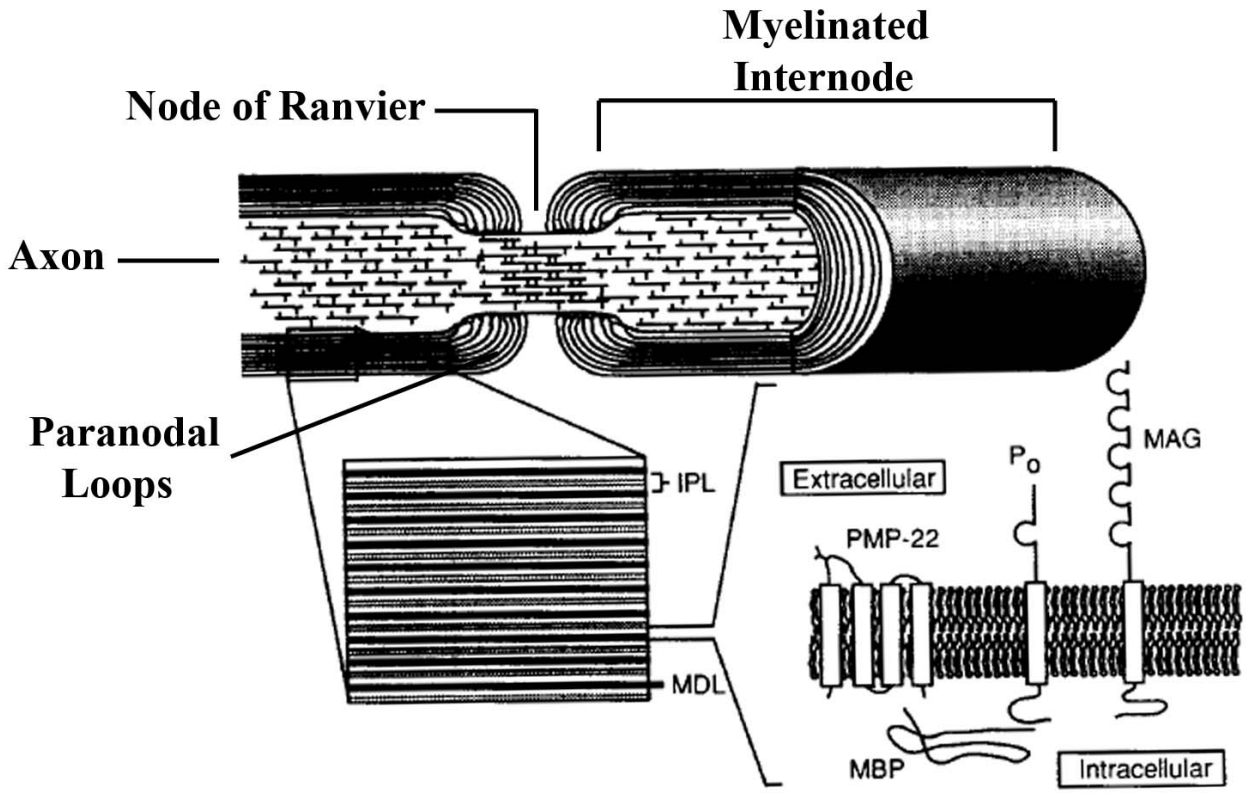

Figure 2: Structure of the myelin sheath. The top image presents a longitudinal view of the structures surrounding the node of Ranvier. The small linear structures within the axon depict the neurofilaments, note the greater axon diameter and reduced neurofilament density in the regions of the axon, which are surrounded by myelin (internodes) than that at the node of Ranvier. At the bottom left is a schematic of the structure of compact myelin with the alternating electron dense major dense lines (MDL) and electron-light intraperiod lines (IPL). The bottom right image is a schematic diagram demonstrating the localization of the major protein components of peripheral nerve myelin as localized on the Schwann cell membrane. *Adapted and reprinted with permission from Suter, Welcher & Snipes (Suter et al. 1993).*

1.4 Axons – Conduits For Communication

1.4.1 Neurofilaments

Myelination is crucial for proper neurological function, with damage to the myelin sheath having potentially devastating consequences. While the nervous system has a moderate innate capacity for remyelination, this process is far from perfect. Axonal injury or demyelination drives Schwann cell dedifferentiation and the acquisition of a reactive phenotype, characterized by prominent GFAP expression (Jessen et al. 1990; Scherer and Salzer 2001). In this state, no new myelin can be elaborated, leaving the axons bare, and therefore vulnerable. One of the challenges associated with demyelinating disorders is the loss of axons due to their vulnerability to degenerative processes (reviewed in (Drenthen et al. 2013; Silber and Sharief 1999)). This loss may be linked to alterations in neurofilament proteins that serve important roles in the radial growth of axons (Friede and Samorajski 1970; Hoffman et al. 1987) thereby impacting axonal caliber and conduction efficiency (Sakaguchi et al. 1993). The neurofilaments (NF) are a group of neuron-specific cytoskeletal proteins and are comprised of three main subtypes, the lowest molecular weight NF-L (~70 kDa), and the larger NF-M (~150 kDa) and NF-H proteins (~200 kDa) (Geisler et al. 1983; Hirokawa et al. 1984; Hoffman et al. 1987; Liem et al. 1978; Schlaepfer 1987; Willard and Simon 1983) all of which share a common central rod domain. Myelinated axons normally display high levels of medium and high molecular weight neurofilament phosphorylation (Lee et al. 1987) at the lysine-serine-proline repeat regions found within the C-terminal domains of their subunits (Elhanany et al. 1994; Jaffe et al. 1998a; Jaffe et al. 1998b). This phosphorylation is accomplished through the actions of proline-directed kinases, such as cyclin-dpendent kinase-5 (cdk5) as well as the extracellular-signal regulated kinases (ERK1/2) (Giasson and Mushynski 1997; Veeranna et al. 1998). The addition of the phosphate groups to these neurofilaments results in an increase axonal caliber through decreasing the packing density of the neurofilament proteins. The negative charges associated with the phosphate groups lead to a re-positioning of the neurofilament side arms, increasing the space between the individual filaments (Elhanany et al. 1994; Jaffe et al. 1998a; Jaffe et al. 1998b;

Kirkpatrick and Brady 1999). These differences in axonal caliber are not only present between individual myelinated and non-myelinated axons, but are also apparent in myelinated and non-myelinated regions of the same axon (Hsieh et al. 1994).

The increased axonal caliber associated with neurofilament phosphorylation is an important signal in determining the onset of myelination (Michailov et al. 2004), with the NF-M and NF-H chains being highly phosphorylated at the internodes, but largely unphosphorylated at the initial axon segment and at the nodes of Ranvier (de Waegh et al. 1992; Hsieh et al. 1994; Mata et al. 1992; Reles and Friede 1991). As the axon caliber increases, the Schwann cell associated with that axonal segment will begin to express the various myelin proteins, beginning with myelin-associated glycoprotein (Sternberger et al. 1979; Trapp et al. 1989), this is a reciprocal relationship as myelin-associated glycoprotein further regulates the expression and phosphorylation of the neurofilaments (Dashiell et al. 2002). The phosphorylation of the neurofilaments is also protective to the axon, with dephosphorylated neurofilaments susceptible to proteolysis by the calcium-dependent protease calpain (Goldstein et al. 1987; Greenwood et al. 1993; Kamakura et al. 1983), while phosphorylated neurofilaments are resistant to degradation (Pant 1988). This degradation can be repressed in injured peripheral nerves through inhibition of the influx of calcium into the axoplasm or via inactivation of the calcium-activated proteases are inhibited (Schlaepfer 1974). Importantly, neurofilament phosphorylation is controlled by the myelination process (Starr et al. 1996) and upon demyelination, these filaments become dephosphorylated, both in experimental models of dysmyelination (de Waegh et al. 1992) and in human demyelinating disease states (Trapp et al. 1998).

1.4.2 Nodes Of Ranvier

Myelinated nerves, with their thick layer of insulation, are able to efficiently and rapidly conduct action potentials along the length of their axons. This rapid conduction is dependent on the highly organized structures at the junctions between the myelinated segments, the nodes of Ranvier (Fig. 2, (Suter et al. 1993)). At the center of these nodes are the voltage gated sodium channels, through which the ions responsible for the depolarization of the axonal membrane will

enter. The clustering of these channels is associated with contact between the axon and a Schwann cell that has begun to express myelin-associated glycoprotein, indicating an intimate relationship between node of Ranvier formation and the initiation of myelination (Vabnick et al. 1996) as well as an instructive role for the Schwann cell in determining the nodal architecture (Wiley-Livingston and Ellisman 1980). Flanking the sodium channels, in the paranodal region, is the contactin-associated protein (Caspr). This protein is an important component of the paranodal junctions between the axon and the paranodal loops of the myelinating Schwann cells (Einheber et al. 1997). These paranodal junctions appear during the later stages of myelination, when the mature, compact, myelin has begun to form (Rosenbluth 1983), and Caspr begins to take on its characteristic regional distribution at this time with an increase in expression at the paranodes, and a corresponding decrease in the internodal regions (Einheber et al. 1997). These paranodal structures are believed to act as a physical barrier that prevents the diffusion of the voltage gated sodium channels away from the node, thereby maintaining the efficiency of the saltatory conduction (Rosenbluth 1983). The juxtaparanodal region contains the Kv1.1 and Kv1.2 subtypes of voltage-gated potassium channels. These channels allow the exit of potassium ions in order to return the membrane back to resting potential following the rapid influx of sodium ions associated with the generation of an action potential. Clustering of the potassium channels near the node of Ranvier may serve to prevent the re-entrant excitation of the membrane (Altevogt et al. 2002; Li et al. 2002) as well as possibly mediating communication between the axon and Schwann cell (Chiu and Ritchie 1984; Vabnick et al. 1999). Disruption in the organization of the nodes of Ranvier is a critical feature of segmental and paranodal demyelination. The distinct organization of the nodal, paranodal and juxtaparanodal proteins is lost following demyelination and can assume a more diffuse axonal distribution, reminiscent of that found in the smaller diameter non-myelinated fibers (Arroyo et al. 2004; Karimi-Abdolrezaee et al. 2004). Recapitulation of the distinct nodal architecture is key during the remyelination process (Rasband et al. 1998) and together with neurofilament phosphorylation serve as important measures of the efficiency of repair processes and axonal health, respectively.

1.5 Macrophages – Neural-Immune Interactions Central For Remyelination

1.5.1 Lineage & Functions

Macrophages are a critical component of the immune system. These phagocytic cells are the terminal differentiation product of bone marrow-derived monocytes. Upon adhesion to, and extravasation from the blood vessels the monocyte will be triggered to differentiate into either a macrophage or a dendritic cell, depending on the nature of the local microenvironment (Serbina et al. 2008). Exposure of the monocyte to the cytokines interleukin-6 (IL-6) and interleukin-10 (IL-10) as well as macrophage colony stimulating factor (M-CSF) shifts the differentiation away from the dendritic cell pathway and towards that of the macrophage (Allavena et al. 2008; Chomarat et al. 2000; Menetrier-Caux et al. 1998). Additionally, the powerful macrophage activator interferon-γ (IFN-γ) further promotes the differentiation of monocytes towards the macrophage lineage through stimulating the autocrine production of IL-6 and M-CSF (Delneste et al. 2003). Once differentiated, macrophages are able to participate in the mounting of both the innate, and acquired arms of the immune response. As an important component of the innate (non-antigen specific) immune response, macrophages are key effector cells. Macrophages are skilled scavengers, and are responsible for the phagocytosis of not only pathogens, but also dead cells and other debris (Geissmann et al. 2010; Gordon and Taylor 2005; Wynn and Barron 2010). Degranulation of platelets rapidly recruits these phagocytes to the site of injury where they not only clear the debris, but also produce a variety of cytokines to recruit neutrophils and other components of the innate immune response (Uutela et al. 2004). In addition to their role in innate immunity, macrophages also function as a component of the acquired immune response. Subsequent to their role as phagocytes, upon digestion of the internalized material, macrophages will present these antigens through the class II major histocompatibility complexes (MHC-II). The antigens are recognized by the CD4+ family of helper T cells (T_H), which ultimately leads to the production of antibodies by B lymphocytes, as well as the expansion of the population of $CD8^+$ cytotoxic T lymphocytes (CTL) (Fearon and Locksley 1996).

1.5.2 Phenotypic Subpopulations Of Macrophages

Macrophages are not a singular population of uniform cells. They exhibit a remarkable degree of phenotypic plasticity, representing a continuum of activation states making them highly dynamic and responsive to factors present within the local microenvironment (Gratchev et al. 2006; Stout et al. 2005; Stout and Suttles 2004). The full macrophage activation spectrum is represented by the "classically activated" M1 macrophages at one end and the "alternatively activated" M2 macrophages at the opposing end (Mantovani et al. 2009; Martinez and Gordon 2014). This nomenclature mirrors the T_H1-T_H2 designation of cytokine classification. Exposure of macrophages to cytokines of the T_H1 class (e.g. IFN-γ) or bacterial products such as lipopolysaccharide induces a polarization towards the M1 phenotype. Macrophages of the M1 phenotype are considered to be pro-inflammatory as they express high levels of the pro-inflammatory cytokines, including tumor necrosis factor-α (TNF-α), IL-1β, IL-12, and IL-23 (Ambarus et al. 2012) and can be distinguished from M2 macrophages by their expression of these markers (Miron and Franklin 2014). The production of both IL-12 and IL-23 are important for connecting these cells to the adaptive immune response through polarizing $CD4^+$ T cells towards the T_H1 subtype, which further perpetuates the inflammatory state. This subclass of macrophages is important for the clearance of invading pathogens, in part by preventing microbial escape from the phagosome and promoting the intracellular killing of phagocytosed pathogens (Shaughnessy and Swanson 2010). In order to produce the reactive oxygen and nitrogen species typical of the M1 macrophage phenotype, these cells express the inducible nitric oxide synthase (iNOS) enzyme, which utilizes L-arginine as its substrate (Hesse et al. 2001). The resulting nitric oxide (NO) produced is highly toxic to the invading pathogens, and is effective in the management of infection, but a fine balance must be struck as NO may also damage the surrounding host tissues (Nathan and Ding 2010).

The generation of an inflammatory response in order to deal with an injury or invading pathogen must be kept in check, and promptly tempered and resolved so as to minimize damage to the host tissues. The M2 polarized class of macrophages performs this important function. In

direct contrast to the pro-inflammatory molecules produced by the M1 macrophages, the M2 cells are characterized by the secretion of anti-inflammatory cytokines including transforming growth factor-β (TGF-β), IL-4, IL-10, and IL-13, as well expression of the scavenger receptors CD206 and CD163, promoting enhanced phagocytic ability and the resolution of inflammation (Stein et al. 1992). These cells are therefore critical for the dampening of the inflammatory response generated by the M1 polarized macrophages as well as in immunoregulation. Furthermore, M2 macrophages play additional critical roles in tissue remodeling, clearance of parasites, and minimizing tumor progression (Biswas and Mantovani 2010). Perhaps one of the most striking differences between the two phenotypes is in their metabolism of the amino acid arginine. Contrary to the use of L-arginine for the production of reactive species, the M2 macrophage expresses the arginase-1 (Arg1) enzyme, which converts L-arginine to ornithine and urea, thereby reducing the available pool of available substrate for nitric oxide production as well as generating intermediate metabolites necessary for tissue repair (reviewed in (Boucher et al. 1999; Bronte and Zanovello 2005; Hesse et al. 2001)). M2 polarized macrophages secrete growth-promoting compounds such as vascular endothelial growth factor (VEGF), IL-8, matrix metalloproteinase-9 (MMP9), and polyamines, promoting processes such as angiogenesis, lymphangiogenesis and fibrosis, which are necessary for the repair and remodeling of damaged tissues (Biswas and Mantovani 2010; Ji 2012). These two opposing phenotypes are both fully reversible, indicating that a single macrophage is able to participate in both the generation and resolution of an inflammatory response (Porcheray et al. 2005).

1.5.3 Role Of Macrophages In Nervous System Injury & Repair

Macrophages have important roles as both cellular mediators and effectors of nervous system inflammation. When peripheral nerves become damaged monocytes quickly leave the circulation to invade the site of injury. Once differentiated to mature macrophages, they play a critical role in removing both axonal and myelin debris through a process termed Wallerian degeneration (Bruck 1997; Griffin et al. 1993; Perry and Brown 1992a), in a process dependent on the activation of the complement cascade (Dailey et al. 1998). The role of peripherally

derived macrophages in damage and subsequent repair of the nervous system is a complex issue, with macrophages being implicated in both demyelination and remyelination. While on one hand macrophages contribute to the pathology associated with nerve injury and demyelination through the release of toxins and via antigen presentation to cytotoxic lymphocytes (Merrill et al. 1993; Myers et al. 1993), they are also beneficial in their ability to phagocytose myelin debris and secrete growth factors (Barouch et al. 2001). Without the aid of macrophages, the process of Wallerian degeneration is slow to occur, which introduces a delay in the regeneration of the damaged axons (reviewed in (Bruck 1997)), the longer an axon remains in a damaged state, the lower the odds of proper repair occurring. The release of IL-1 by the infiltrated macrophages can trigger the release of neurotrophins (e.g. nerve growth factor (NGF)) from the surrounding fibroblasts (Perry and Brown 1992a; Perry and Brown 1992b), as well as the release of neurotrophins (e.g. brain-derived neurotrophic factor (BDNF)) from the macrophage itself (Barouch et al. 2001) which can potentially aid in promoting the regeneration of the damaged axons.

The polarization state or rather the ratio of M1:M2 appears to play an important role in whether or not effective repair/remyelination will occur. While few peripheral nerve studies have examined the link between macrophage polarity and PNS repair, it does appear that it is not only the presence of macrophages at the site of injury, but also their phenotype that matters for efficient repair and protection from further injury (Mokarram et al. 2012; Ydens et al. 2012). The importance of macrophage phenotype for proper nervous system repair has been examined in experimental models of CNS demyelination (such as experimental autoimmune encephalomyelitis (EAE)). At the peak of EAE severity there is an imbalance in the M1:M2 ratio with an overabundance of M1 polarized cells (Okuda et al. 1995), while supplementation with additional exogenous M2 polarized monocytes improves both oligodendrocyte differentiation and clinical presentation (Mikita et al. 2011). Indeed, there is a switch from M1 to M2 phenotype that correlates with the onset of myelination. In a recent study by Miron et al. (Miron et al. 2013), M1 macrophages were shown to be important in the recruitment phase of

oligodendrocyte precursor cells (OPCs) when they proliferate and divide. Indeed, selective depletion of this population impairs this proliferation (Kotter et al. 2001; Kotter et al. 2005). The subsequent switch to an M2 polarization state, which occurs in both macrophages and microglia, is essential for effective remyelination (Miron et al. 2013). They also went on to show macrophage-conditioned medium and in particular one molecule activin-A, a member of the TGF-β superfamily effects OPC differentiation into an oligodendrocyte. This group was also able to restore myelination efficiency through heterochromic parabiosis (pairing old mouse with a young (Ruckh et al. 2012)) which resulted in increased densities of M2 polarized cells and improved remyelination. Thus, it appears that therapies that can favorably impinge on the M2 polarization axis hold tremendous promise for improved clinical outcomes.

1.6 Neurotrophins – Molecules Implicated In Myelination

1.6.1 Structure & Function of Neurotrophins And Their Receptors

The neurotrophins are a family of proteins which play a number of critical roles in development and maintenance of both the peripheral and central nervous systems (Notterpek et al. 1999), mostly through regulating neuronal survival, differentiation, synaptic strength and plasticity, and cell death (Cosgaya 2002; Rosenberg et al. 2006). The four members of this family, nerve grown factor (NGF), brain-derived neurotrophic factor (BDNF), neurotrophin-3 (NT-3), and neurotrophin-4/5 (NT-4/5), are all secretory proteins which are initially synthesized as larger precursor peptides before being processed by proteases (e.g. the tissue plasminogen activator (tPA)/plasmin system is responsible for the cleavage of pro-BDNF to the mature peptide (Baranes et al. 1998; Pang et al. 2004)) to their mature form (Chao and Bothwell 2002). Each of the neurotrophin proteins is capable of interacting preferentially with its own cognate tyrosine kinase receptor from the tropomyosin-related kinase (Trk) family; NGF with TrkA, BDNF and NT-4/5 with TrkB, and NT-3 with TrkC, with all neurotrophins capable of binding to the common p75 neurotrophin receptor ($p75^{NTR}$). The larger pro-neurotrophins perform a distinct set of functions from their processed, mature, products. It is the pro-domain of the peptide that is critical for both the targeting of the peptide to the secretory pathway, as well as for

the correct folding of the mature protein (Chen et al. 2004; Egan et al. 2003). In addition to the targeting and processing role of the pro-domain, the pro-neurotrophin itself performs a variety of signalling functions, usually contrary to the function of the mature peptide (Lu et al. 2005). For example, in contrast to the role of the mature BDNF peptide in promoting neuronal survival through the binding of the BDNF homodimer to the receptor tyrosine kinase TrkB, the pro-BDNF molecule will preferentially bind to $p75^{NTR}$ leading to the initiation of the apoptotic cascade (Je et al. 2012; Taylor et al. 2012; Teng et al. 2005), axonal degeneration (Park et al. 2010), or the cessation of neurite outgrowth (Sun et al. 2012).

1.6.2 Role Of Neurotrophins In Myelination

While the various members of the neurotrophin family play a critical role in the survival of different population of neurons, it is their involvement in myelination that is of particular interest here. Through binding to the common neurotrophin receptor $p75^{NTR}$, BDNF has been shown to enhance myelin formation by Schwann cells in the peripheral nervous system (Cosgaya 2002). Further, BDNF along with NT-3 is important for the induction of oligodendrocyte proliferation and differentiation in the CNS through modulation of the expression of MBP, a major protein component of the myelin sheath (Rosenberg et al. 2006).

In the PNS, it is the mature form of BDNF that is important for initiation of the myelination program (Chan 2001; Chan et al. 2006) primarily via activation of the $p75^{NTR}$ expressed by Schwann cells (Cosgaya 2002). The expression of BDNF provides a negative signal that halts the migration and replication of the Schwann cells, while at the same time providing a positive signal for the expression of the myelin-associated genes (Chan 2001; Cosgaya 2002; Yamauchi et al. 2004). Sensory neurons of the dorsal root ganglia express, anterogradely transport, and secrete BDNF in order to promote this myelination by Schwann cells (Ng et al. 2007). This finding is requisite if BDNF is to be an active participant in the axon/glial cell interaction necessary for the myelination process to occur. The recruitment of $p75^{NTR}$ receptors to the Schwann cell membrane by the partitioning defective-3 (Par-3)

scaffolding protein helps to ensure that the released BDNF is able to interact with this receptor and initiate the downstream signalling events necessary for myelin formation (Chan et al. 2006).

Following injury to, and the subsequent repair of PNS axons, many of the events that occurred during development are recapitulated, including axon myelination. This remyelination process is also BDNF-dependent, with potential sources for this needed factor including neurons (Mannion et al. 1999; Ng et al. 2007; Tonra et al. 1998; Zhou et al. 1999; Zhou and Rush 1996), Schwann cells (Meyer et al. 1992; Zhang et al. 2000), or activated macrophages which have infiltrated the injury site (Barouch et al. 2001; Dougherty et al. 2000). Collectively, this results in an accumulation of BDNF at the site of demyelination that appears to be crucial for enhancing the remyelination process. Furthermore, when fibroblast cells engineered to express BDNF are transplanted into contused spinal cord tissue there is an increase in the degree of remyelination, likely through the activation of the endogenous pool of precursor cells (McTigue et al. 1998). The data presented in these studies indicate that activation of the neurotrophin mediated signalling pathways is a viable therapeutic target to promote effective repair of sites of demyelination.

1.7 Demyelination

1.7.1 Problems Associated With Remyelination

Demyelination may occur as a consequence of injury or disease, as previously discussed. Efficient and effective clearance of myelin debris is critical for remyelination following traumatic injury in both the peripheral and central nervous systems. While myelin-associated glycoprotein is an important component of the mature myelin sheath, it appears to have a negative influence on both axonal repair and remyelination following injury (Filbin 1995). Its presence in the remaining myelinated axons as well as in the myelin debris at the lesion site serve as an inhibitory signal for repair. In the PNS, axonal regeneration and subsequent remyelination occurs after Wallerian degeneration, where the myelin has been effectively removed (Filbin 1995). Furthermore, it has been hypothesized that one of the major obstacles to remyelination of nervous system tissue is overcoming the inhibitory effect of the myelin proteins

themselves. In models of CNS demyelination, it has been demonstrated that the presence of myelin proteins prevents the differentiation of oligodendrocyte precursor cells (Kotter 2006). This finding emphasizes the potential importance of the population of infiltrating macrophages in the process of neural repair as these phagocytic cells are responsible for the clearance of the debris present at the lesion site. This role for macrophages has been proposed partially based on the finding that depletion of macrophages leads to a delay in the proliferation and differentiation of the population of oligodendrocyte precursor cells (Kotter et al. 2005), presumably due to a delay in the clearance in the myelin debris. The requirement of the monocyte lineage cells for the repair of the myelin sheath highlights the double-edge sword of the inflammatory response in demyelination; not only are macrophages effector cells in the destruction of the myelin sheath, but they also play a critical role in its repair.

1.7.2 Role Of Electrical Stimulation In Nerve Repair

Remyelination can occur in response to damage to the myelin sheath of peripheral (Griffin et al. 1990; Rubinstein and Shrager 1990) or central nervous system axons (McTigue et al. 1998), although it is less effective in the latter. While it has been shown that spontaneous nervous system remyelination can occur (McTigue et al. 1998) a key question that remains to be answered is whether this repair response can be enhanced/upregulated following a demyelinating insult. Studies have shown that when a transected and repaired femoral nerve is immediately briefly electrically stimulated (one hour at 20 Hz) just proximal to the surgical repair site, regeneration is greatly improved, and is associated with an activity-dependent upregulation in the expression of both BDNF and its receptor TrkB in both motor neurons (Al-Majed et al. 2000a) and sensory neurons (Geremia et al. 2007). This surgical repair strategy following traumatic nerve injury and increase in neurotrophin expression correlates not only with an acceleration in the rate of nerve regeneration, but it has also been associated with improved remyelination (Singh et al. 2012).

However, the issue of how to promote early and rapid activation of this response following a demyelinating insult remains unresolved. That increased neuronal electrical activity

may serve as an important intrinsic signal for remyelination, is supported by *in vitro* experiments demonstrating that electrical stimulation of DRG neurons co-cultured with OPCs promotes expression of MBP (a major protein constituent of the myelin sheath), and that myelin formation is restricted to electrically active axons (Wake et al. 2011). Electrical stimulation (ES) of DRG neurons halts the proliferation of co-cultured Schwann cells, an important first step in the maturation of the Schwann cell into a mature, myelinating phenotype (Stevens 2000), and that specific patterns of neural activity are capable of influencing myelination in these same culture systems (Stevens et al. 1998). However, it still remains to be determined what effects this ES may have on the *in vivo* repair of demyelinated axons. As mentioned above, this strategy of increasing neuronal activity to improve remyelination also appears to have benefits *in vivo* in the traumatically injured and repaired peripheral nerve as discussed above (Al-Majed et al. 2000b; Back et al. 2005; Brushart et al. 2005; Geremia et al. 2007) and is associated with enhanced remyelination following crush injury of the sciatic nerve (Singh et al. 2012). The improved regeneration is associated with increases in the neuronal expression of both BDNF and its receptor TrkB (Al-Majed et al. 2000a), and neurotrophin signaling (English et al. 2006; Geremia et al. 2010). Collectively, these findings raise the question of whether the beneficial effects of brief ES will still be apparent in an experimental model of demyelinating disease.

1.7.3 Experimental Demyelination

A number of models of experimental demyelination exist, and they all have their place as valuable tools for research, however each is not without limitations. The immunization of either mice or rats with myelin proteins (e.g. MBP, or myelin oligodendrocyte glycoprotein) and the subsequent generation of sensitized T lymphocytes produces an immune-associated attack on the central nervous system, termed experimental autoimmune encephalomyelitis (EAE), and is commonly used as a model to study multiple sclerosis, as it can have a chronic, relapsing course, and displays common histopathological evidence of demyelination (reviewed in (Gold et al. 2000; Rawji and Yong 2013)). The EAE model has two major drawbacks, the first being the inability to know the precise location where the demyelinated lesions will develop, and secondly,

its use is limited to examining demyelination within the CNS. The addition of the copper chelating compound cuprizone to the diet of laboratory rodents is able to overcome one of the drawbacks to the EAE model, the imprecise localization of the demyelinating lesions. Cuprizone produces a copper deficiency and demyelinating lesions localized to the corpus callosum and the superior cerebellar peduncle, which is reversible upon removal of the chelator from the diet, allowing for the study of both the generation and resolution of demyelinating insults (reviewed in (Matsushima and Morell 2001; Rawji and Yong 2013)). While this model offers greater precision in the localization of the demyelinating lesions, once again it is restricted to studies pertaining to the CNS, and therefore is of no use in examining demyelination of peripheral nerves.

For over 40 years, lysophosphatidyl choline (LPC) has been used as an agent for the induction of focal demyelination in both the central and peripheral nervous systems. This agent allows for the creation of a precise focal lesion, in which axons have been focally demyelinated but remain intact (Hall 1972; Hall and Gregson 1971). This model largely spares axonal structure (Allt et al. 1988), and provides one with the opportunity to selectively treat a predicted focally demyelinated region. Such a model allows researchers to examine in isolation the intricate process of myelin sheath production. The injection of LPC into peripheral nerves induces a lysis of the myelin sheath, while the axolemma and plasma membrane of the myelin-producing Schwann cell remain intact (Allt et al. 1988). This demyelination has a rapid onset, with visible changes to the myelin sheath present within 30-60 minutes of injection, including the splitting of the intraperiod line and a thickening of the major dense line similar to changes observed during Wallerian degeneration. The loss of myelin reaches a peak within 96 hours, with debris found within the endoneurium as well as the macrophages that have infiltrated the lesion site (Hall and Gregson 1971). The injection of LPC induces a potent inflammatory response, increasing permeability of vascular endothelium and expression of adhesion molecules and cytokines, allowing for easier extravasation of recruited cells (Qiao et al. 2006), and furthermore has been shown to be a chemoattractant for cells of the monocyte lineage (Quinn et al. 1988), facilitating

the recruitment of phagocytic cells to the site of demyelination. Once these cells have been recruited, LPC further enhances the generation of an inflammatory response through inducing the production of pro-inflammatory cytokines. One drawback to the LPC model of focal demyelination is that the lesions are self-limiting, and therefore this model is not an ideal candidate for the study of chronic demyelination (Rawji and Yong 2013). It does however serve as an excellent experimental system for assessing myelin damage and repair. It is preferable to traumatic peripheral nerve injury models, such as a crush injury model, which despite also leading to demyelination in a defined region of the nerve, also have axonal damage inherent to the nerve crush injury. The latter complicates the study of inflammation and remyelination substantially, as one is unable to study myelin repair in isolation of axon regeneration, as one can do in the LPC focal demyelination model.

1.8 Hypotheses & Specific Aims

It is these observations that have lead to the following hypothesis:

> *The brief electrical stimulation protocol (1 hour at 20 Hz) shown to optimally promote peripheral nerve regeneration will beneficially impact cellular axes and molecular events associated with the effective repair of a peripheral nerve that has a pre-existing focal demyelinating lesion.*

The specific goals of this research are:

i) To employ the LPC model of focal demyelination to assess the effects of brief electrical stimulation on the degree of remyelination following LPC-induced demyelination of the peripheral nervous system.

ii) To examine the effect of brief ES on the axonal state, a key factor in determining whether remyelination will be possible.

iii) To examine the effect of brief ES on the local immune microenvironment, including the polarization state of the macrophages that have infiltrated the zone of focal demyelination.

CHAPTER 2:

METHODS

2.1 Surgical Procedures

2.1.1 Focal Demyelinating Lesion

All procedures were approved by the University of Saskatchewan Animal Research Ethics Board (protocol number 20090087) and adhered to the Canadian Council on Animal Care guidelines for humane animal use. Animals were given analgesics (buprenorphine/Temgesic; 0.05- 0.1 mg/kg) subcutaneously pre- and postoperatively to minimize incisional discomfort. A total of 190 young adult male Wistar rats (150-200g) were employed for the studies presented in this thesis. Rats were deeply anaesthetized with inhaled isoflurane (2% delivered at a rate of 2L/min).

To create a focal demyelinating lesion, the right sciatic nerve was exposed at the level of the trifurcation into the common peroneal, tibial and sural branches and 2 μl of a 1% LPC / 1% Fluorogold (FG; Fluorochrome Inc. Denver, CO, USA) solution were injected into the tibial branch of the sciatic nerve, just distal to the trifurcation (Fig 3A), using a 20-30 micron tip glass needle connected to a Hamilton syringe. Fluorogold served to demarcate the demyelination zone, while an epineural 10-0 suture marked the injection site.

2.1.2 Electrical Stimulation (ES)

Five days post-LPC injection, the animals were randomly assigned to experimental groups (5, 6, 8, 10 and 12 days post-LPC injection). The 5-day post LPC group served as the demyelination baseline control group. In all other groups, half of the animals were anaesthetized and the right sciatic nerves re-exposed to perform ES. Insulated stainless steel wires bared of insulation (2-3 mm for the anode, 5-10 mm for the cathode) were connected to a Grass (Quincy, MA) SD-9 stimulator. The cathode wire was wrapped around the exposed nerve, 2-3 mm proximal to the injection site. The anode was placed between the skin and muscle. ES was performed as previously described by Al-Majed et al (Al-Majed et al. 2000b). Briefly, the Grass stimulator delivered a continuous 20 Hz train of supramaximal pulses (100 msec; 3V) for one

hour. Epineural 10-0 suture served to mark the stimulation site. The stimulation parameters employed in this study were selected as they closely mimic the firing patterns of both motor and sensory neurons (Al-Majed et al. 2000b; Fitzgerald 1987).

For histological studies, animals were processed for analysis at various time points post-LPC injection with stimulated groups being paired with non-stimulated groups in the same cryomolds to ensure processing under identical conditions (5 days, n=19; 6 days, n= 8 LPC and 8 LPC+ES; 8 days, n= 16 LPC and 16 LPC+ES; 10 days, n= 16 LPC and 16 LPC+ES; and 12 days, n=11 LPC and 12 LPC+ES).

2.1.3 Experimental Controls

In addition to the LPC-injected +/- ES animals, the following controls were generated - naïve rats (n=3); naïve animals with brief ES as above (n=3); LPC-injected animals with sham stimulation where electrodes were connected but the stimulator was not turned on (n=3); and LPC-injected animals treated with 2% lidocaine soaked gelfoam applied to the sciatic nerve proximal to ES 30 minutes prior to and during ES (n=3) followed by thorough rinsing with sterile phosphate-buffered saline (PBS) before closing the incision.

2.1.4 Preparation Of Tissue For Analysis

For fixed, frozen (FiFr) immunohistochemistry, animals (n= 124) were euthanized with Euthanyl Forte overdose (Bimeda-MTC, Cambridge, ON) and transcardially perfused with 0.1 M phosphate buffered saline (PBS) followed by 4% paraformaldehyde. One cm of ipsilateral sciatic nerve (bordering both sides of the sites of LPC injection and electrical stimulation) and a contralateral equivalent section of nerve were removed, post-fixed and cryoprotected overnight in 20% sucrose. Tissues were embedded in cryomolds with OCT compound (Tissue Tek, Miles INC, Elkhart, IN) frozen in cooled isopentane and stored at -80°C until processing. For fresh, frozen (FrFr) immunohistochemistry, animals (n=14) were euthanized via CO_2 inhalation and one cm of ipsilateral sciatic nerve (bordering both sides of the sites of LPC injection and electrical stimulation) and equivalent contralateral were removed. Tissues were immediately embedded in cryomolds with OCT compound (Tissue Tek, Miles INC, Elkhart, IN) frozen in

cooled isopentane and stored at -80°C until processing.

2.2 Histochemistry

2.2.1 Immunofluorescence

Longitudinal and transverse/cross sections of fixed frozen (FiFr) nerve tissue were cut at 10 μm on a Microm cryostat and thaw-mounted onto silanized glass slides. Slides were air-dried for 15 minutes and washed 3 x 5 minutes in 0.1 M PBS prior to blocking in 10% normal donkey serum and 0.1% Triton X-100 in 0.1 M PBS for one hour at room temperature. Primary antibodies (see Table 1) diluted in 2% normal donkey serum and 0.1% Triton X-100 in 0.1 M PBS were applied and slides incubated overnight at 4 °C in a humidified chamber. Slides were washed 3 x 10 minutes in 0.1 M PBS and secondary antibodies (see Table 1) diluted in 0.1 M PBS applied for one hour at room temperature. Slides were washed 3 x 10 minutes in 0.1 M PBS and mounted with a glass coverslip using 50% glycerol in 0.1M PBS.

For fresh frozen (FrFr) immunohistochemistry, tissue was cut as above and slides immediately fixed in 4% paraformaldehyde for 15 minutes at room temperature. Slides were washed 3 x 5 minutes in 0.1 M PBS, and blocked for 1hr at room temperature in 10% normal donkey serum and 0.3% Triton X-100 in 0.1 M PBS. Primary antibodies (see Table 1) diluted in 2% normal donkey serum and 0.3% Triton X-100 in 0.1 M PBS and incubated overnight at 4 °C in a humidified chamber. Slides were washed 3 x 10 minutes in 0.1 M PBS. Secondary antibodies (see Table 1) diluted in 0.1 M PBS were applied for one hour at room temperature. Slides were washed 3 x 10 minutes in 0.1 M PBS and mounted with a glass coverslip using 50% glycerol in 0.1 M PBS.

2.2.2 3.3' – Diaminobenzidine (DAB) Immunohistochemistry

Longitudinal and cross sections of fixed frozen tissue were cut as above. Slides were air-dried overnight at 37^{o}C, washed 3 x 5 minutes in 0.1 M PBS and endogenous peroxidase activity quenched with 0.3% hydrogen peroxide in distilled water for 30 minutes at room temperature. Slides were blocked in 0.1 M PBS containing 10% fetal bovine serum (FBS) prior to overnight

incubation at 4 °C with a primary antibody recognizing the 70 kDa subunit common to all neurofilament chains (see Table 1) diluted in 3% human serum and 10% FBS applied and incubated overnight in a humidified chamber. Slides were washed 3 x 10 minutes in 0.1 M PBS and biotinylated secondary antibody (see Table 1) diluted in 10% fetal bovine serum in 0.1 M PBS was applied for one hour at room temperature. Slides were washed 3 x 10 minutes in 0.1 M PBS and HRP-conjugated avidin applied for one hour at room temperature before developing with DAB for approximately five minutes.

2.2.3 Histological Stains

Sections processed for DAB immunohistochemistry also underwent Luxol Fast Blue staining to detect myelin, with Nuclear Fast Red as a counterstain. To do this, slides were washed 3 x 5 minutes in distilled water, then passed through a 70% and 95% alcohol gradient (5 minutes each). Slides were immersed up to the frosted region in a 1% Luxol Fast Blue solution (in 95% alcohol, 10% acetic acid), and incubated in a 60^{o}C oven overnight. After cooling to room temperature, slides were rinsed in 95% alcohol and distilled water before differentiation in 0.05% lithium carbonate for approximately 1-2 minutes. Slides were then briefly rinsed in 70% alcohol and distilled water before immersion in the 0.1% Nuclear Fast Red stain solution (in 5% aluminum sulfate solution) for 5-10 minutes at room temperature. Slides were rinsed in distilled water, dehydrated through an alcohol gradient (70%, 90%, 95%, 100%) and cleared in xylene prior to mounting with a coverslip using Permount (Fisher Scientific, catalog # SP15-500). Slides were imaged using an Olympus BX53 microscope and images digitally captured using cellSens Standard software (Olympus).

2.3 Protein Analysis

2.3.1 ENZYME-LINKED IMMUNOSORBENT ASSAY (ELISA)

To generate tissue samples for the ELISA, a separate cohort of animals received a LPC focal demyelinating lesions with or without brief ES as above (n=22 animals total, with 4 animals per condition and with 2 naïve rats and 5d LPC contralateral nerves serving as controls).

Animals were euthanized at 5, 8, and 10 days post-LPC. One centimeter lengths of sciatic nerve bordering both sides of the demyelinating lesion equally were removed, along with corresponding levels of control nerves, placed in lysis buffer (137mM NaCl, 20mM Tris-HCl (pH 8.0), 1% NP40, 10% glycerol, 1mM PMSF, 10μg/mL aprotinin, 1μg/mL leupeptin, 0.5mM sodium vanadate) and stored at -80°C until processing. BDNF content was measured using the BDNF E_{max} Immunoassay System kit (Promega, Madison, WI), using all antibodies and reagents supplied by the kit and as per the manufacturer's instructions. Briefly, polystyrene ELISA plates (sealed with an acetate sheet to prevent evaporation) were coated overnight at 4^{o}C with an anti-BDNF monoclonal antibody diluted 1:1000 in pH 9.7 carbonate coating buffer. The coating buffer was removed and the plates were washed in Tris-buffered saline with 0.05% Tween 20 (TBST, 20mM Tris, 150 mM NaCl), before being blocked in 1X block & sample buffer for one hour at room temperature. Plates were washed 3x in TBST. Duplicate wells of samples (diluted 1:4 in 1x block & sample buffer) and the BDNF standard curve (500, 250, 125, 62.5, 31.3, 15.6 and 7.8 pg/mL) were applied and incubated for two hours at room temperature with gentle shaking. Plates were then washed 5x in TBST. Anti-human BDNF polyclonal antibody (diluted 1:500 in 1X block & sample buffer) was applied; followed by a two-hour incubation with gentle shaking at room temperature. The plates were washed 5x in TBST before applying HRP-conjugated anti-IgY (diluted 1:200 in 1X block & sample buffer) and leaving it for one hour at room temperature with gentle shaking. Plates were washed 5x in TBST, before color development using the TMB substrate. After 10 minutes, 1N HCl was added to all wells to stop the reaction. Plates were read immediately at a wavelength of 450 nm in a SpectraMax 340 (Molecular Devices, Sunnyvale, CA) spectrophotometric plate reader equipped with SoftMax Pro 5 software (Molecular Devices, Sunnyvale, CA).

2.3.2 Western Blotting

Surgical procedures were performed as above on a separate cohort of animals (n = 32 animals total with 2 naïve controls, 6 LPC and 6 LPC+ES animals per time point). Animals were euthanized at 5, 8 and 10 days post-LPC injection. Three naïve animals served as controls.

A one cm segment of sciatic nerve bordering both sides of the injection site equally was removed from each rat, along with corresponding levels of contralateral and control naïve nerves. The nerve segments were placed in lysis buffer (137mM NaCl, 20mM Tris-HCl (pH 8.0), 1% NP40, 10% glycerol, 1mM PMSF, 10μg/mL aprotinin, 1μg/mL leupeptin, 0.5mM sodium vanadate), homogenized and stored at -80°C until processing. Extracted proteins from pooled samples (N=3 rats/experimental condition/ sample) at each time point and a protein molecular size marker (Licor, catalog #928-40000) were separated by either standard SDS-PAGE (10% acrylamide gels) at 150V for approximately one hour in standard Tris-glycine running buffer (25 mM Tris, 0.2M Glycine, 0.05% SDS), before transfer to PVDF membranes (Bio-Rad, catalog # 162-0177) by semi-dry electroblotting using a Bio-Rad Trans-Blot apparatus for 15 minutes at 15V using chilled transfer buffer (25mM Tris, 192 mM Glycine, 20% methanol). Membranes were blocked overnight at 4^{o}C with gentle agitation using Licor Odyssey blocking buffer (catalog # 927-40000). Membranes were briefly rinsed in 0.01 M PBS with 0.05% Tween 20 (PBST), and primary antibodies (see Table 1) diluted in PBST were applied at 4^{o}C for 72 hours with gentle agitation. The membranes were then washed 3 x 5 minutes in PBST. Infrared dye-conjugated secondary antibodies (see Table 1) were applied for one hour at room temperature with gentle agitation. Membranes were washed 2 x 5 minutes in PBST, followed by washing 1 x 5 minutes in 0.01 M PBS before scanning on a Licor Odyssey 9120 infrared scanning system.

For total protein and equal sample loading determination Coomassie Blue staining was used as the injury model employed made traditional immunostaining for a standard housekeeping marker (such as GAPDH) difficult as all housekeeping proteins examined change expression levels. This method has been evaluated thoroughly (Eaton et al. 2013), and is compatible with the infrared detection systems used to visualize the protein bands. The probed PVDF membranes were stained in a solution of 0.1% Coomassie Blue R-250 (Sigma-Aldrich, catalog# 27186) (in 50% methanol, 7% acetic acid) for ~ 5 minutes at room temperature with gentle agitation. Stain solution was removed, replaced with destain solution #1 (50% methanol, 7% acetic acid) and membranes incubated for ~ 5 minutes at room temperature with gentle agitation. Solution was

discarded, and membranes were submerged in destain solution #2 (90% methanol, 10% acetic acid) and agitated by hand until bands reached desired level of differentiation. Membranes were rinsed twice in distilled water before scanning on a Licor Odyssey 9120 infrared scanning system.

2.4 Data Analysis

2.4.1 Histochemical

To ensure accurate analysis of relative changes in immunofluorescence (IF) signal between experimental groups, nerve segments ipsilateral and contralateral to LPC injection from both experimental and control groups were always mounted on the same slide so that processing was conducted under identical conditions. Immunofluorescence data was gathered from digital images of the site of demyelination captured under identical exposure conditions using Northern Eclipse v7.0 software (EMPIX Imaging Inc.) and a Zeiss Axio Imager M.1 fluorescence microscope. Demyelinated regions of interest for each image (identified by the presence of FG-positive staining) were demarcated with a 1300 x 900 μm box overlaid on the image using Photoshop CS5. Analysis was carried out by tracing the outline of the FG-positive region that fell within the overlaid box of interest using Northern Eclipse, which then calculates the Average Gray and total area (in microns^2) for the image, yielding average Gray per micron^2. For each time point examined, all values obtained at that time point were normalized to the mean value of the Average Gray per micron^2 value for the nerves ipsilateral to LPC treatment for the *LPC Only* animals at that time point. The relative fluorescence signal for each marker with and without ES was compared using the Kruskal-Wallis one-way ANOVA with Dunn's post-test analysis (6, 8, 10 or 12 days post-injection) or Student's t-test (5 days post-injection). Results achieved statistical significance at a p value <0.05.

To evaluate changes in macrophage phenotype between experimental groups, nerve segments ipsilateral and contralateral to LPC injection from both experimental and control groups were always mounted on the same slide so that processing would be conducted under identical conditions. Immunofluorescence data was gathered from digital images of the site of

demyelination captured under identical exposure conditions using Northern Eclipse v7.0 software (EMPIX Imaging Inc.) and a Zeiss Axio Imager M.1 fluorescence microscope. Demyelinated regions of interest were identified by the presence of FG-positive staining. Analysis was carried out by merging images captured from double labeled slides (ED-1/CD206; ED-1/Arg1; ED-1/iNOS; ED-1/TNF-α), and manually determining the proportion of ED-1-positive cells within each of 10 fields of view that also strongly expressed either CD206, Arg1, iNOS or TNF-α. The number of cells indentified as strongly positive for each marker were compared using the Kruskal-Wallis one-way ANOVA with Dunn's post-test analysis (5, 8, or 10 days post-injection). Results achieved statistical significance at a p value <0.05.

2.4.2 ELISA

BDNF protein levels in samples of sciatic nerve assessed via ELISA were determined by interpolation from the standard curve included in the assay, followed by background correction done by subtracting the average background OD_{450} (obtained from the mean OD_{450} of three wells containing only water) from that of each of the experimental values as well as the standard curve. For each sample the mean BDNF concentration was determined for the duplicate wells. Statistical analysis was performed using a one-way ANOVA with Tukey's multiple comparison test. Results achieved statistical significance at a p value <0.05.

2.4.3 Western Blot

Data (from two replicates using protein isolated from pooled nerves from 3 animals per experimental group) was analyzed using the ImageJ software application. Mean densitometry values for all experimental conditions were normalized to the β-III tubulin loading control and expressed as a fold difference of the mean densitometry reading for two lanes of protein extract from naïve animals run on the same gel. Student's t-tests were performed to determine the significance of changes relative to naïve controls in the abundance of the marker of interest at each time point with and without ES. Results achieved statistical significance at a p value <0.05.

TABLE 2.1: LIST OF ANTIBODIES USED

Primary Antibodies			
Target	**Supplier**	**Catalog No.**	**Dilution**
Chicken α-BDNF	Promega	G1641	IHC 1:150
Goat α-CD206	Santa Cruz	sc-34577	IHC 1:100, WB 1:500
Mouse α-β-III	Millipore	MAB1637	IHC 1:00, WB 1:100
Mouse α-CD68 (ED-1)	Cedarlane	MCA341R	IHC 1:250, WB 1:500
Mouse α-Kv1.2	Millipore	MABN77	IHC 1:1000
Mouse α-MBP	Covance	SMI-94R	IHC 1:250
Mouse α-NF	Dako	M0762	IHC 1:800, WB 1:1000
Mouse α-NF-p (SMI-31)	Covance	SMI-31R	IHC 1:1000
Rabbit α-Arg1	Santa Cruz	sc-20150	IHC 1:100, WB 1:500
Rabbit α-β-III	Sigma-Aldrich	T 2200	IHC 1:1000
Rabbit α-Caspr	Abcam	ab34151	IHC 1:4500
Rabbit α-GFAP	Dako	Z 0334	IHC 1:800
Rabbit α-iNOS	Cedarlane	ab3523	IHC 1:100, WB 1:500
Rabbit α-TNF-α	Cedarlane	ab6671	IHC 1:100; WB 1:500
Secondary Antibodies			
Target	**Supplier**	**Catalog No.**	**Dilution**
Donkey Cy3 α-Chicken	Jackson ImmunoResearch	703-165-155	IHC 1:1000
Donkey DyLight594 α-Goat	Jackson ImmunoResearch	705-515-003	IHC 1:1000
Donkey IR680 α-Goat	Licor	925-68074	WB 1:5000
Donkey Alexa488 α–Mouse	Jackson ImmunoResearch	715-546-151	IHC 1:1000
Biotinylated α-Mouse	Amersham	RPN1001	IHC 1:200
Donkey IR800 α-Mouse	Licor	926-32212	WB 1:5000
Donkey Cy3 α–Rabbit	Jackson ImmunoResearch	711-166-152	IHC 1:1000
Donkey IR800 α-Rabbit	Licor	926-32213	WB 1:5000

CHAPTER 3:
RESULTS

3.1 IMPACT OF DELAYED ELECTRICAL STIMULATION ON MYELINATION, MOLECULES INVOLVED IN MYELINATION AND SCHWANN CELL ACTIVATION STATE

Rapid and efficient axon remyelination aids in restoring strong electrochemical communication with end organs and in preventing axonal degeneration often observed in demyelinating neuropathies. The signals from axons that can trigger more effective remyelination *in vivo* are still being elucidated. In the next three sections I assess the impact of delayed brief electrical nerve stimulation (ES; 1 hour @ 20 Hz 5 days post-demyelination) on ensuing reparative events in a focally demyelinated adult rat peripheral nerve.

3.1.1 Creation & Identification Of A Reproducible Focal Demyelination Zone

In order to test the first part of my hypothesis that delayed brief nerve electrical stimulation (ES; 1 hour at 20 Hz) delivered proximal to a site of focal demyelination induced five days prior, will induce cellular changes that result in more effective remyelination, I had to select a reliable and reproducible focal demyelination model in which the impact of brief ES could be assessed. For this purpose, I chose the LPC model of focal demyelination in the tibial nerve branch of the sciatic nerve at the level immediately distal to the nerve trifurcation.

The ability to clearly demarcate the initial region of demyelination in the affected nerve is necessary in order to reliably assess alterations in cellular events and proteins within zones of demyelination and remyelination. Thus, the retrograde fluorescent tracer Fluorogold (FG) was co-injected with the demyelinating agent LPC into the tibial nerve (Fig 3A) creating a readily identifiable injection zone and subsequent region of demyelination and remyelination. The tibial branch of the sciatic nerve was selected as the site of LPC/FG injection as it is not only the largest of the three branches, but also allows for precise, and readily reproducible focal demyelinating lesions. While some FG was retrogradely transported back to the neuronal cell bodies contributing axons to the tibial branch, sufficient FG remained at the zone of demyelination to readily demarcate it. Figure 3 shows a longitudinal section of a demyelinated

nerve, 5 days post-LPC/FG injection, which is representative of the size of the demyelination zone observed across all time points examined. The site of demyelination was readily identified by the joint presence of FG (Fig 3C), diminished myelin basic protein (MBP; a component of myelin, Fig 3D) immunofluorescence (IF) and β-III tubulin IF, an axonal marker (Fig 3E). There was tight register between the region of demyelination and the co-injected FG (Fig 3C and Fig 3D), as shown by a relative lack of MBP in the most FG intense region. These FG intense regions were used to create regions of interest (ROIs) in which the intensity of IF signal for individual markers examined in this study were quantified. For all sections examined, the loss of MBP signal did not extend beyond the FG-positive ROI, with consistent demyelination observed in the FG-defined ROI at 5 days post-LPC (Fig 3B). There was also no evidence of a contralateral effect in response to ES, as the contralateral tibial nerves did not differ from naïve controls with respect to the various markers examined (data not shown). Finally, ES did not appear to impact the integrity of the nerve, as levels of β-III tubulin IF signal over sections of naïve nerve were not discernibly different from sections of nerve that had undergone only brief ES (no demyelination) seven days previous (data not shown).

3.1.2 Impact Of Delayed ES On Remyelination-Associated Events

By 5 days post-LPC there is little structural myelin left within the zone of demyelination in the injected peripheral nerve (Hall and Gregson 1971). In order to assess whether ES effects more rapid remyelination of the LPC-demyelinated axons, I chose to examine select indicators associated with this process, namely, increased expression of MBP, a molecule important in maintaining correct myelin structure; reestablishment of the nodes of Ranvier, important in efficient impulse propagation; expression of a key molecule involved in this process, BDNF; and whether the dedifferentiated reactive state of the Schwann cell is attenuated.

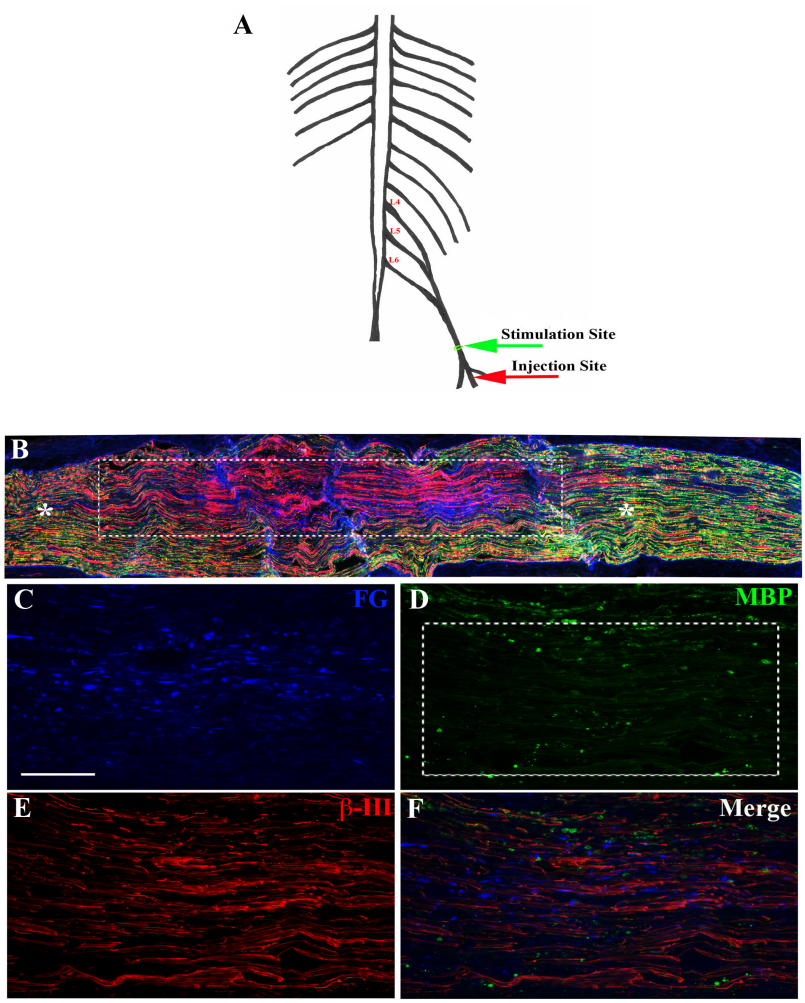

Figure 3: **FluoroGold (FG) staining delineates the demyelination zone**. Representative fluorescence photomicrographs from a longitudinal section of tibial nerve six days after injection with a lysophosphatidyl choline (LPC)/FG mixture and doubly immunostained for myelin basic protein (MBP; green, D) and β-III tubulin (red, E). Note: FG was taken up by cells in the injection site region and diffused beyond the injection site. There was good register between the most intensely stained region of FG (blue, B, C) and the area of demyelination as defined by the punctate immunostaining for MBP and a lack of the normally uniform linear MBP staining (B, D). The presence of positive linear β-III tubulin IF indicates that axons within the demyelination site persist (B, E). The demyelination site was identified by the joint presence of FG, axonal (β-III tubulin) and paucity of myelin marker (MBP) (boxed areas B, D) in contrast to the robust MBP immunostaining outside the zone of demyelination (asterisks, B). Thus, FG serves to identify the regions of interest (ROIs; similar to that outlined by dashed lines in (D)), where alterations in various markers impacted by the LPC and electrical stimulation were quantified (see Figs 2, 6). Scale bar = 100 μm.

3.1.2.1 Brief ES Increases MBP Expression

Injection of LPC into the tibial branch of the sciatic nerve induced a rapid, focal demyelinating lesion. The contralateral control (noninjected) nerves at all time points examined

displayed intense immunostaining for MBP. The MBP immunopositive profiles of the contralateral nerves displayed a linear, organized pattern, which is typical of myelinated internodes (Fig 4A). By five days post-LPC injection, a near complete demyelination of the axons within the injection site was observed (Fig 3, 4B). There was clear disruption of the normal linear pattern of MBP IF (Fig 4B vs. 4A), consistent with segmental demyelination. The MBP IF signal within the demyelination zone was greatly diminished and when detected was punctate, likely representing myelin debris that was either free within the endoneurium or that had been taken up by phagocytic macrophages. Analysis comparing the relative alterations in MBP IF signal over contralateral versus ipsilateral tibial nerves revealed a significant decrease in MBP, consistent with myelin loss in the LPC-injected (ipsilateral) nerves (Fig 4C). Alterations in MBP expression induced by the one hour ES treatment (applied at 5d post-LPC injection) were assessed relative to nerves that had undergone LPC-induced demyelination only at the same time point following ES. At 6d post-LPC (1d post-ES), the levels of MBP detected in the focally demyelinated tibial nerves of animals were not significantly different between the experimental group that received ES and those that did not (Fig 4D & 3D). The lesion sites in both groups were nearly devoid of linear MBP signal and differed significantly from the intact contralateral nerve (Fig 4F).

By 8d post-LPC injection (3d post-ES), however, clear differences between the stimulated and non-stimulated nerves began to emerge. While the non-stimulated nerves continued to be largely devoid of MBP immunoreactivity, their stimulated counterparts began to display a more intense MBP IF signal. Not only was there a greater degree of total MBP immunoreactivity, but the distribution of the immunopositive signal also displayed changes. Beginning at this time point, there was less visible MBP-positive myelin debris present, and there was a more linear pattern of MBP signal in the ES-treated nerves, suggestive of early segmental remyelination (Fig 4G, H, I). While the stimulated nerves did not differ greatly in the level of MBP IF detected 10d post-LPC as compared to that detected in nerves at 8d post-LPC (Fig 4H, K,), there was a distinct and significant difference between the stimulated and non-

stimulated nerves at 10d post-LPC, both in terms of the amount of immunofluorescence and in the localization of the IF signal. As in the 8d post-LPC nerves, the MBP IF signal displayed a much more linear appearance in the ES group, while in the LPC only nerves its localization remained predominantly associated with small, round cells morphologically consistent with activated macrophages (Fig 4J, K, L). By 12d post-LPC there was an even greater divergence in the IF signal for MBP between the non-ES treated and ES treated nerves (Fig 4M, N, O; 7d post-ES). At this last time point examined, nerves receiving ES had clear evidence of greater remyelination than controls, albeit incomplete. There was definite organization of the MBP IF signal into structures resembling normal myelin internodes, with little evidence of myelin debris. The non-stimulated nerves at this time point had just began to display the first signs of possible remyelination, with a few structures resembling internodes present (Fig 4M).

When naïve (non-LPC injected) nerves were subjected to the stimulation procedure there were no discernable changes in MBP expression. These nerves displayed a level of MBP IF indistinguishable from that observed in naïve nerves, suggesting that hypermyelination did not occur (Fig 5A, B). This implies that the increased MBP expression observed in the LPC-injected nerves is likely due to an enhanced repair response. Further, the observed changes in MBP expression appeared to be due to the ES procedure itself, rather than the mere surgical re-exposure of the demyelinated nerves. When sham ES was performed, (nerve exposed, electrodes put in place for one hour, but without the stimulator turned on) there was no discernable increase in MBP expression by 12d post-LPC, as opposed to the significant increase observed when the stimulator was active (Fig 5C vs 4N). Furthermore, the impact of ES on MBP expression was likely due to neuronal activation, and dependent on action potential conduction, as the application of the sodium channel blocking agent lidocaine prior to, and throughout the one hour ES procedure abolished the observed increases in MBP expression and axonal remyelination (Fig 5D).

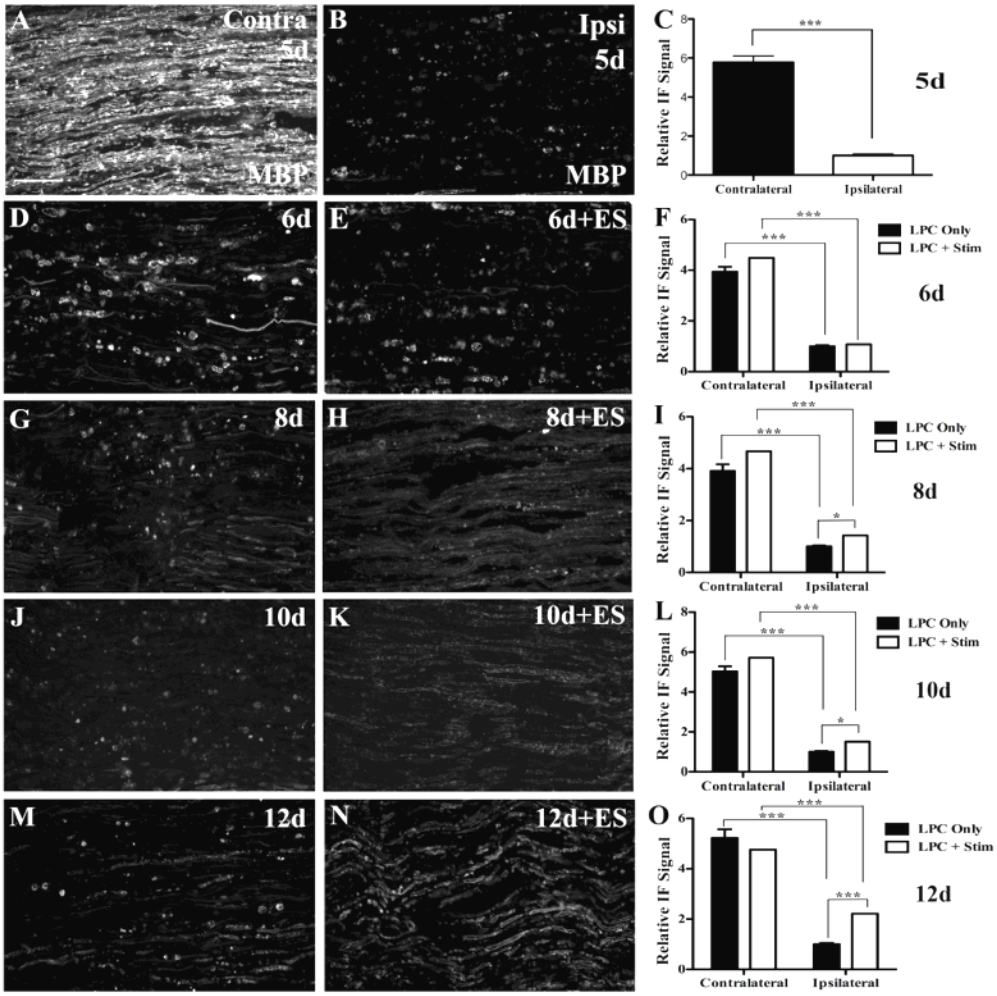

Figure 4: **Increased myelin basic protein (MBP) expression following 1hr ES delivered 5 d post-LPC demyelination.** Representative photomicrographs from FG-positive areas on longitudinal sciatic nerve sections processed for MBP immunofluorescence (IF) reveal extensive demyelination 5d post lysophosphatidyl choline (LPC)/FG demyelinating injection (B) as compared to *contralateral* normal control nerves (A). Temporal analysis of LPC) focal demyelination +/- electrical stimulation (ES) as indicated in days post-LPC: 6d (D), 6d+ES (E), 8d (G), 8d+ES (H), 10d (J) 10d+ES (K) and 12d (M) 12d+ES (N) post-LPC. Note: In the LPC only group, MBP IF was localized in distinct patches consistent with uptake by phagocytosing cells (D, G, J) with faint linear regions similar to periaxonal MBP localization observed by 12 days post-LPC only injection (M). In contrast, in the LPC + ES group faint regions of MBP peri-axonal-like IF were already apparent 8d post-LPC (3d post-ES; H) and consistently stronger in the 10d post-LPC (5d post-ES; K) and 12d post-LPC (7d post-ES; N). Summary bar graphs of relative changes in immunofluorescence signal for MBP in focal demyelination zones (C, F, I, L, O). Note: values obtained from individual slides at each time point were normalized to the mean value of the Average Gray per micron^2 readings for the nerves ipsilateral to LPC treatment for the LPC only animal on that slide and for that time point. N = 4-6 animals analyzed per condition; regions quantified per condition: 49 ipsi and 38 contra (5d, LPC only); 128 ipsi and 76 contra (6d, LPC only); 81 ipsi and 54 contra (6d LPC+Stim); 83 ipsi and 49 contra (8d, LPC only); 60 ipsi and 58 contra (8d, LPC+Stim); 62 ipsi and 52 contra (10d, LPC only); 54 ipsi and 48 contra (10d, LPC+Stim); 155 ipsi and 73 contra (12d, LPC only); 119 ipsi and 104 contra (12d LPC+Stim). Asterisks indicate significant differences between experimental groups; *P<0.05, **P<0.01, ***P<0.001. Scale bar = 100 μm.

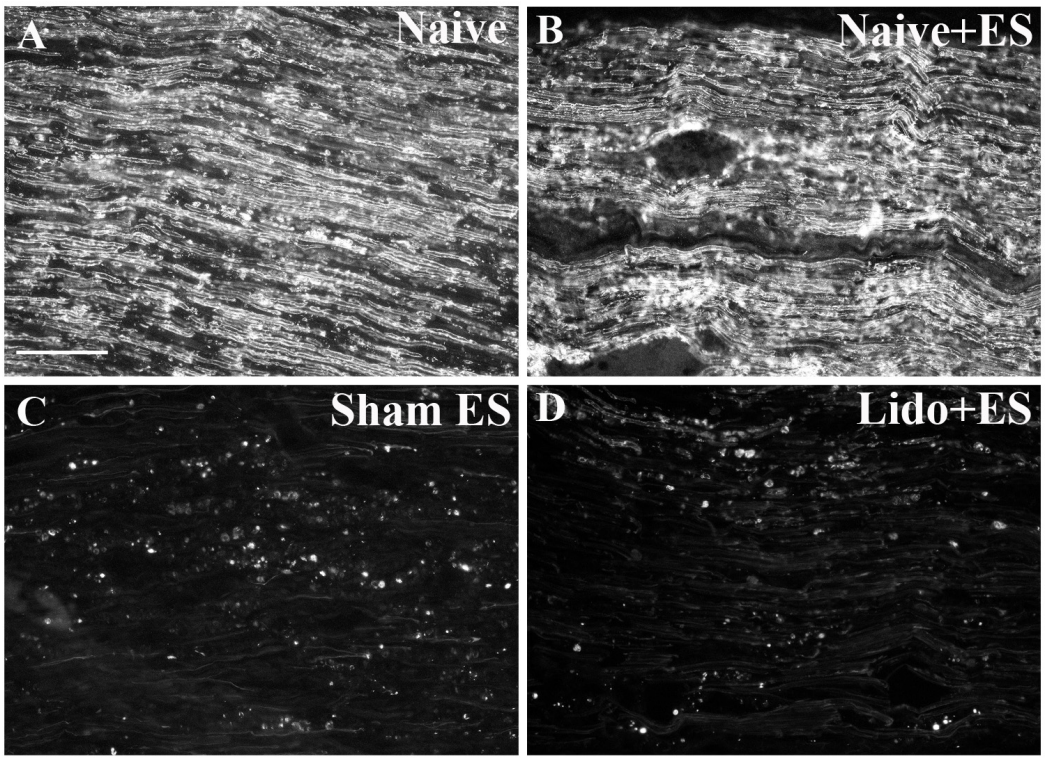

Figure 5: Impact of ES on MBP expression in naïve nerves or focally demyelinated nerves subjected to action potential blockade. Representative immunofluorescence photomicrographs of tibial nerve sections immunostained for MBP. Naïve control nerves displayed intense MBP immunoreactivity (A). Electrical stimulation (ES) of naïve nerves did not discernibly alter MBP expression (B). Neither sham stimulation, nor blockage of action potential conduction through local application of lidocaine prior to and at time of electrical stimulation of 5d LPC-injected nerves effected the increase in MBP expression within the focal demyelination zone (C,D) normally observed at the 12 day post-LPC timepoint examined. This supports that the increased MBP immunoreactivity observed in the stimulated focally demyelinated nerves is due to the increased axonal activity effected by the ES procedure. Scale bar = 100 μm.

3.1.2.2 Accelerated Node Of Ranvier Reorganization In Electrically Stimulated Demyelinated Nerves

The node of Ranvier has a highly structured molecular organization, with the Nav1.6 sodium channels clustered at the node (Schafer et al. 2006), flanked by the contactin-associated protein (Caspr) at the paranode, and voltage gated potassium channels (including Kv1.2) in the juxtaparanodal region (Arroyo et al. 2004). Axonal demyelination resulted in a loss of the discrete regional localization of the two node of Ranvier associated markers. Both paranodal Caspr and juxtaparanodal Kv1.2 assumed a diffuse distribution with the two markers often colocalized (Fig 6B, C, E), instead of being highly localized and distinct from each other

((Arroyo et al. 2004); Fig 6A and insert, Fig 6A). At 5d post-LPC injection there was nearly a complete loss of the distinct restricted Caspr and Kv1.2 staining, with an average of 1.5 visible organized nodal regions in the fields of view examined, compared to 24.1 nodal regions in an equivalent field in the contralateral control nerve. Disruption of the nodal organization largely persisted in both the ES and non-stimulated nerves at 8d post-LPC injection (3d post-ES; Fig 6C, D). At this time point however, early evidence of reorganization of nodal regions began to emerge, especially in the ES group (Fig 6D), with an average of 13.28 Caspr-positive nodal regions observed per field of view, compared to 5.19 for the non-stimulated nerves (Fig 6I). By 10d post-LPC (5d post-ES) the incidence of Caspr- and Kv1.2-positive organized nodal regions in the stimulated nerves (Fig 6F) was equivalent to that observed in the normal nerve with an average of 21.53 distinct Caspr-positive nodal regions per field of view (Fig 6I). Despite this, there was still some faint diffuse Kv1.2 staining in the axons. This differed markedly from the non-stimulated nerves that continued to display a disorganized, predominantly diffuse pattern of Caspr- and Kv1.2-positive IF signal (Fig 6E) with an average of only 9.96 visible Caspr-positive nodal regions per field of view (Fig 6I). By 12d post-LPC (7d post-ES) there is a return to the normal pattern of Caspr and Kv1.2 localization in ES nerves (Fig 6H). By this time, nerves that received only the LPC injection had also begun to display more highly organized nodal structures with Caspr once again assuming a distinct discrete localization. Kv1.2 was seen to localize to regions adjacent to some of these Caspr-positive distinct regions, and co-localized with Caspr less frequently (Fig 6G), similar to the pattern observed 5d after ES (Fig 6F), albeit less organized.

3.1.3 Impact Of Delayed ES On Molecules Important For Myelination

The increased MBP expression and more rapid re-establishment of the node of Ranvier architecture made us posit whether molecules involved in the myelination process may also be

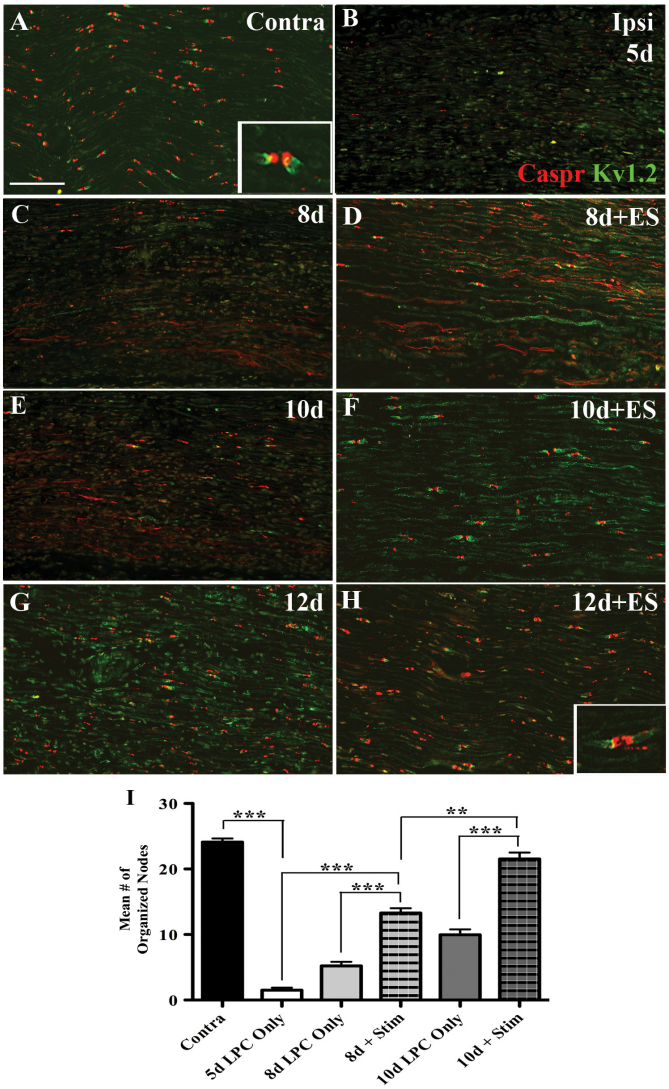

Figure 6: **Accelerated node of Ranvier reorganization in focally demyelinated nerves subjected to 1hr ES.** Representative photomicrographs of FG-positive (i.e focally demyelinated) regions of longitudinal tibial nerve sections dually immunostained for the paranodal protein Caspr (red) and the juxtaparanodal Kv1.2 ion channel (green). Contralateral control nerves display well-organized nodes of Ranvier with Caspr IF in the paranodal region and Kv1.2 IF at the juxtaparanodal region (A, insert reveals nodal staining at higher magnification) and an average of 24.1 visible nodes per field of view as defined by a 1300 x 900 pixel rectangle superimposed on the photomicrograph (I). A marked loss of nodal organization was observed 5d post-lysophosphatidyl choline (LPC)/FG injection, with an average of 1.5 nodal regions per field of view (B, I). Temporal analysis of LPC +/- ES delivered 5 d post-LPC and indicated in days post-LPC: 8d (C), 8d+ES (D), 10d (E), 10d+ES (F) and 12d (G) 12d+ES (H) post-LPC, revealed that ES delivered 5 d post-LPC resulted in nodal reorganization apparent as early as 8d post-LPC (8d+ES - 3d post-ES; D), with a mean of 13.28 nodes per field of view, as compared to 5.19 in the non-stimulated nerves (8d post-LPC only; C, I). The reorganization continued at 10d post-LPC in the ES nerves, approaching contralateral control nerve levels (10d+ES - 5d post-ES; F), with a mean of 21.53 nodes per field of view in the stimulated nerves (I), compared to 9.96 in the non-stimulated (10d post-LPC; E, I) that continued at the 12d post-LPC (12d+ES - 7d post-ES; H and insert). Tissue from the LPC only group displayed modest nodal re-organization (G) 12d post-LPC consistent with the appearance of only faint remyelination (see Fig 1). Scale bar = 100 μm.

coordinately regulated. One such molecule is BDNF. It has been previously reported that BDNF plays a key role in peripheral nerve myelination (Chan 2001; Chan et al. 2006) and that in models of axonal transection and repair, immediate brief ES results in increased BDNF expression that is presumably being released from growing axon tips (Al-Majed et al. 2000a; Geremia et al. 2007; McTigue et al. 1998; Singh et al. 2012). However, in the LPC model of focal demyelination employed in this study, the axons are still structurally intact. Therefore, I examined if delayed brief ES could affect an increase in BDNF at the site of focal demyelination.

Using BDNF immunohistochemistry and ELISA analysis, a persistent low level of BDNF was detected in control sciatic nerves (Fig 7A). Five days post-LPC increased BDNF levels were detected within the demyelination zone, localizing predominantly to cells identified as ED-1-positive macrophages (Fig 7B, colocalization data not shown). Measurement of the local BDNF content via ELISA confirmed an increase in the amount of BDNF within the demyelination zone 5d post-LPC injection, and was determined to be 38.6 +/-0.3 pg/ml (s.e.m.), as compared to 7.6 +/- 1.6 pg/ml (s.e.m.) in an equivalent region of the contralateral nerve (Fig 7C). Eight days post-LPC injection (3d post-ES) the ES nerves contained even higher levels of BDNF at 53.8 +/- 3.1 pg/ml (s.e.m.), as compared to the LPC-only nerves, which had declined relative to the 5 days post-LPC levels to 19.7 +/- 4.9 pg/ml (s.e.m.). This is a similar timeline to that observed for the increase in MBP immunofluorescence, and appears to indeed correlate with an early onset of remyelination. Notably, at this time point the increased BDNF IF signal colocalized with the axonal marker βIII-tubulin, the Schwann cell marker GFAP and the macrophage marker ED-1 (colocalization data not shown; Fig 7D, E, F). This suggests that there are additional sources of BDNF in the stimulated nerve not observed in the non-stimulated nerves. The levels of BDNF in the demyelination zone were still elevated in the ES-treated nerves 10d post-LPC (five days post-ES). Nerves receiving brief ES had greater BDNF IF signal and mean BDNF content (66.3 +/- 3.7 pg/ml, s.e.m.), compared to the non-stimulated LPC-treated nerves that had declined to almost the baseline levels of control contralateral nerves (9.5 +/- 0.3 pg/ml, s.e.m.), with BDNF expressed by macrophages, Schwann cells, and the axons

(colocalization data not shown; Fig 7G, H, I). Once again, there was agreement between the BDNF ELISA and IF data, with the latter appearing similar to that observed in the 8d post-LPC group.

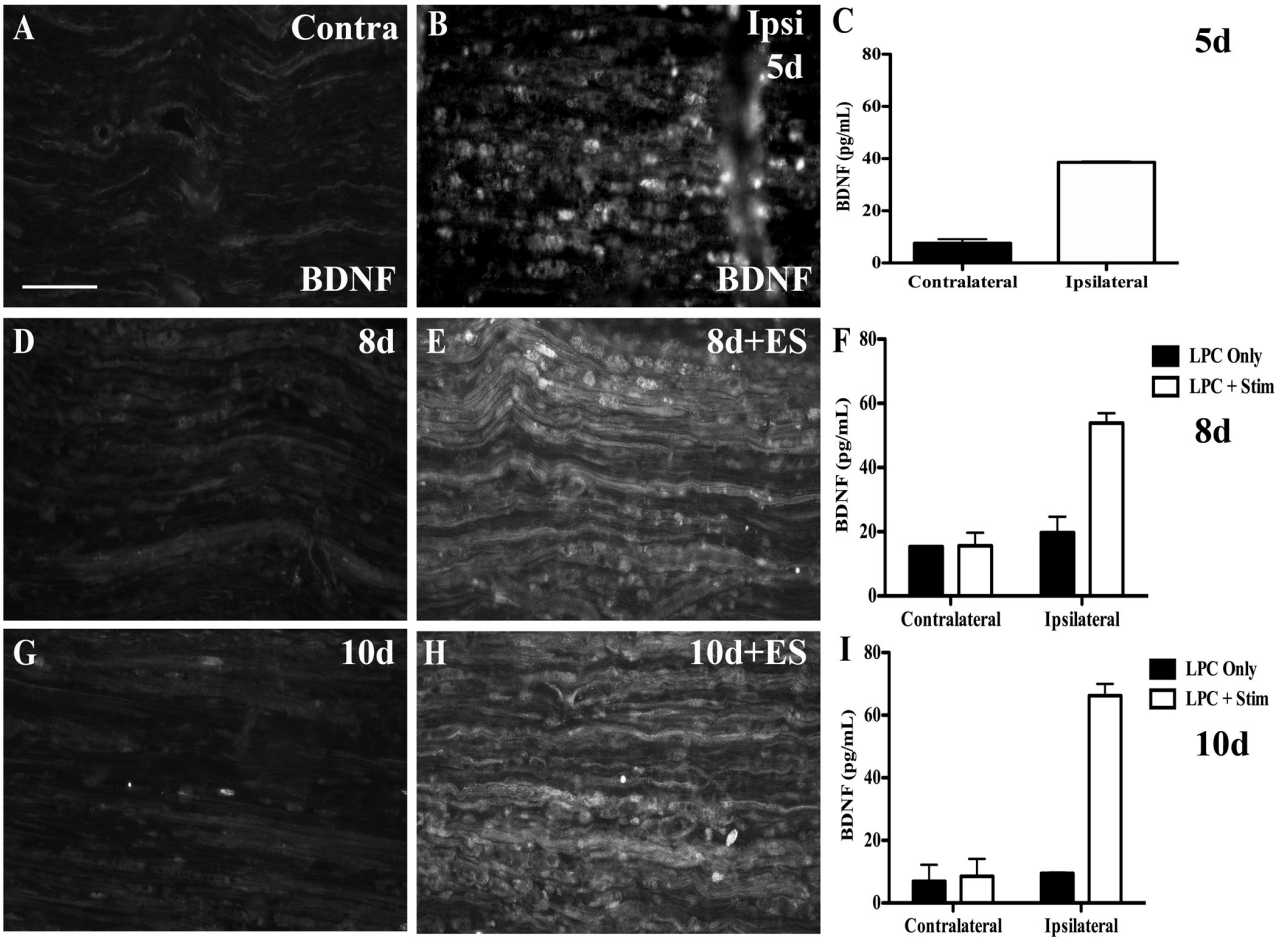

Figure 7: Increased BDNF protein in demyelination zone following 1 hr ES. Representative immunofluorescence (IF) photomicrographs from FG-positive focally demyelinated areas of tibial nerve sections immunostained for BDNF. Contralateral control nerves displayed only minimal BDNF IF (A). There was a marked increase in BDNF observed 5d post- lysophosphatidyl choline (LPC)/FG injection (B), largely within cells identified as ED-1 positive macrophages (data not shown). Temporal analysis of LPC focal demyelination +/- ES delivered 5 d post-LPC and as indicated in days post-LPC: 8d (D), 8d+ES (E), 10d (G), 10d+ES (H). Note: ES results in an increase in the BDNF IF signal detected 8 and 10 d post-LPC (3 and 5 days post-ES; E,H) relative to LPC only nerves (D,G). Summary bar graphs of BDNF protein levels measured by ELISA in samples of sciatic nerve bridging the site of demyelination are in agreement with BDNF IF (C, F, I). Asterisks indicate significant differences between experimental groups; **P<0.01. Scale bar = 100 μm.

3.1.4 Gradual Attenuation Of The Schwann Cell Reactive State Following Brief ES

An important consideration when examining aspects surrounding myelin repair is the state of the glial cells responsible for the elaboration of the myelin sheath. Demyelination drives Schwann cells into a de-differentiated state, which shares many properties with their non-myelinating counterparts. This de-differentiation is associated with the acquisition of a reactive phenotype characterized by prominent glial fibrillary acidic protein (GFAP) expression (Scherer and Salzer 2001). In order to affect proper repair, a prompt conversion of these Schwann cells back to a myelinating phenotype is desirable and thus the impact ES on SC GFAP expression was assessed.

The focal demyelination observed following LPC injection was also associated with increased Schwann cell reactivity, as evidenced by increased IF signal for the cytoskeletal protein GFAP in the LPC-injected tibial nerves (Fig 8B). In the contralateral control nerves there was a persistent, low level of GFAP expression, likely expressed by the population of non-myelinating Schwann cells, but at a significantly lower level than that of the focally demyelinated nerves (Fig 8A, C). Nerves examined at the 6, 8, and 10 days post-LPC injection (1d, 3d, and 5d post-ES) time points displayed similar, elevated levels of GFAP expression in both the stimulated and non-stimulated nerves (Fig 8D-F, G-I, J-L). However, by 12d post-LPC injection (7d post-ES) a marked difference between the animals that received the brief ES and those that did not had emerged. The LPC-only animals still expressed high levels of GFAP (Fig 8M). However, in ES nerves the GFAP IF levels were now reduced compared to that observed in the LPC-only animals (Fig 8N, O), but still remained elevated above the IF intensity of the contralateral control nerves. This suggests that ES gradually results in a more rapid resolution of the activated state of SCs in the demyelination zone.

When naïve (non-LPC injected) nerves were subjected to the stimulation procedure there were no discernible changes in GFAP expression. Because the naïve, stimulated nerves did not display a measurable increase in GFAP expression, this suggests that the stimulation procedure

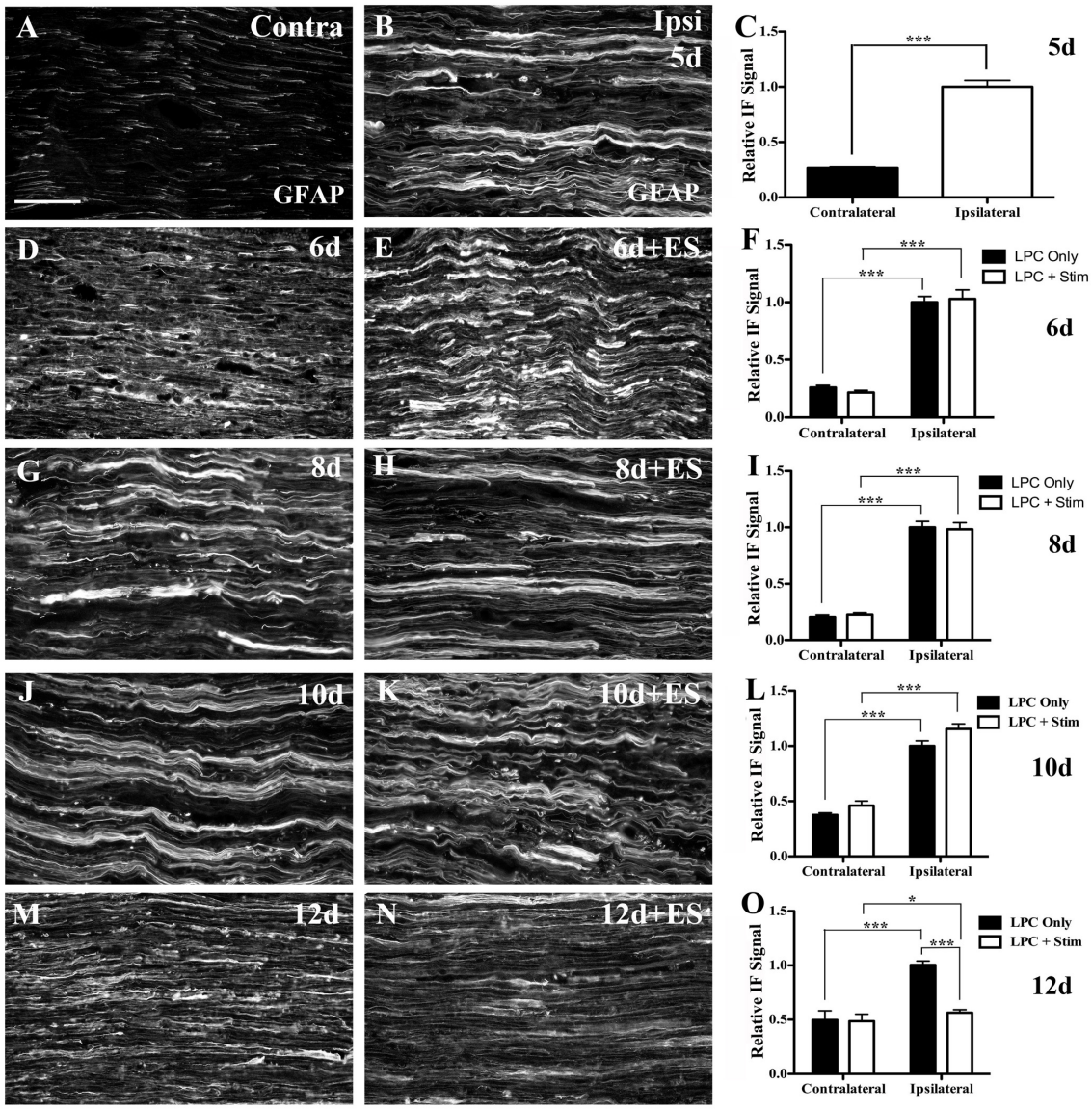

Figure 8: Decreased reactive gliosis following 1hr electrical stimulation (ES) delivered 5d post-demyelination. Representative immunofluorescence photomicrographs from FluoroGold (FG) positive areas of tibial nerve sections processed for glial fibrillary acidic protein (GFAP) immunofluorescence (IF) to detect reactive Schwann cells. Contralateral intact control nerves displayed only minimal GFAP IF (A). However 5d post-lysophosphatidyl choline (LPC)/FG injection there was a marked increase in GFAP IF (B). Temporal analysis of LPC focal demyelination +/- ES as indicated in days post-LPC: 6d (D), 6d+ES (E), 8d (G), 8d+ES (H), 10d (J) 10d+ES (K) or 12d (M) 12d+ES (N) post-LPC. Note: ES resulted in a significant decrease in the GFAP IF signal detected at 12d post-LPC (7 days post-ES; N) relative to 12d LPC only (M). Summary bar graphs of relative changes in immunofluorescence signal for GFAP within the focal demyelination zone in sections of tibial nerve bridging this zone (C, F, I, L, O). N = 4-6 animals analyzed per condition; regions quantified per condition: 49 ipsi and 32 contra (5d, LPC only); 73 ipsi and 64 contra (6d, LPC only); 60 ipsi and 48 contra (6d, LPC+Stim); 84 ipsi and 68 contra (8d, LPC only); 53 ipsi and 60 contra (8d, LPC+Stim); 89 ipsi and 74 contra (10d, LPC only); 86 ipsi and 76 contra (10d, LPC+Stim); 142 ipsi and 74 contra (12d, LPC only); 108 ipsi and 80 contra (12d, LPC+Stim). Asterisks indicate significant differences between experimental groups; *P<0.05, ***P<0.001. Scale bar = 100 μm.

alone is not sufficient to induce a reactive state in the SCs (Fig 9A, B). As was observed with the immunostaining for MBP, when sham ES was performed, (nerve exposed, electrodes put in place for one hour, but without the stimulator turned on) there was no observable change/attenuation in GFAP expression by 12d post-LPC, compared to the significant attenuation in GFAP expression observed when the stimulator was active (Fig 9A, C). Furthermore, the impact of ES on GFAP expression was likely due to neuronal activation, and dependent on action potential conduction. The application of the sodium channel blocking agent lidocaine prior to, and throughout the one hour ES procedure abolished the observed decreases in GFAP expression and Schwann cell reactivity (Fig 9D).

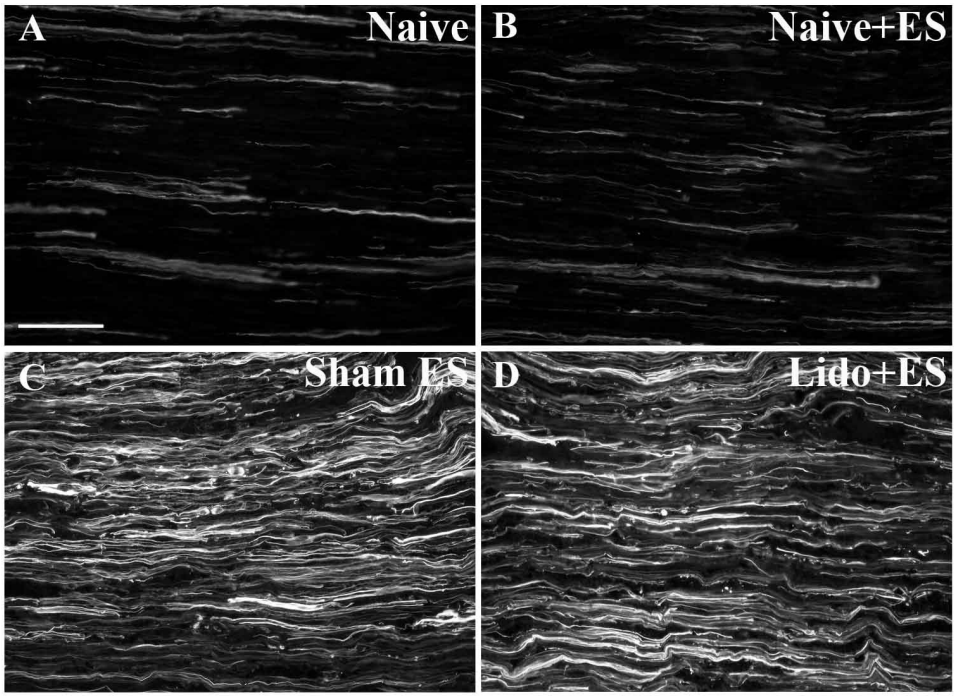

Figure 9: Impact of ES on Schwann cell reactive state in naïve nerves or focally demyelinated nerves subjected to action potential blockade. Representative immunofluorescence photomicrographs (20x magnification) of sciatic nerve sections immunostained for glial fibrillary acidic protein (GFAP). Naïve nerves display some GFAP immunoreactivity, reflecting the population of non-myelinating Schwann cells present within peripheral nerves (A). Electrical stimulation of naïve nerves did not induce reactive gliosis (B). Neither sham stimulation, nor blockage of action potential conduction through local application of lidocaine at time of electrical stimulation of 5d LPC-injected nerves effected a decrease in GFAP expression (reactive gliosis) within the focal demyelination zone normally observed at the 12 day post-LPC timepoint examined (C, D). This supports that the reduction in Schwann cell reactivity normally observed at 12 days post-LPC within the demyelination zones in animals receiving ES 1 week previously is due to the increased neuronal activity effected by the electrical stimulation procedure. Scale bar = 100 μm.

Taken together, these results indicate that a single bout of electrical stimulation delivered five days following a demyelinating insult has a beneficial effect on processes involved in myelination, namely expression of MBP, reformation of proper nodal architecture, increased local BDNF, and the attenuation of Schwann cell reactivity. When examining the effect of an intervention on an in vivo system, it is not enough to merely consider what is occurring within a single cell type, one must consider the other vital components to the system. As axons that have lost their myelin sheath are vulnerable to degeneration, it was thus prudent to examine what effect, if any, the stimulation procedure has on the axons themselves.

3.2 IMPACT OF DELAYED NERVE STIMULATION ON AXONAL PROPERTIES IN FOCALLY DEMYELINATED NERVES

Rapid and efficient axon remyelination is critical for the prevention of axonal degeneration, a common occurrence in demyelinating disease, and a source of permanent disability (Drenthen et al. 2013; Silber and Sharief 1999). The maintenance of the components of the cytoskeleton, namely the neurofilament class of intermediate filament proteins, is an important factor affecting the overall health and integrity of the axon. In addition to providing protection against degeneration, there is a complex and intimate link between the neurofilaments and the process of myelination (Starr et al. 1996). In this section I assess the impact of delayed brief electrical nerve stimulation (ES; 1 hour @ 20 Hz 5 days post-demyelination) on the preservation and protection of axons in focally demyelinated adult rat peripheral nerve.

3.2.1 The Re-Expression Of Axonal Neurofilaments Is Enhanced By ES

A classic histological approach was used to examine the overall impact of ES on the neurofilament content of LPC demyelinated nerves. To do this, sections were processed for neurofilament immunohistochemistry (using a pan-neurofilament antibody recognizing the common core of all three neurofilament subtypes) then stained with the classic histological stains Luxol Fast Blue (LFB) and Nuclear Fast Red (NFR) to detect both myelin and presumptive macrophages, respectively. In naïve control nerves immunoreactivity for neurofilament proteins was readily visible as prominent dark brown/black structures (Fig 10A) and assumed a linear

pattern. Intense LFB staining, also arranged in a linear pattern parallel to the neurofilament protein immunopositive structures, as one would expect with normal myelin content accompanied this. Numerous elongated nuclei (consistent with the appearance of Schwann cell nuclei) were also observed in close association with and parallel to the myelin stain and neurofilaments. When examined in cross section, the neurofilaments were visible as dark brown/black rings, surrounded by an outer ring of blue stained myelin (Fig 11A, arrow). In sharp contrast, by 5d post-LPC injection there was a near complete loss of the normal, organized myelin structure, and an extensive infiltration of macrophages had occurred. These cells were round and contained globules of myelin, consistent with the appearance of foamy, activated macrophages (Fig 10B, Fig 11B, arrow). In both longitudinal and cross sections, there was also a distinct loss of neurofilament, with little to none of the normal linear arrangement of neurofilaments protein immunopositive structures present, suggesting that the focal demyelination had indeed impacted neurofilament expression.

Eight days post-LPC (three days post-ES), the non-stimulated nerves still had dramatically reduced myelin levels, a continued presence of a large number of myelin debris-containing macrophages and were largely lacking in detectable neurofilament immunostaining (Fig 10C, Fig 11C). In contrast, the ES nerves had once again begun to display positive immunostaining for neurofilament proteins, which, although less numerous than in the uninjured nerves, were still linear in nature (Fig 10D). In addition, thin segments of myelin were detected in a close, parallel association with the neurofilament immunoreactive signal, suggestive of early remyelination (Fig 10D). Cross sections also showed an increase in the neurofilament immunoreactive signal, with myelin found surrounding these axons in a typical circular pattern, though of a much lower intensity of myelin staining (Fig 11D, arrow). This is consistent with the previously outlined results of the MBP immunohistochemistry in which the appearance of thinly myelinated internodes were once again apparent at this time point. While the stimulated nerves still had numerous macrophages (many containing myelin debris), there was also an emergence of some smaller, less foamy macrophages largely devoid of visible myelin (Fig 10D,

arrow). Similar results were observed at 10d (Fig 10E,F) and 12d (Fig 10G,H) post-LPC (5d and 7d post-ES, respectively). The nerves not receiving ES displayed only minimal recovery of neurofilament immunoreactivity at 10d post-LPC, remaining largely demyelinated with numerous foamy macrophages still present (Fig 10E,G, Fig 11E). In contrast, the stimulated nerves displayed higher levels of detectable neurofilaments with myelinated axon profiles more evident and elongated nuclei resembling those of Schwann cells aligned with the neurofilaments (Fig 10F, arrow, Fig 11F). The stimulated nerves were also largely devoid of macrophages by 12d post-LPC. At each of these time points the intensity of the neurofilament immunostaining increased in the stimulated nerves until it began to approximate normal levels. The density of the closely associated myelin also increased, although the LFB staining never did perfectly recapitulate the intensity of that found in the contralateral control (Fig 10H) nerves, consistent with the notion that remyelinated internodes will be both shorter, and thinner than they were prior to the demyelinating insult. By 12d post-LPC the nerves that did not receive brief ES displayed increased neurofilament immunoreactivity (Fig10G), similar to that observed in the ES nerves at eight days post-LPC. At this time point the non-stimulated nerves also showed the first indication that the inflammatory process was resolving, by the presence of non-myelin containing macrophages.

3.2.2 ES Promotes The Re-Phosphorylation Of Axonal Neurofilaments

While increased expression of neurofilament proteins is important in order to fully resolve a demyelinating insult, alone it is insufficient to prevent axonal loss and ensure a full return to normal structure and function. A variety of post-translational modifications are important final steps in the synthesis of many proteins, and the neurofilaments are no exception. The post-translational processing of the neurofilament proteins, namely the addition of phosphate groups to the medium and heavy isoforms (Lee et al. 1987) does not occur in isolation. Rather, an important extrinsic factor, namely myelination, plays an important role in modulating this process (Starr et al. 1996). As both the wrapping of the axon in a myelin sheath and the

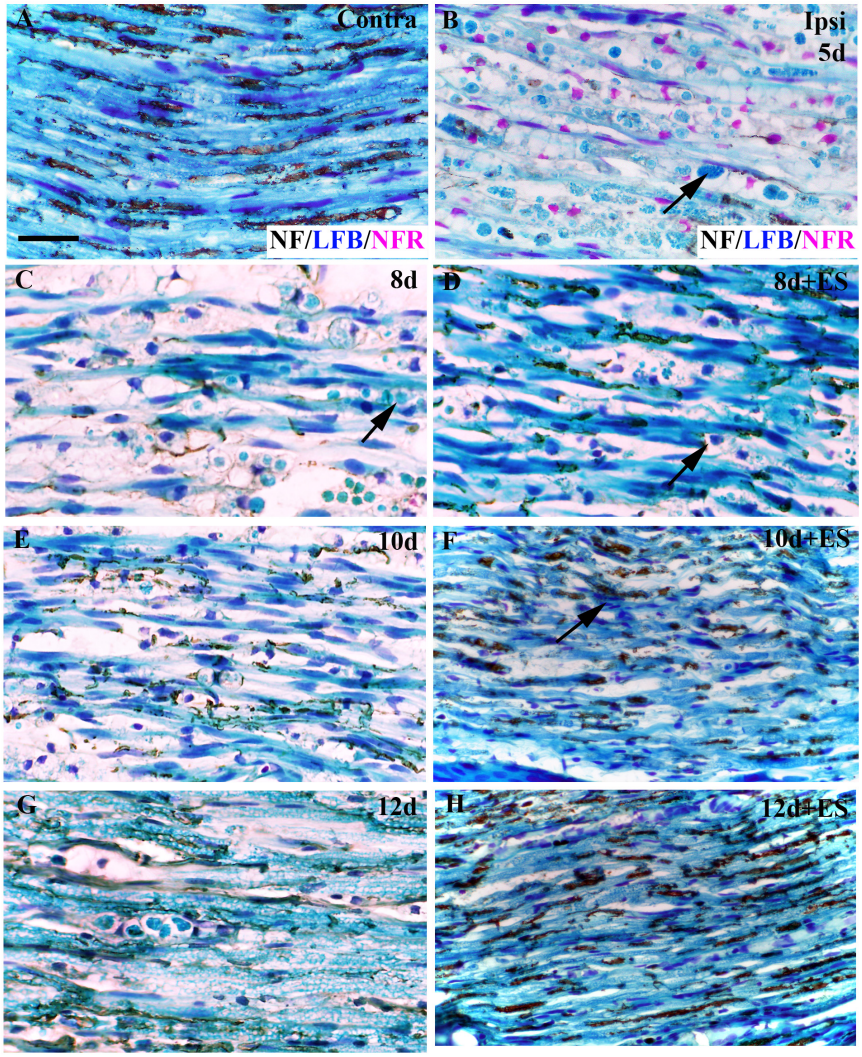

Figure 10: **Neurofilament expression increases coincident with reappearance of myelinated axons in focally demyelinated nerves subjected to ES.** Representative photomicrographs from FluoroGold (FG)-positive areas of longitudinal tibial nerve sections immunostained for neurofilament proteins (NF – brown/black) then stained for the presence of myelin (Luxol Fast Blue [LFB] - blue) and nuclei (nuclear fast red [NFR] – purple/darkblue). Uninjured (*contralateral*) control tibial nerves displayed intense uniform LFB staining, indicative of abundant myelin with prominent linear NF immunostaining (A) and elongated dark blue Schwann cell nuclei. Five days post tibial nerve injection of lysophosphatidyl choline (LPC)/FG, extensive NF and myelin loss is observed coupled with infiltration by numerous macrophages filled with largely unprocessed myelin debris (B,C arrow). Temporal analysis of LPC-focally demyelinated nerves +/- ES as indicated in days post-LPC. Note: In the LPC+ES group there was increasing linear NF immunoreactivity detected (F,H) with higher levels of uniform LFB staining consistent with myelinated axons, and the appearance of macrophages devoid of myelin debris apparent as early as 8d post-LPC (3d post-ES; D, arrow). The LFB staining was even stronger in the 10d (5d post-ES) animals where presumptive Schwann cells now display elongated nuclei (F, arrow) and 12d (7d post-ES; H) post-ES tissue. In contrast, in the LPC only group there was just a slight increase in NF immunoreactivity beginning 10d post-LPC (E), but it was much less robust than that observed in the stimulated as well as the contralateral control nerves. Notably in the nonstimulated nerves the immune cell infiltration is still largely unresolved at the 12d post-LPC time point. Scale bar = 5μm.

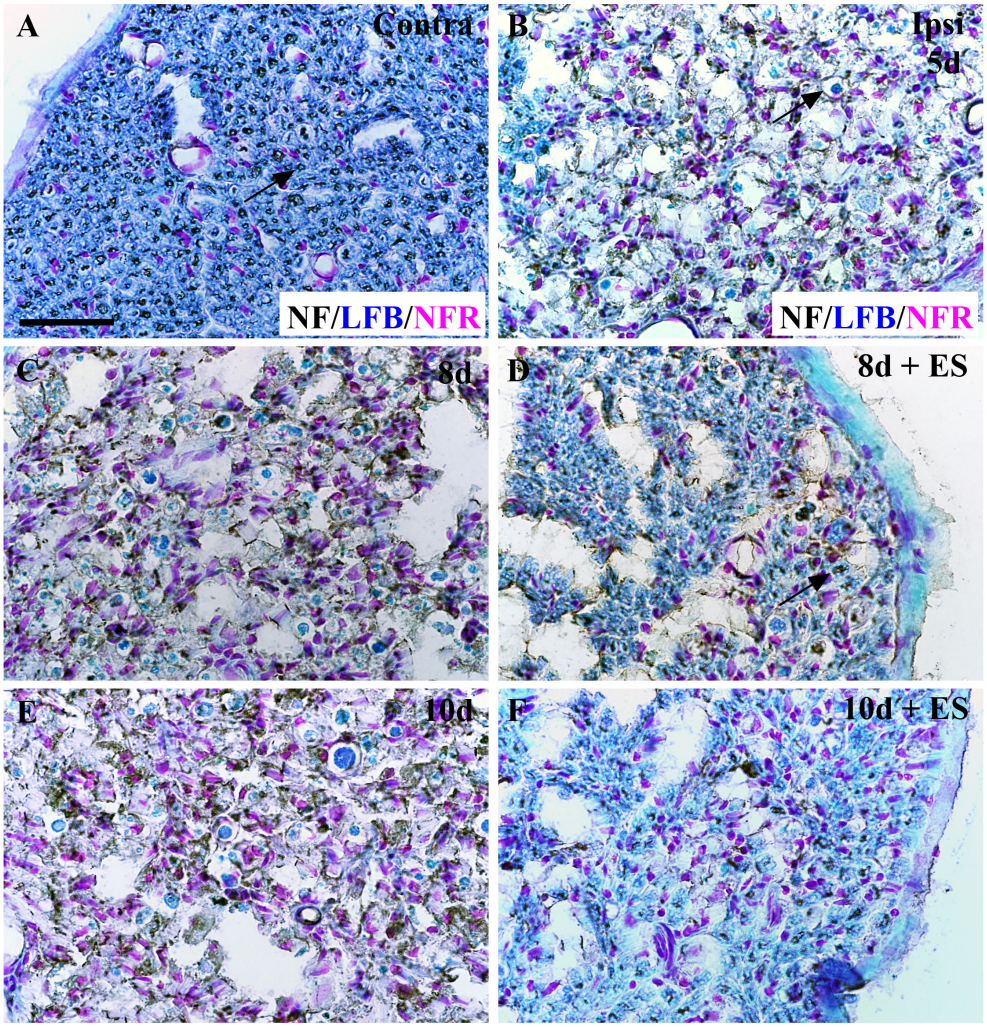

Figure 11: Increased neurofilament expression is coincident with myelin in focally demyelinated nerves subjected to ES. Representative photomicrographs from FluoroGold (FG)-positive areas of tibial nerve cross sections immunostained for neurofilament proteins (NF – brown/black) then stained for the presence of myelin (Luxol Fast Blue [LFB] - blue) and nuclei (nuclear fast red [NFR] – purple). Uninjured (*contralateral*) control tibial nerves displayed intense uniform LFB staining, indicative of abundant myelin with prominent linear NF immunostaining (A) and elongated dark blue Schwann cell nuclei. Five days post tibial nerve injection of lysophosphatidyl choline (LPC)/FG, extensive NF and myelin loss is observed coupled with numerous macrophages filled with largely unprocessed myelin debris (B). Temporal analysis of LPC-focally demyelinated nerves +/- ES as indicated in days post-LPC. Note: In the LPC+ES group increasing NF immunoreactivity was detected (D,F) with higher levels of uniform LFB staining surrounding regions of NF immunoreactivity consistent with myelinated axons, and the appearance of macrophages devoid of myelin debris apparent as early as 8d post-LPC (3d post-ES; D). The LFB staining was even stronger in the 10d (5d post-ES) animals with increased numbers of presumptive Schwann cell nuclei (F). In contrast, in the LPC only group there was just a slight increase in NF immunoreactivity beginning 10d post-LPC (E), but it was much less robust, and not associated with a ring of myelin like that observed in the stimulated as well as the contralateral control nerves. Notably in the nonstimulated nerves the immune cell infiltration is still largely unresolved at the 10d post-LPC time point. Scale bar = 20μm.

phosphorylation of the neurofilaments are important factors in determining axonal health and protecting the axon from degradation, it is prudent to examine not only their expression, but also posttranslational modifications (i.e. phosphorylation) relevant to recovery from a demyelinating insult.

In longitudinal sections of naïve control nerves, axons display robust phosphorylated neurofilament expression arranged in a distinctly linear pattern as detected by SMI-31 IF (Fig 12A). Five days following LPC injection, the amount of immunoreactivity for phosphorylated neurofilaments was dramatically reduced in the LPC-injected nerves (Fig 12B) consistent with the overall reduction in total neurofilament observed (Figs 10C; 11C). This is suggestive of both a loss of neurofilaments and/or neurofilament dephosphorylation in response to the focal demyelination. In LPC-injected nerves that underwent brief ES there is a recovery of immunoreactivity for phosphorylated neurofilaments observed at 8d post-LPC injection (3d post-ES; Fig 12E), consistent with the timing of the observed onset of increased MBP expression and the re-appearance of thinly remyelinated axonal profiles. This increase in phosphorylated neurofilament expression was not observed in the focally demyelinated nerves not subjected to ES (Fig 12D,F). The stimulated nerves continued to display increasing levels of SMI-31 immunoreactivity at both 10d and 12d post-LPC injection (5d and 7d post-ES respectively; Fig 12H,K). By the final time point examined the amount of phosphorylated neurofilament in the stimulated nerves was no longer significantly different than that observed in the contralateral (uninjured) nerves. The non-stimulated nerves only displayed a limited recovery of phosphorylated neurofilament expression beginning 10d post-LPC (Fig 12G,J). However, the intensity of the immunoreactivity remained consistently lower than that of the stimulated nerves, and at all time points examined remained significantly lower than that of the contralateral nerves (Fig 12F, I, L).

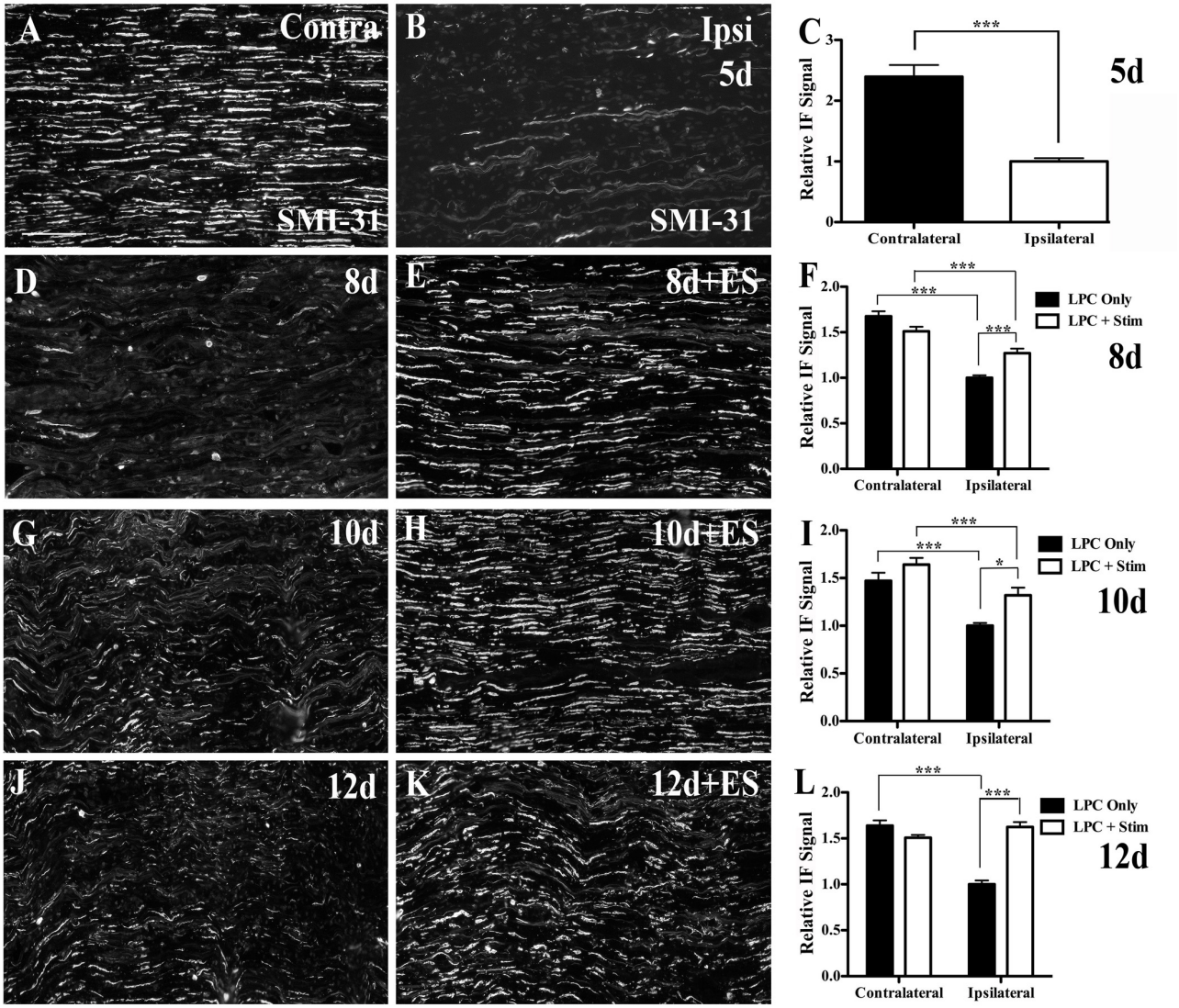

Figure 12: Increased neurofilament phosphorylation in electrically stimulated focally demyelinated nerves. Representative photomicrographs from FG-positive (i.e focally demyelinated) areas of longitudinal tibial nerve sections processed for phosphorylated neurofilament (SMI-31) IF reveal extensive loss of SMI-31 IF (B) as compared to contralateral control nerves which displayed intense SMI-31 immunoreactivity (A). Temporal analysis of LPC focal demyelination +/- ES as indicated in days post-LPC. Note: In the LPC+Stim group there was dramatically increased SMI-31 IF signal apparent as early as 8d post-LPC (3d post-ES; D), which was increasingly stronger in the 10d (5d post-ES; F) and 12d (7d post-ES; H) tissue. In contrast, in the LPC only group there was just a slight increase in SMI-31 IF signal beginning 10d post-LPC. Note: for each time point examined, all values obtained were normalized to the mean value of the Average Gray per micron^2 readings for the nerves ipsilateral to LPC treatment for the LPC only animal on that slide and for that time point. N = 4-6 animals analyzed per condition; regions quantified per condition: 45 ipsi and 59 contra (5d, LPC only); 57 ipsi and 82 contra (8d, LPC only); 83 ipsi and 72 contra (8d, LPC+Stim); 72 ipsi and 70 contra (10d, LPC only); 83 ipsi and 72 contra (10d, LPC+Stim); 75 ipsi and 82 contra (12d, LPC only); 50 ipsi and 41 contra (12d, LPC + ES). Scale bar = 100 μm.

The β-III tubulin protein is an abundantly expressed marker of the axonal cytoskeleton, and therefore is a useful marker for evaluating the co-expression of other cytoskeletal proteins, such as the neurofilaments. To confirm that the increased SMI-31 expression observed in longitudinal sections of LPC-injected sciatic nerve was indeed axonal in nature double-labeled immunohistochemistry was performed on transverse sections of nerve. Consistent with the above observations, there was prominent SMI-31 IF observed in the contralateral (uninjured) control nerves (Fig 13A), which demonstrated near perfect colocalization with the β-III tubulin IF. By 5d post-LPC injection, there was a near complete loss of the immunoreactivity for SMI-31, but without a reduction in β-III tubulin IF, indicating that the axons were still present (Fig 13B). As was observed in the longitudinal IF sections, in the stimulated nerves, both at 8d and 10d post-LPC there was an increase in SMI-31 IF, which was co-localized with the β-III tubulin IF (Fig 13D, F). The SMI-31 IF signal increased to a level of intensity that was nearly indistinguishable from the contralateral nerves by 10d post-LPC. The non-stimulated nerves remained largely devoid of SMI-31 IF at 8d post-LPC (Fig 13C), but showed a modest increase at 10d post-LPC, similar to what had been observed in the longitudinal sections (Fig 13E, G).

To confirm the immunohistochemical and histological observations, Western blot analysis was performed. The levels of total neurofilament (NF) and phosphorylated neurofilament (SMI-31) expression at 5d, 8d and 10d post-LPC with or without ES were compared to naïve and contralateral control nerves (Fig 14). Consistent with the histochemical observations, by 5d post-LPC, there was a dramatic decrease in the level of both total and phosphorylated neurofilament that could be detected. In protein extracts from stimulated nerves obtained 8 and 10 days post-LPC (3d and 5d post-ES) there was a steady and consistent increase in the amount of both total neurofilament and phosphorylated neurofilament protein that could be detected (Fig 14). These findings suggest that not only does brief ES promote the re-expression of axonal neurofilament proteins in previously demyelinated nerves, but that these proteins are in the phosphorylated state that is critical to maintaining axonal integrity and health.

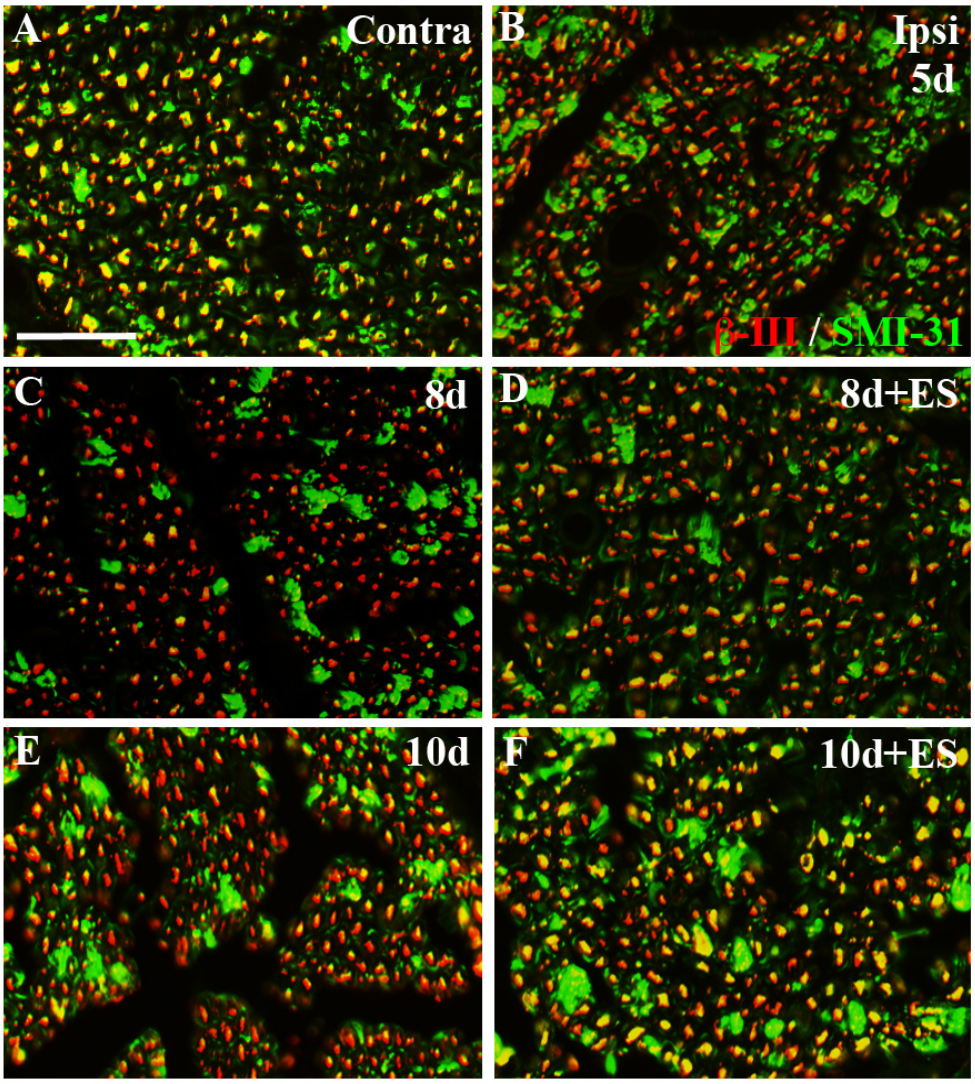

Figure 13: Increased neurofilament phosphorylation in axons of electrically stimulated focally demyelinated nerves. Representative photomicrographs from FG-positive (i.e focally demyelinated) areas of transverse tibial nerve sections dually processed for the axonal marker β-III tubulin (β-III) and phosphorylated neurofilament (SMI-31) IF reveal extensive loss of the colocalization of the two axonal markers and decreased packing density of the fascicles, indicative of inflammation/edema (B) as compared to contralateral control nerves which displayed intense near perfect colocalization (A), as well as tight packing of the fascicles. Temporal analysis of LPC focal demyelination +/- ES as indicated in days post-LPC. Note: The round structures displaying bright SMI-31 IF without any detectable β-III IF likely represent macrophages, which have taken up debris associated with the demyelinating insult. In the LPC+ES group there was dramatically increased β-III/SMI-31 IF signal colocalization apparent as early as 8d post-LPC (3d post-ES; D), which was increasingly stronger in the 10d (5d post-ES; F) tissue at which time it approximates that found in the contralateral (uninjured) nerves. In contrast, in the LPC only group there was a slight increase in colocalization of the β-III/SMI-31 IF signals beginning 10d post-LPC, however, it consistently remained less than that observed in the stimulated nerves. Scale bar = 20 μm.

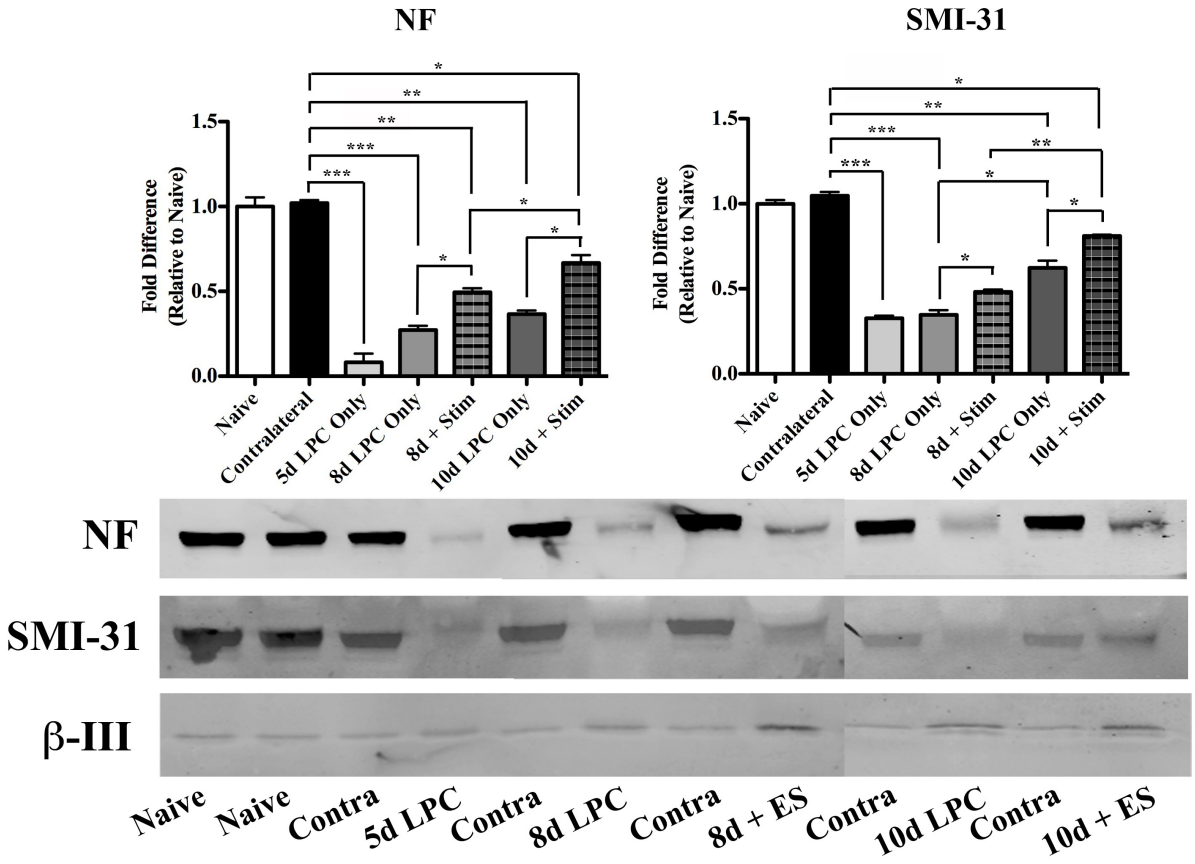

Figure 14: 1hr brief electrical stimulation (ES) results in increased expression of total and phosphorylated neurofilament proteins. Representative Western blot of tibial nerve demyelination zone protein extract and probed for total (NF) and phosphorylated neurofilaments (SMI-31). Immunoblots were run in duplicate from pooled nerve samples from 3 animals per experimental condition. Densitometry readings were normalized to the loading control β-III tubulin within each lane and compared to the mean densitometry reading of the two lanes of naïve sciatic nerve protein extract run alongside the demyelinated nerve extracts in each gel. Naïve and contralateral control nerves displayed intense NF and SMI-31 immunoreactivity. There was a marked decrease in both NF and SMI-31 band intensity observed 5d post-lysophosphatidyl choline (LPC)/FG injection into the tibial branch of the sciatic nerve. ES resulted in an increase in the amount of detectable NF and SMI-31 proteins 3 and 5 days post-ES (8 and 10 days post-LPC), consistent with the immunohistochemical observations and quantification (see Fig 3). In focally demyelinated nerves that did not undergo ES the levels of NF and SMI-31 remained low. Asterisks indicate significant differences between experimental groups; *P<0.05, **P<0.01, ***P<0.001, Student's t-test.

Taken together, the above results suggest that brief ES promotes not only the re-appearance of the neurofilament proteins, but also promotes a more rapid return to an axon-protective phosphorylated state amenable to remyelination. The return to this favorable state occurs at a time point that is coincident with the onset of the remyelination observed in the

stimulated nerves. Injection of LPC into nervous tissue evokes a strong inflammatory response, with prominent infiltration of the demyelinated zone by immune cells such as macrophages. The histological findings presented in Figures 10 and 11, namely the changes in the numbers of macrophages present in the stimulated nerves, have also indicated that the stimulation procedure may be impinging upon aspects of this inflammatory response. This is explored in detail in the next section.

3.3 EFFECT OF DELAYED NERVE STIMULATION ON IMMUNE CELL DYNAMICS AND PHENOTYPIC PROPERTIES IN FOCALLY DEMYELINATED PERIPHERAL NERVE

As outlined in the previous two sections of this chapter, the application of delayed brief ES has a remarkable impact on a number of parameters associated with recovery from a focal demyelinating insult. An important factor to consider when examining repair of any form of injury is the dynamics of the accompanying inflammatory response. There is a complex and intimate interaction between Schwann cells and macrophages during all stages of peripheral nerve demyelination and remyelination: the demyelination of the axons, the removal of the myelin debris, and the termination of the inflammatory response (Martini et al. 2008). The different stages of the induction and resolution of inflammatory demyelination and remyelination are also closely linked to macrophage plasticity, as their different functional phenotypes play important roles in these processes (Miron et al. 2013; Miron and Franklin 2014). In this section, I examine the influence of brief electrical stimulation on the inflammatory response induced by injection of LPC into the tibial nerve and correlate this with remyelination efficiency.

3.3.1 ES leads to enhanced macrophage clearance in demyelinated nerves

Injection of LPC into the tibial branch of the sciatic nerve induces an inflammatory demyelination. By 5d post-LPC injection, numerous macrophages were observed to have infiltrated the injected tibial nerve, demonstrated by intense immunostaining for the macrophage surface marker ED-1 (Fig 15B). The ED-1-positive non-neuronal cells were large, oval shaped cells with a “foamy” appearance, suggestive of active phagocytosis. In contrast, the contralateral

(non-injected) sciatic nerve had very few detectable ED-1 immunopositive cells (Fig 15A). At 6d post-LPC (one day post-ES) the stimulated and non-stimulated nerves were indistinguishable from each other. Longitudinal sections of nerves from both groups contained numerous ED-1 positive macrophages distributed throughout (Fig 15D, E, F). At 8d post-LPC injection (3d post-ES), early differences in the levels of ED-1 IF detected in ES and non-stimulated nerves began to emerge. Though visually there appeared to be an almost equal number of cells still present in both the stimulated and non-stimulated nerves, the intensity of the immunostaining of the ED-1 positive cells in the stimulated nerves was reduced (Fig 15G, H, I). By 10d post-LPC injection (5d post-ES) the differences between the stimulated and non-stimulated nerves were not only statistically significant, but were also visually apparent. While numerous macrophages were still detected in LPC-only injected nerves (Fig 15J), the LPC+ES nerves had significantly fewer (Fig 15K, L). The differences between the two groups were even more apparent and significant at 12d post-LPC (7d post-ES; Fig 15M, N, O). Further, beginning at the 10d post-LPC time point, there was a shift in the distribution of the activated macrophages within the lesion site from a general scattered one in the non-stimulated nerves, to one localized mainly to the periphery in response to ES, suggestive of immune cell clearance from the endoneurium to the epineurial connective tissue (Kuhlmann et al. 2001; Martini et al. 2008). This supports that the application of brief ES may enhance clearance of immune cells from the demyelination zone.

Qualitative examination of transverse (cross) sections of LPC-injected tibial branches of sciatic was also conducted to verify whether there was an ES enhanced clearance of macrophages toward the periphery of the focally demyelinated nerve. Qualitative assessment was only conducted on nerve sections with Fluorogold present throughout the entire nerve. The results confirmed an enhanced clearance of macrophages from stimulated nerves. As in the longitudinal sections examined, very few ED-1 immunopositive cells were present in contralateral (uninjured) nerve sections (Fig 16A). At 5d post-LPC injection numerous macrophages had infiltrated the zone of demyelination, and were distributed throughout the

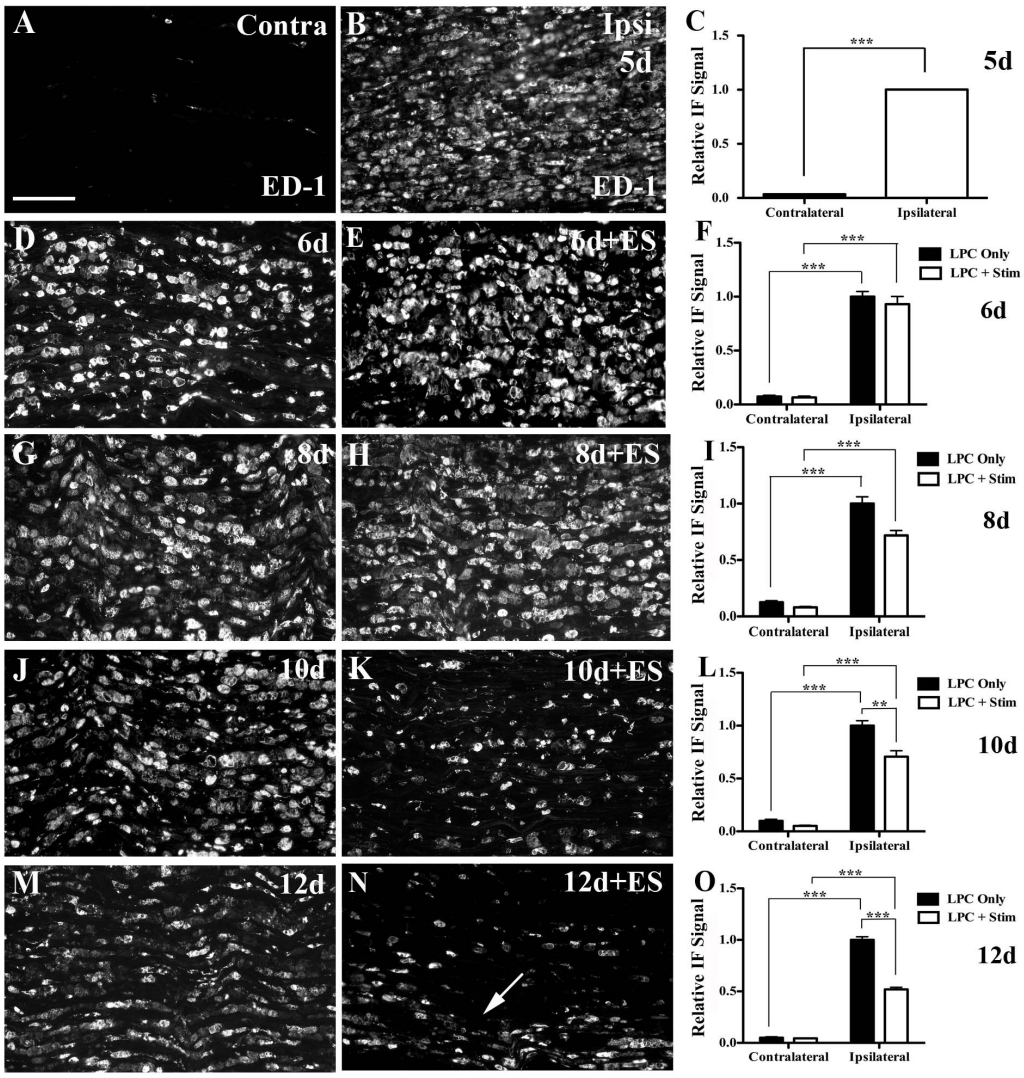

Figure 15: Decrease in number of activated macrophages in focally demyelinated nerve subjected to 1hr ES. Representative photomicrographs from FG-positive (i.e. focally demyelinated) areas of longitudinal tibial nerve sections processed for ED-1 IF to detect activated macrophages. There was marked macrophage infiltration into the demyelination zone 5d post- lysophosphatidyl choline (LPC)/FG injection (B), while contralateral control nerves displayed only minimal ED-1 IF (A). Temporal analysis of LPC focal demyelination +/- ES delivered at 5 d post-LPC as indicated in days post-LPC: 6d (D), 6d+ES (E), 8d (G), 8d+ES (H), 10d (J), 10d+ES (K), 12d (M) or 12d+ES (N) post-LPC. Note: ES results in a significant decrease in the ED-1 IF 10d post-LPC (5d post-ES; K) and 12d post-LPC (7d post-ES; N) relative to LPC only in a pattern suggestive of movement toward lateral edges and egress (arrow). Summary bar graphs of relative changes in IF signal for ED-1 in the zone of demyelination (C, F, I, L, O). Note: for each time point examined, all values were normalized to the mean value of the Average Gray per micron^2 readings for the nerves ipsilateral to LPC treatment for the LPC Only animal on that slide and for that time point. N = 4-6 animals analyzed per condition; regions quantified per condition: 35 ipsi and 36 contra (5d, LPC only); 89 ipsi and 69 contra (6d, LPC only); 52 ipsi and 53 contra (6d, LPC+Stim); 74 ipsi and 50 contra (8d, LPC only); 66 ipsi and 70 contra (8d, LPC+Stim); 79 ipsi and 64 contra (10d, LPC only); 87 ipsi and 61 contra (10d, LPC+Stim); 122 ipsi and 52 contra (12d, LPC only); 98 ipsi and 71 contra (12d, LPC+Stim). Asterisks indicate significant differences between experimental groups; *P<0.05, ***P<0.001. Scale bar = 100 μm.

nerve (Fig 16B). At 8d post-LPC (3d post-ES) stimulated nerves contained fewer total ED-1 positive macrophages than their non-stimulated counterparts (Fig 16C, D). The macrophages present in the stimulated nerves were also beginning to assume a different distribution, and appear to be localizing towards one side of the nerve. This shift in cell localization was even more evident at 10d post-LPC (5d post-ES). At this time point there was both an obvious reduction in the number of ED-1 immunopositive cells present within the stimulated nerve and a clear localization of the macrophages towards the periphery of the nerve (Fig 16F). At 10d post-LPC, the non-stimulated nerves also began to show a decrease in the number of ED-1 immunopositive cells present, however this decrease was similar to what was observed in the stimulated nerves at the 8d post-LPC time point (Fig 16D). These results are consistent with the reduction in ED-1 IF signal quantified in the longitudinal nerve sections being a product of a reduction in the number of macrophages present within the zone of demyelination.

In control experiments, nerves from naïve animals were virtually indistinguishable from the contralateral (uninjured) nerves from LPC-injected animals with only a few ED-1 positive cells detected. To examine whether ES alone recruited significant numbers of macrophages, naïve nerves were subjected to the one-hour ES procedure. These nerves displayed a very small rise in ED-1 immunoreactivity seven days post-ES. However, rather than the robust and widespread infiltration of activated macrophages observed following LPC injection, the ED-1 positive cells were restricted to the site of electrode contact and therefore likely due to the process of surgical exposure and contact of the electrode on the nerve (Fig 17A,B). LPC-injected nerves were also subjected to sham stimulation (electrodes placed but stimulator not activated) at 5d post-LPC and then examined at 12d post-LPC. Examination of the sham-stimulated nerves revealed that these nerves displayed similar numbers of activated macrophages to the 12d post-LPC injection only nerves (Fig 17C). Finally, the observed enhanced clearance of macrophages from the site of demyelination appears to be dependent on neuronal activity as application of lidocaine prior to, and during the stimulation procedure abrogated the effects of

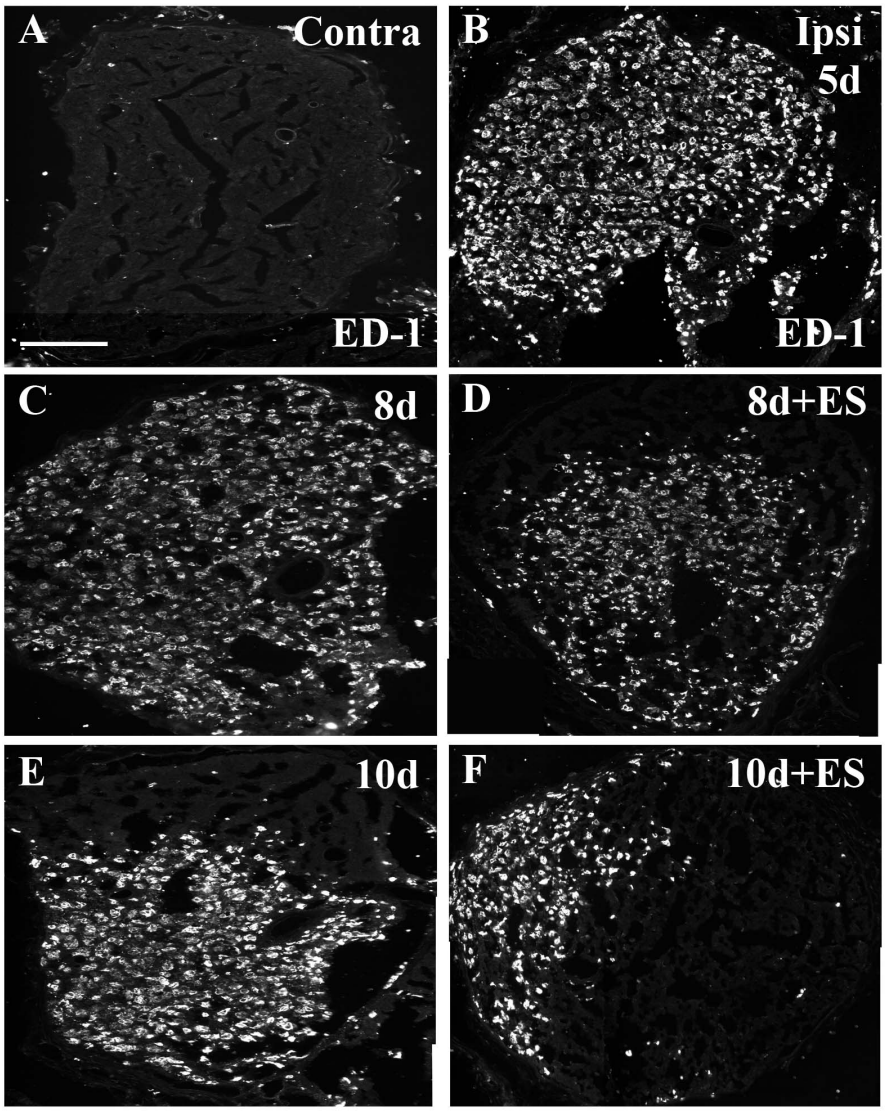

Figure 16: Enhanced clearance of macrophages in focally demyelinated nerve subjected to 1hr ES. Representative photomicrographs from FluoroGold (FG)-positive areas of tibial nerve transverse (cross) sections immunostained for ED-1 IF. Uninjured (*contralateral*) control tibial nerves displayed minimal ED-1 immunoreactivity (A) and elongated dark blue Schwann cell nuclei. Five days post tibial nerve injection of lysophosphatidyl choline (LPC)/FG, extensive infiltration by macrophages is observed throughout the entire nerve (B). Temporal analysis of LPC-focally demyelinated nerves +/- ES as indicated in days post-LPC. Note: In the LPC+ES group there was decreasing ED-1 immunoreactivity detected apparent as early as 8d post-LPC (3d post-ES; D) with a clear reduction in the number of macrophages present by 10d post-LPC (5d post-ES, F). This was also accompanied by a clear shift in distribution, with the majority of the remaining macrophages localizing to the periphery of the nerve. In contrast, in the LPC only group there was still just a slight decrease in ED-1 immunoreactivity beginning 10d post-LPC (C, E). Notably in the non-stimulated nerves the immune cells still largely remain distributed throughout the entire nerve. Scale bar = 100μm.

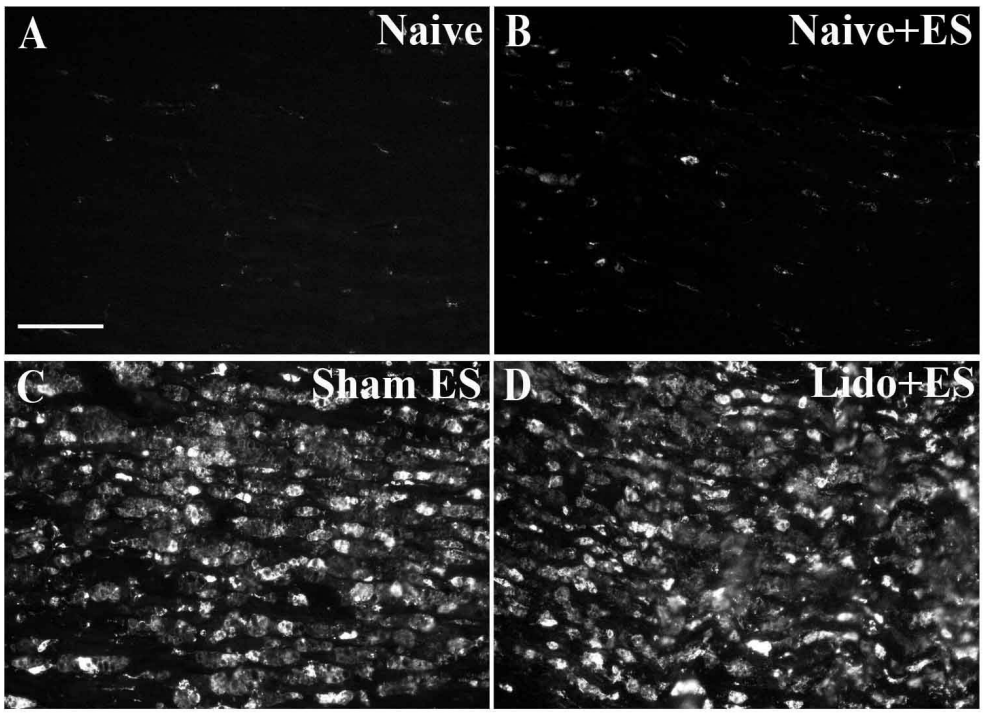

Figure 17: Increased neuronal activity is required to effect reductions in activated macrophage (ED1) immunoreactivity in focally demyelinated regions. Representative immunofluorescence photomicrographs of tibial nerve sections immunostained for ED1. Naïve (uninjured) nerves displayed minimal ED1 immunoreactivity (A). Electrical stimulation (ES; delivered 5d post-LPC) alone did not trigger an inflammatory response nor an infiltration of activated macrophages into the stimulation site (B). Sham stimulation and blockade of action potential conduction through local application of lidocaine did not result in an increase in macrophage clearance from the lesion site at 12d post-LPC (C, D). This indicates that the enhanced clearance of macrophages from the demyelinated lesions of animals receiving electrical stimulation (ES) is related to the activity induced by the ES procedure. Scale bar = 100 μm.

the stimulation (Fig 17D) in agreement with the effects reported on myelination and neurofilament expression.

The ED-1 immunofluorescence findings were confirmed by Western blot analysis (Fig 18). The observed infiltration of numerous activated macrophages into the zone of demyelination correlated with a significant increase in the amount of the ~100 kDa ED-1 protein detected via Western blotting for LPC-injected sciatic nerves as compared to both naïve and contralateral (uninjured) sciatic nerves (Fig 18). The ED-1 protein as measured by Western blotting decreased in the stimulated nerves at 8d post-LPC (3d post-ES), the same time point as the observed decrease in the IF signal, and was further decreased at the 10d post-LPC (5d post-

ES) time point. In those nerves that did not receive the one-hour ES procedure there were continually elevated levels of ED-1 protein detected via Western blot. While there was a measurable reduction in detectable ED-1 from the 5d post-LPC baseline at the 8d and 10d time points in the non-stimulated nerves, at all times examined post 5d, the levels remained significantly higher than that of both the contralateral (uninjured) and the ES-treated nerves (Fig 18).

3.3.2 Impact Of ES On Immune Cell Phenotype

The macrophage is a highly plastic cell, capable of adapting its phenotype according to the local microenvironment in order to perform their various functions (Gratchev et al. 2006; Stout et al. 2005; Stout and Suttles 2004). It is important to consider not only whether there are macrophages present at the site of demyelination, but also their functional phenotype. In experimental models of CNS demyelination an overabundance of M1 (pro-inflammatory) macrophages has been associated with increased severity of symptoms (Okuda et al. 1995), while increasing the population of M2 (pro-repair) macrophages promotes oligodendrocyte proliferation and improves remyelination (Mikita et al. 2011). As the ES procedure has a remarkable effect of promoting remyelination, a prudent question to address is the impact of the stimulation procedure on the macrophage polarization state. Thus, in order to assess whether the infiltrated macrophages were polarized toward a pro-inflammatory (M1) or pro-repair phenotype, the macrophages were dually immunostained for ED-1 to identify the activated macrophages and individual markers of the two polarization states.

3.3.2.1 ES reduces expression of markers associated with M1 (pro-inflammatory) phenotype

LPC, when injected into the tibial branch of the sciatic nerve produces an inflammatory focal demyelination (Hall 1973; Hall and Gregson 1971), with a prominent infiltration of

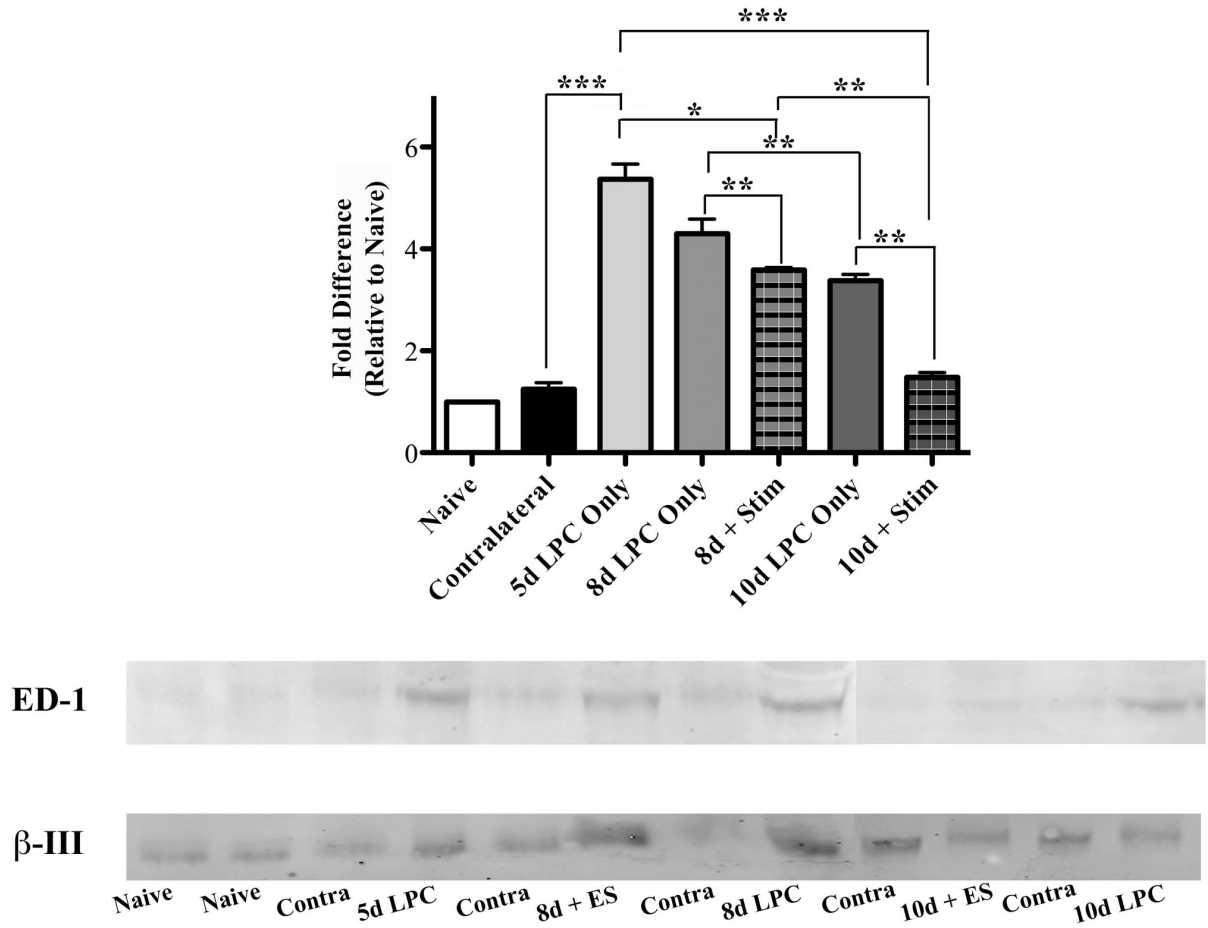

Figure 18: 1hr electrical stimulation (ES) 5 days post-lysophosphatidyl choline (LPC) results in decreased ED-1 content beginning 8d post-LPC. Representative Western blots of sciatic nerve extract probed for ED-1. Immunoblots were run in duplicate from pooled nerve samples from 3 animals/experimental condition. Densitometry readings were normalized to the loading control β-III tubulin within each lane and compared to the mean densitometry reading of the two lanes of naïve sciatic nerve protein extract run alongside the demyelinated nerve extracts in each gel. There was a marked increase in detectable ED-1 observed 5d post-lysophosphatidyl choline (LPC) injection into the tibial branch of the sciatic nerve, as compared to that observed in protein extract from both naïve and contralateral (uninjured) nerves. As early as three days post-ES (8d post-LPC), there was a decrease in the amount of detectable ED-1 in the stimulated nerves. This drop preceded the visual differences observed immunohistochemically (Fig 4J, K). Levels of detectable ED-1 showed further decline 5d post-ES (10d post-LPC), where they reached levels not significantly different than that of the naïve or contralateral (uninjured) controls. Asterisks indicate significant differences between experimental groups; *P<0.05, **P<0.01, ***P<0.001, Student's t-test.

activated macrophages into the demyelination zone (Fig 15A, Fig 19A, Fig 20A). The large cells have a foamy appearance, consistent with active phagocytosis, and express high levels of the ED-1 surface marker which serves to identify those cells of the mononuclear phagocyte system

(Damoiseaux et al. 1994). Manual counting of these double-labeled immunostained cells in the zone of demyelination indicated that a large number of the cells (55.6%) also express the inducible form of nitric oxide synthase (iNOS; Fig 19B, C) associated with a polarization of the macrophage towards the M1 pro-inflammatory phenotype. Application of a single 1hr episode of brief electrical stimulation (ES) resulted in a significant reduction in the proportion of ED-1 positive macrophages that also expressed iNOS. This was evident at 8d post-LPC (3d post-ES) as well as at 10d post-LPC (5d post-ES) compared to their non-stimulated counterparts. At 8d-post-LPC, 38.4% of the ED-1 positive macrophages also expressed iNOS in the stimulated nerves, compared to 56.2% of the ED-1 positive macrophages from non-stimulated nerves. Similarly, by 10d post-LPC 37.8% of the ED-1 cells were iNOS-positive positive in ES-treated nerves compared to 55.6% in the non-stimulated nerves (Fig. 19P). This indicates that the application of ES results in a reduction of markers associated with the pro-inflammatory state.

Another hallmark of polarization towards the M1 phenotype is the expression and secretion of the inflammatory cytokine tumor necrosis factor alpha (TNF-α). At 5d post-LPC a large proportion of the population of infiltrated macrophages are dually immunopositive for ED-1 and TNF-α (57.7%, Fig 20B, C, P). Similar to the reduction in the number if iNOS-expressing cells in the demyelination zone observed following ES, there was also a reduction in the number of macrophages also expressing TNF-α following ES (Fig 20E, F vs H, I and Fig 20K, L vs N, O). In ES-treated nerves, at 8d post-LPC (3d post-ES) 39.3% of ED-1 positive cells were immunopositive TNF-α, compared to 54.6% of macrophages in non-stimulated nerves (Fig 20P). This trend continued at 10d post-LPC (5d post-ES) with 35.2% of macrophages examined TNF-α immunopositive in the stimulated nerves as compared to 56.4% of macrophages in the non-stimulated nerves (Fig 20P). Thus, when taken together with the ED-1/iNOS co-localization data it supports that ES drives an overall reduction in M1 phenotype-associated proteins, suggesting that the polarity of the macrophages within the stimulated nerves shifts away from the pro-inflammatory state. This shift is coincidental with the reported reduction in ED-1 expression and onset of remyelination following LPC-mediated focal demyelination.

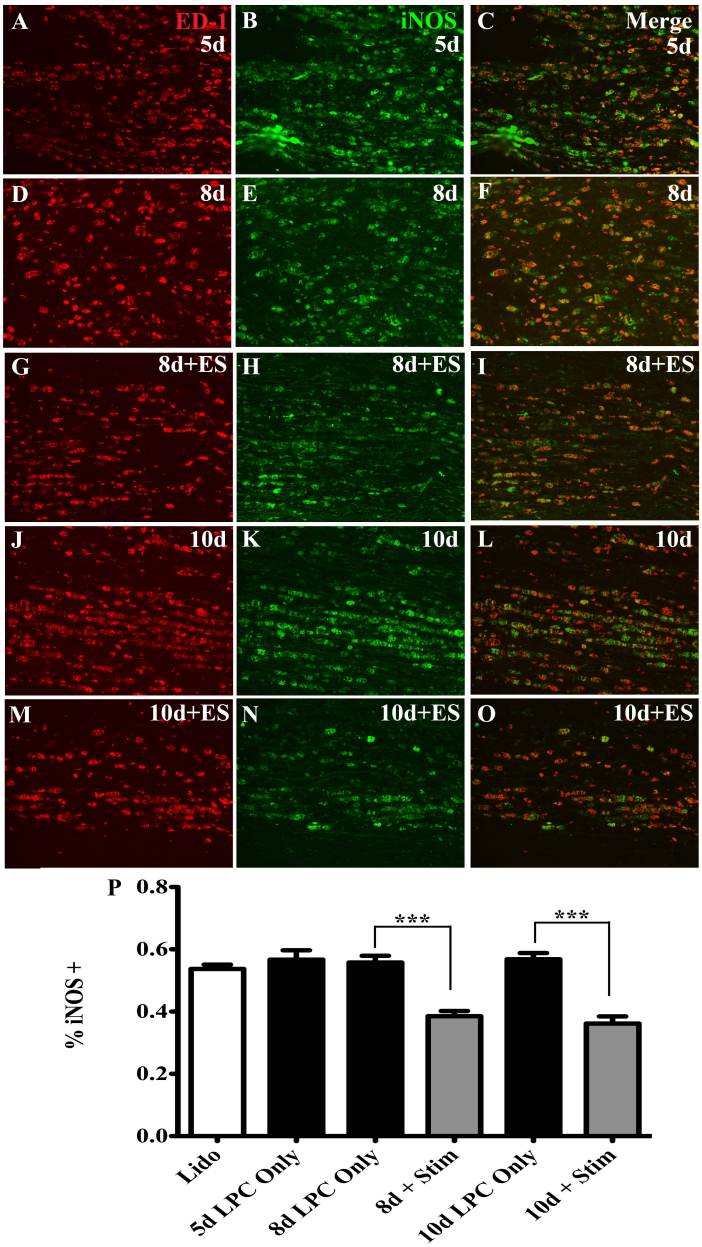

Figure 19: Diminished numbers of iNOS-expressing macrophages in focally demyelinated nerves subjected to 1hr ES. Representative photomicrographs of focally demyelinated regions of tibial nerve sections doubly immunolabeled for ED-1 (red) and iNOS (green) to detect activated macrophages. There was a prominent infiltration of ED-1 positive activated macrophages into the zone of demyelination 5d post-lysophosphatidyl choline (LPC)/FG injection (A), the majority of which (55.6%, P) were also immunopositive for iNOS (B, C). Temporal analysis of LPC focal demyelination +/- ES delivered at 5d post-LPC as indicated in days post-LPC: 8d (D, E, F), 8d+ES (G, H, I), 10d (J, K, L), 10d+ES (M, N, O). Note: ES results in a significant reduction in the number of doubly ED-1/iNOS positive macrophages 8d post-LPC (3d post-ES; H, I) relative to LPC only (E, F) (38.4% vs 56.2%, P) as well as at 10d post-LPC (5d post-ES; N, O) relative to LPC only (K, L) (37.8% vs 55.6%, P). Note: for each time point examined the number of strongly immunopositive cells were counted from ten fields of view. N=3 animals analyzed per condition, with a total number of 846-1824 cells counted. Asterisks indicate significant differences between experimental groups; ***P<0.001. Scale bar = 100 μm.

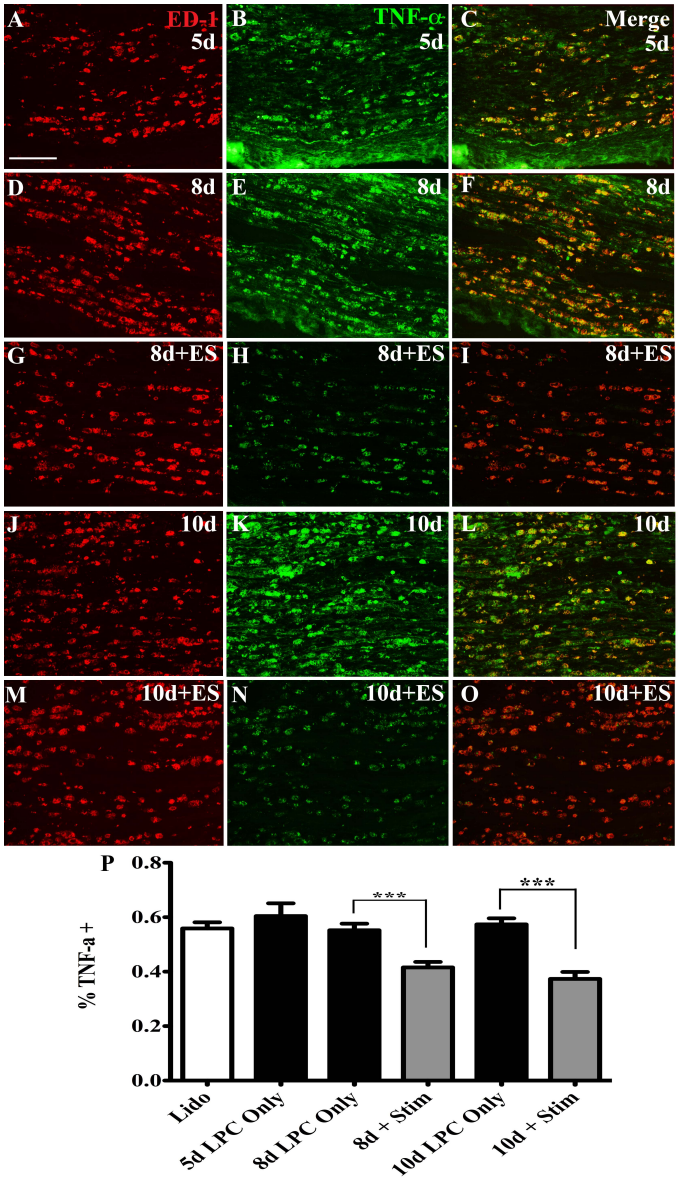

Figure 20: Diminished numbers of TNF-α-expressing macrophages in focally demyelinated nerves subjected to 1hr ES. Representative photomicrographs of focally demyelinated regions of tibial nerve sections doubly immunolabeled for ED-1 (red) and TNF-α (green) to detect activated macrophages. There was a prominent infiltration of ED-1 positive activated macrophages into the zone of demyelination 5d post-lysophosphatidyl choline (LPC)/FG injection (A), the majority of which (57.7%, P) were also immunopositive for TNF-α (B, C). Temporal analysis of LPC focal demyelination +/- ES delivered at 5d post-LPC as indicated in days post-LPC: 8d (D, E, F), 8d+ES (G, H, I), 10d (J, K, L), 10d+ES (M, N, O). Note: ES results in a significant reduction in the number of doubly ED-1/TNF-α positive macrophages 8d post-LPC (3d post-ES; H, I) relative to LPC only (E, F) (39.3% vs 54.6%, P) as well as at 10d post-LPC (5d post-ES; N, O) relative to LPC only (K, L) (35.2% vs 56.4%, P). Note: for each time point examined the number of strongly immunopositive cells were counted from ten fields of view. N=3 animals analyzed per condition, with a total number of 820-1964 cells counted. Asterisks indicate significant differences between experimental groups; ***P<0.001. Scale bar = 100 μm

The observed visual decrease and manual count of the number of macrophages bearing markers associated with an M1 (pro-inflammatory) phenotype was confirmed by Western blot analysis of the LPC-injected nerves. A significant increase in the amount of the ~130 kDa iNOS and ~50 kDa TNF-α proteins detected via Western blotting 5d post-LPC injection was observed (Fig 21). The elevation in both iNOS and TNF-α protein in non-stimulated LPC-injected nerves was sustained at the 8 and 10d post-LPC timepoints examined, consistent with the manual counts of dually-labeled ED-1 and iNOS or TNF-α macrophages present within the demyelination zone (Fig 19 & 20 vs Fig 21). Likewise, in the stimulated nerves there was a significant reduction in the amount of iNOS and TNF-α proteins detected in isolates from both the 8d and 10d post-LPC (3d and 5d post-ES) time points. This decrease in detectable protein was consistent with the observed decrease in the numbers of dually labeled ED-1 and iNOS or TNF-α macrophages present in the regions of focal demyelination.

3.3.2.2 ES increases expression of markers associated with M2 (pro-repair) phenotype

By 5d post-LPC injection there was an abundance of ED-1 positive macrophages (Fig 22A) within the demyelination zone. While the majority of these cells expressed markers associated with polarization to an M1 pro-inflammatory state (e.g. iNOS and TNF-α), a minority (27.1%) expressed Arginase-1 (Arg1) (Fig 22B, C); a marker associated with the M2 pro-repair polarization state. By 8d post-LPC (3d post-ES) injection stimulated nerves contained a higher proportion of macrophages dually-immunolabeled for ED-1and Arg1 (52.6%), compared to non-stimulated nerves (29.7%) (Fig 22E, F vs H, I) with the latter containing a similar proportion of Arg-1 expressing macrophages as that observed at the baseline 5d post-LPC time point (Fig 22P). A similar trend continued at 10d post-LPC (5d post-ES), with the majority (53.4%) of macrophages within the demyelination zone of stimulated nerves immunopositive for Arg1 and only a minority of macrophages in non-stimulated nerves (36.2%) (Fig 22K, L vs. N, O).

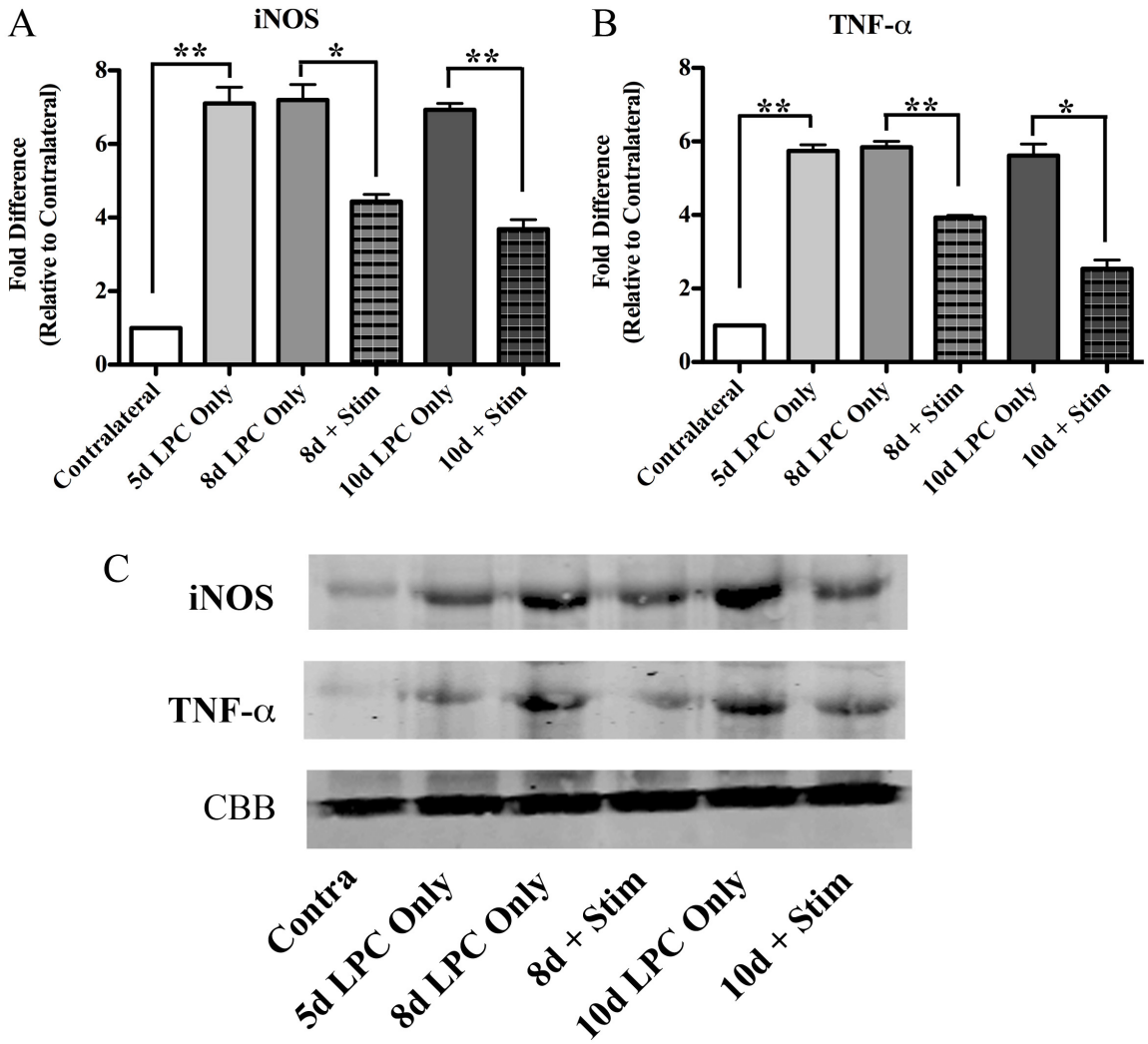

Figure 21: 1hr electrical stimulation (ES) 5 days post-lysophosphatidyl choline (LPC) results in decreased M1-associated protein content beginning 8d post-LPC. Representative Western blots of sciatic nerve extract probed for the M1 (pro-inflammatory) macrophage markers iNOS and TNF-α. Immunoblots were run in duplicate from pooled nerve samples from 3 animals/experimental condition. Densitometry readings were normalized to one band of protein stained by Coomassie Brilliant Blue within each lane and compared to the mean densitometry reading of the contralateral (uninjured) sciatic nerve protein extract run alongside the demyelinated nerve extracts in each gel. There was a marked increase in detectable iNOS and TNF-α observed 5d post-lysophosphatidyl choline (LPC) injection into the tibial branch of the sciatic nerve, as compared to that observed in protein extract from contralateral (uninjured) nerves. As early as three days post-ES (8d post-LPC), there was a decrease in the amount of detectable iNOS (A, C) and TNF-α (B, C) in the stimulated nerves. This drop in detectable protein content correlates the visual differences observed immunohistochemically, and quantified via manual counting of immunopositive cells (Fig 17, Fig 18). Levels of detectable iNOS and TNF-α showed a further, but not statistically significant decline 5d post-ES (10d post-LPC), and never reached levels not significantly different than that of the contralateral (uninjured) controls, and for all experimental conditions remained significantly different than the contralateral nerves. Asterisks indicate significant differences between experimental groups; *P<0.05, **P<0.01, Student's t-test.

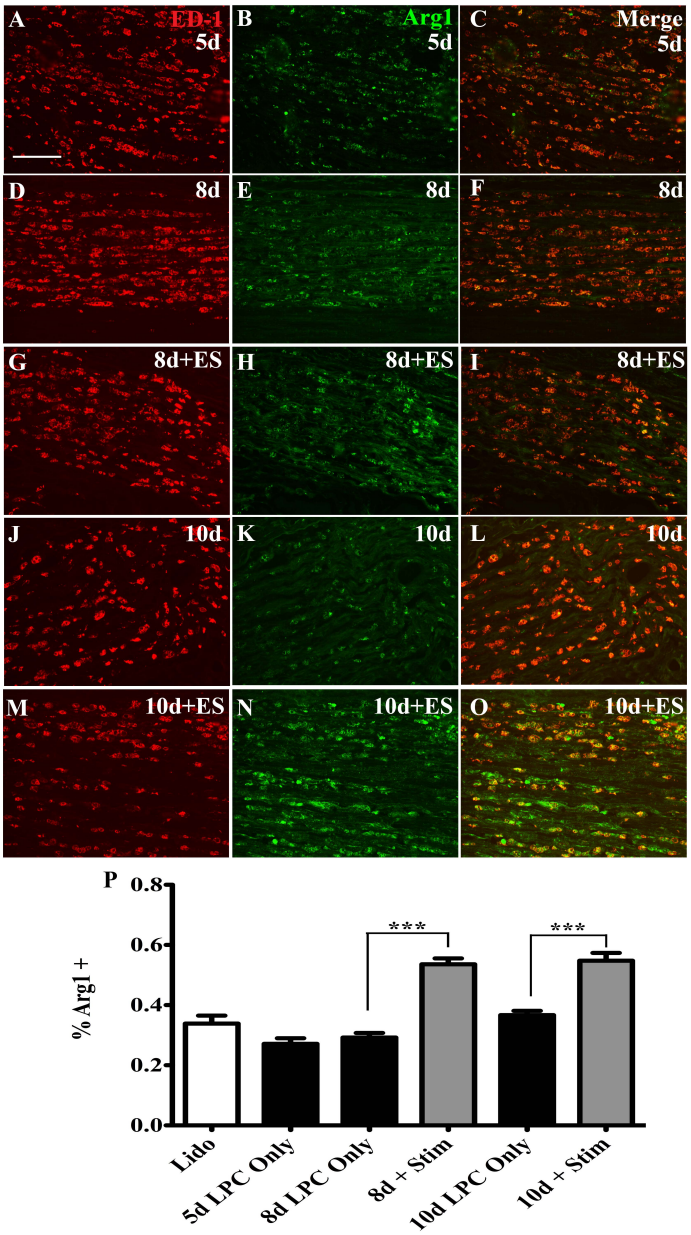

Figure 22: Increased numbers of Arg1-expressing macrophages in focally demyelinated nerves subjected to 1hr ES. Representative photomicrographs of focally demyelinated regions of tibial nerve sections doubly immunolabeled for ED-1 (red) and Arg1 (green) to detect activated macrophages. There was a prominent infiltration of ED-1 positive activated macrophages into the zone of demyelination 5d post-lysophosphatidyl choline (LPC)/FG injection (A), a minority of which (27.1%, P) were also immunopositive for Arg1 (B, C). Temporal analysis of LPC focal demyelination +/- ES delivered at 5d post-LPC as indicated in days post-LPC: 8d (D, E, F), 8d+ES (G, H, I), 10d (J, K, L), 10d+ES (M, N, O). Note: ES results in a significant increase in the number of doubly ED-1/Arg1 positive macrophages 8d post-LPC (3d post-ES; H, I) relative to LPC only (E, F) (52.6% vs 29.7%, P) as well as at 10d post-LPC (5d post-ES; N, O) relative to LPC only (K, L) (53.4% vs 36.2%, P). Note: for each time point examined the number of strongly immunopositive cells were counted from ten fields of view. N=3 animals analyzed per condition, with a total number of 877-1359 cells counted. Asterisks indicate significant differences between experimental groups; ***P<0.001. Scale bar = 100 μm.

A second marker associated with the polarization of macrophages towards the M2 (pro-repair) state was also examined, namely, the expression of the mannose receptor (CD206) (Stein et al. 1992). In a similar pattern to the expression of Arg1, there a minority of cells (31.3%) co-expressed ED-1 and CD206 at 5d post-LPC (Fig 23B, C). ES resulted in an increased incidence of macrophages co-expressing ED-1 and CD206 at both 8d and 10d post-LPC (3d and 5d post-ES respectively) (Fig 23H, I and N, O), similar to the increased presence of ED-1/Arg1 positive macrophages observed in the demyelination zone following a single episode of ES. The majority of macrophages at these time points were dually positive for these markers (54.2% and 62.2% respectively). Those nerves that were not stimulated had only a small proportion of ED-1 immunopositive cells dually labeled for CD206, and this incidence was similar to that observed at the initial time point of 5d post-LPC (31.9% at 8d and 31.2% at 10d vs 31.3% at 5d post-LPC; Fig 23P). Notably, the patterns of expression of the chosen M2 phenotypic markers (Arg1, CD206) were the inverse variation of the two M1 polarization markers examined (iNOS, TNF-α).

These observed changes in the incidence of macrophages expressing pro-repair M2 phenotypic markers were supported by similar trends in the levels of these markers detected by Western blot analysis of isolates obtained from the zones of demyelination under the different experimental conditions. The infiltration of activated macrophages (defined as ED-1 immunopositive) that also expressed the M2-associated proteins Arg1 and CD206 resulted in increased amounts of the ~160 kDa CD206 and ~37 kDa Arg1 proteins detected via Western blotting 5d post-LPC injection (Fig 24). There was a sustained elevation above that found in contralateral (uninjured) nerves of both CD206 and Arg1 content in non-stimulated nerves that did not change significantly at all time points examined, consistent with the trends observed when determining the incidence of CD206 or Arg1 expression in ED-1 positive macrophages within demyelination zones (Fig 22 & 23 vs Fig 24). Similarly, in the stimulated nerves there was a significant increase in the amount of CD206 and Arg1 proteins detected at both the 8d and 10d post-LPC (3d and 5d post-ES) time points examined by Western blot (Fig 24). These

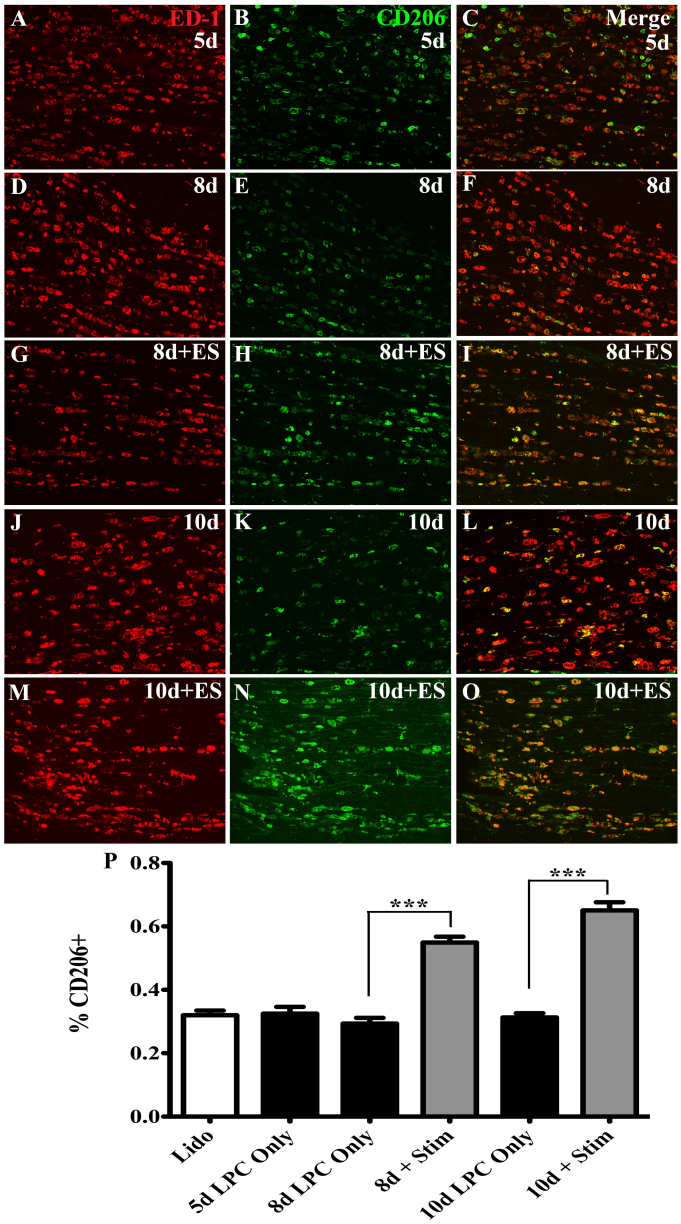

Figure 23: Increased numbers of CD206-expressing macrophages in focally demyelinated nerves subjected to 1hr ES. Representative photomicrographs of focally demyelinated regions of tibial nerve sections doubly immunolabeled for ED-1 (red) and CD206 (green) to detect activated macrophages. There was a prominent infiltration of ED-1 positive activated macrophages into the zone of demyelination 5d post-lysophosphatidyl choline (LPC)/FG injection (A), a minority of which (31.3%, P) were also immunopositive for CD206 (B, C). Temporal analysis of LPC focal demyelination +/- ES delivered at 5d post-LPC as indicated in days post-LPC: 8d (D, E, F), 8d+ES (G, H, I), 10d (J, K, L), 10d+ES (M, N, O). Note: ES results in a significant increase in the number of doubly ED-1/Arg1 positive macrophages 8d post-LPC (3d post-ES; H, I) relative to LPC only (E, F) (54.2% vs 31.9%, P) as well as at 10d post-LPC (5d post-ES; N, O) relative to LPC only (K, L) (62.2% vs 31.2%, P). Note: for each time point examined the number of strongly immunopositive cells were counted from ten fields of view. N=3 animals analyzed per condition, with a total number of 671-948 cells counted. Asterisks indicate significant differences between experimental groups; ***P<0.001. Scale bar = 100 μm.

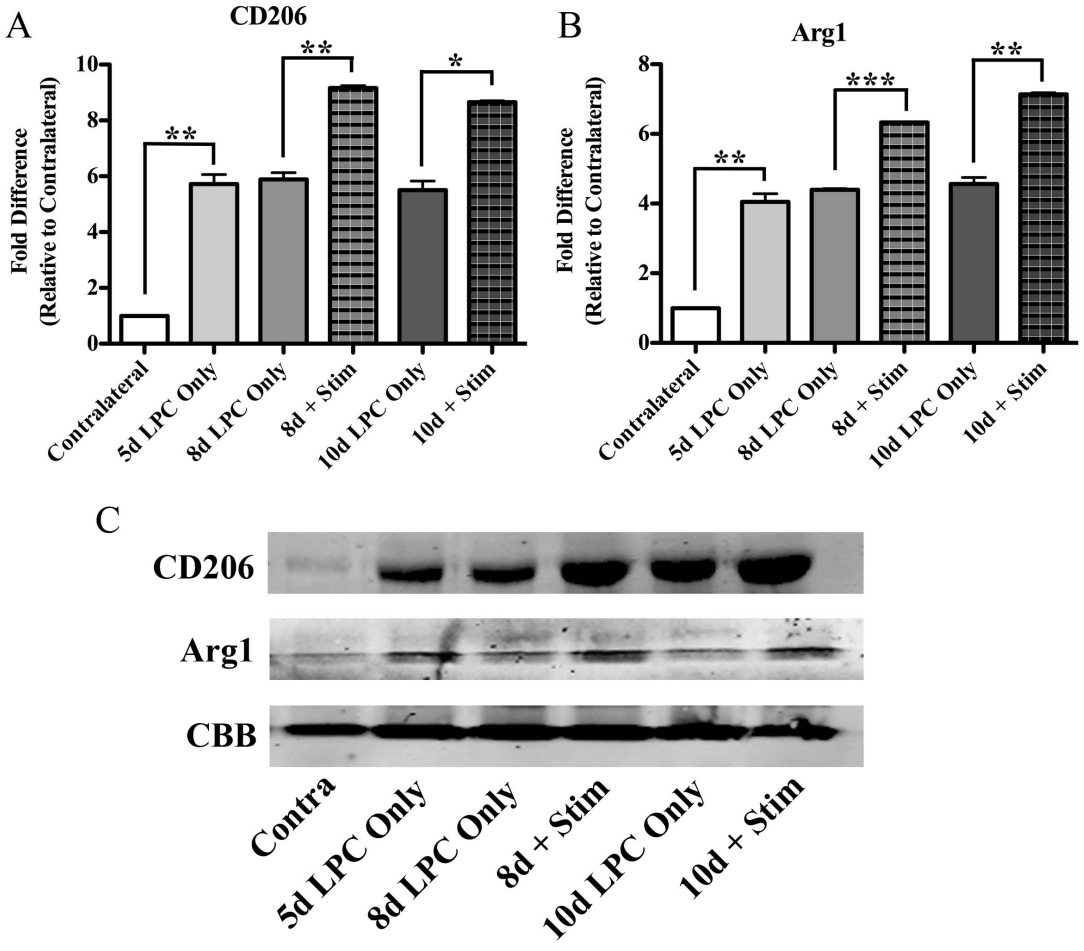

Figure 24: 1hr electrical stimulation (ES) 5 days post-lysophosphatidyl choline (LPC) results in increased M2-associated protein content beginning 8d post-LPC. Representative Western blots of sciatic nerve extract probed for the M2 (pro-repair) macrophage markers CD206 and Arg1. Immunoblots were run in duplicate from pooled nerve samples from 3 animals/experimental condition. Densitometry readings were normalized to one band of protein stained by Coomassie Brilliant Blue within each lane and compared to the mean densitometry reading of the contralateral (uninjured) sciatic nerve protein extract run alongside the demyelinated nerve extracts in each gel. There was a marked increase in detectable CD206 and Arg1 observed 5d post-lysophosphatidyl choline (LPC) injection into the tibial branch of the sciatic nerve, as compared to that observed in protein extract from contralateral (uninjured) nerves. As early as three days post-ES (8d post-LPC), there was a further increase in the amount of detectable CD206 (A, C) and Arg1 (B, C) in the stimulated nerves. This increase in detectable protein content correlates the visual differences observed immunohistochemically, and quantified via manual counting of immunopositive cells (Fig 20, Fig 21). At all time points examined, levels of detectable CD206 and Arg1 were significantly different than that of the contralateral (uninjured) controls. Asterisks indicate significant differences between experimental groups; *P<0.05, **P<0.01, Student's t-test.

increased levels of expression in M2 phenotypic markers were in agreement with the increased incidence of CD206 and Arg1 expression within ED-1 positive macrophages in the zones of

demyelination. These data indicate that the application of a single, 1hr episode of ES is sufficient to shift the majority of the infiltrated macrophages towards the pro-repair, M2 phenotype.

Thus, delayed brief ES has a dramatic impact on the polarization of macrophages towards a pro-repair M2 phenotype, in addition to its impact on faster resolution of the LPC-induced inflammation. Consistent with this, the non-stimulated nerves contained both a greater number of macrophages, and a greater proportion of pro-inflammatory M1 polarized cells, indicative of an ongoing more robust inflammatory response. When these findings are considered in combination with the data supporting enhanced remyelination and axonal protection with the application of ES, it is evident that this single intervention has a remarkable impact on the microenvironment surrounding the zone of demyelination. With the enhanced clearance and pro-repair polarization of the macrophages in the stimulated nerves a permissive environment is established I posit aids in both the initiation of the remyelination process and the protection of the vulnerable axons within the zone of demyelination.

CHAPTER 4:
DISCUSSION

4.1 Major Findings

In this thesis the therapeutic potential of *in vivo* brief electrical stimulation (ES) of focally demyelinated nerves was examined for the first time. The data identify ES as a novel and effective strategy to promote remyelination of the demyelinated nerve, as evidenced by the improvement of a number of parameters associated with peripheral nerve demyelinating pathologies. Further, they provide insights into the potential underlying mechanisms and cellular events associated with ES' beneficial effects. Focally demyelinated nerves receiving a single bout of electrical stimulation 5 days post-demyelination, remyelinated more rapidly relative to nerves that were demyelinated but not stimulated. The cellular events associated with the ES-enhanced remyelination include: elevated levels of BDNF in the zone of demyelination; a more rapid return of the Schwann cells to a non-activated state within the demyelination zone; the increased expression and re-appearance of neurofilaments in the axon-protective phosphorylated state; increased remyelination as indicated by increased Luxol Fast Blue staining and accelerated re-establishment of node of Ranvier architecture. Lastly, delayed nerve ES has a remarkable impact on the inflammatory response associated with the LPC-mediated focal demyelination. The stimulation procedure not only resulted in an accelerated reduction of macrophages from the zone of demyelination, but also promoted their polarization from a pro-inflammatory (M1) state towards one associated with tissue regeneration and repair (M2). These findings are summarized and placed together in temporal order in Figure 25.

4.2 Delayed ES impacts Schwann cell-associated parameters

4.2.1 Axon remyelination can be accelerated by ES

Neuronal activity has been linked to myelination of both central and peripheral axons, with exogenous electrical stimulation of DRG sensory neurons revealing that specific patterns of electrical activity can influence the process of myelination (Ishibashi et al. 2006; Stevens et al. 1998; Wake et al. 2011). It is speculated that this may be due to resulting changes in axonal

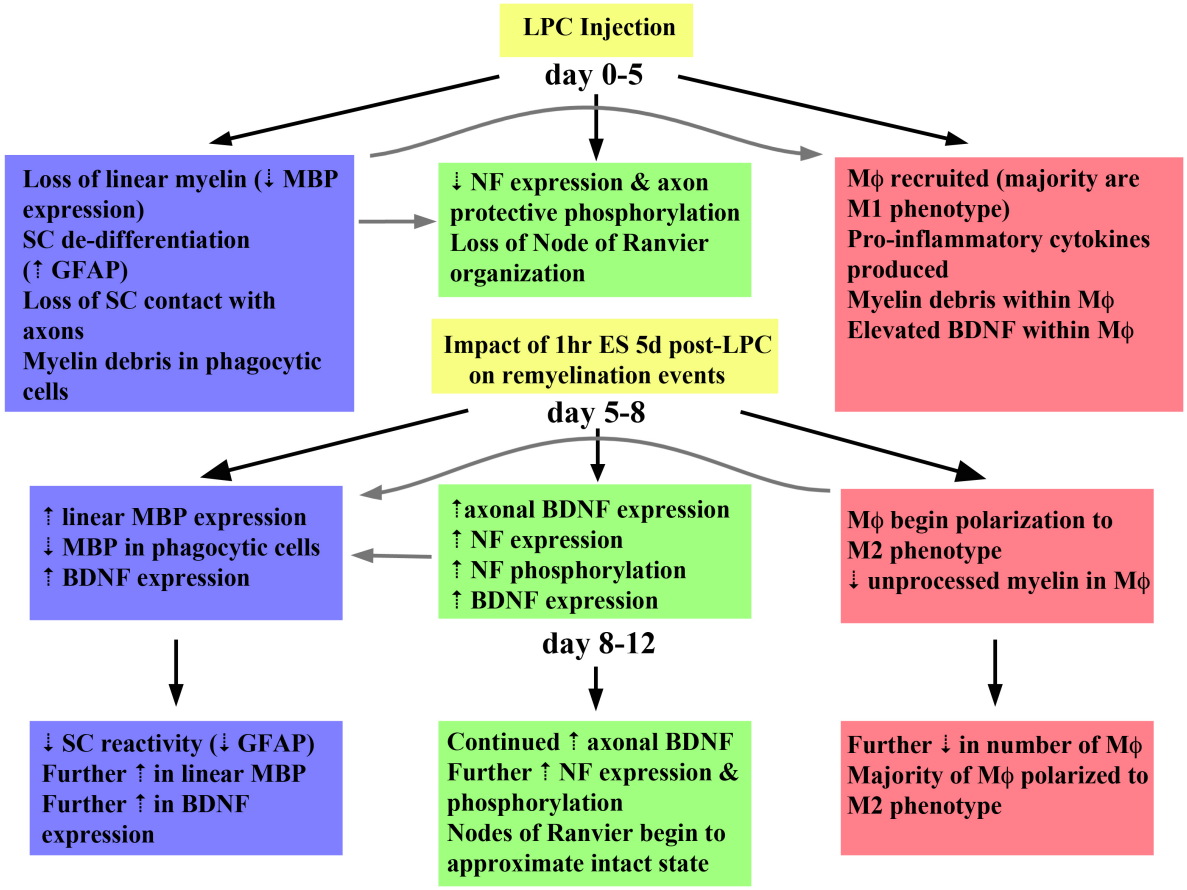

Figure 25: Temporal Changes in Remyelination Events Effected by ES. Schematic diagram outlining temporal changes occurring in Schwann cells (SC, blue), axons (green), and macrophages (red) following focal demyelination via LPC injection and delayed brief ES. Cellular events that are under mutual influence are indicated via grey arrows. The loss of SC-axon contact, and SC de-differentiation following LPC injection was not measured directly, but presumed to have occurred as is typical of peripheral demyelinating processes (Mirsky and Jessen 1996). The myelinolytic action of LPC produces debris, which promotes the recruitment of immune cells (grey arrow). The loss of myelin also impacts the expression and phosphorylation of the axonal neurofilaments (grey arrow). Following ES these same interactions may occur in the reverse direction, macrophage-mediated debris clearance sets up a permissive environment for myelination to occur (grey arrow), and axon-derived BDNF promotes myelination by Schwann cells. The increased linear MBP observed 8d post-LPC is consistent with the proliferation, differentiation and myelin sheath production by Schwann cells (Mirsky and Jessen 1996). The decreased numbers of macrophages is presumed to be due to cellular egress out of the nerve and a return to the peripheral circulation.

expression of proteins such as the L1 cellular adhesion molecule (Stevens et al. 1998). Axons that are electrically active (i.e. firing action potentials) display greater myelination by oligodendrocytes than those axons that have been silenced through the blocking of sodium channels with tetrototoxin (Ishibashi et al. 2006). The conduction of action potentials by axons,

and the release of factors (e.g. neurotransmitters, neurotrophins) along their length promotes the formation of signaling domains that mediate an interaction between the glial cell and the axon, which in turn results in the expression of a variety of proteins that comprise the myelin sheath (Wake et al. 2011), thereby supporting the doctrine of axonal activity having a strong influence on the process of myelination. Indeed, a body of *in vitro* studies already has demonstrated that the axon is not a passive entity during the formation of myelin. Rather, the electrical activity of the axon is a crucial component of the axo-glial interactions necessary for the process of myelination. One important caveat to this previous work is that it was performed in culture, an artificial environment that may not necessarily reflect the more complex *in vivo* scenario. It highlights a need for *in vivo* studies to be performed in order to corroborate these findings.

The work presented in the current study extends those previous *in vitro* findings and evaluates the impact of increased neuronal activity affected by brief ES of the sciatic nerve on myelin formation in the living animal. In the LPC model of focal peripheral nerve demyelination, maximal demyelination of axons occurs within four to six days, with the first appearance of thinly remyelinated fibers normally evident only around 14d post-LPC injection (Hall and Gregson 1971). I found that the ES promoted axon remyelination, and this was apparent 6 days earlier than usual, being detectable by 3d post-ES (8d post-LPC injection) and was clearly progressed by 5d and 7d post-ES (10 and 12d post-LPC) relative to the non-stimulated nerves. The ES effect on remyelination was likely the result of increased neuronal activity, as it was neither observed with sham ES, nor if the action potential generation was blocked at the time of stimulation with lidocaine. These results demonstrate that strategies aimed at increasing the electrical activity of axons will likely have therapeutic benefits.

ES also impacted the Schwann cell reactive state induced by the LPC injection. A clear attenuation in Schwann cell GFAP expression associated with this reactive state was observed within the zone of demyelination, and was evident by the last time point examined, 12d post-LPC (7d post-ES). Normally in the uninjured nerve, GFAP expression is largely restricted to the population of non-myelinating Schwann cells. However, upon injury there is a rapid increase in

GFAP immunoreactivity that also includes the myelin forming population of Schwann cells distal to the lesion site as the cells de-differentiate to an actively proliferating, reactive phenotype in which a new myelin membrane is not able to be elaborated (Cheng and Zochodne 2002; Wang et al. 2010). Perhaps the ability of brief ES to attenuate GFAP expression in the demyelination zone is linked to a switch of the de-differentiated Schwann cell back to a mature, myelinating phenotype. This may also be linked to the ES-associated observed egress/resolution of activated macrophages in the affected zone, as they have been shown to contribute to the reactive state of Schwann cells (Martini et al. 2008). The observed impact of brief ES on the myelinating function of Schwann cells does not occur in isolation; rather it is likely acting in concert with an impact upon the axons themselves, which I also observed. This highlights the intimate connection that exists between the myelinating Schwann cell and the axon which it ensheaths.

Parallels may also be drawn between the observed loss of myelin in response to LPC injection and the loss of myelin that occurs in the Wallerian degenerating distal nerve stump when axons are damaged and must subsequently undergo regeneration. Although the molecular environment following axotomy is quite different to that of a focal demyelinating insult where the axon is left intact, there are parallels that include the influx of immune cells, the removal of myelin debris and the induction of a reactive state in Schwann cells. The outcomes of my studies are also consistent with the previously reported ability of ES to promote remyelination of regenerating peripheral neurons (Singh et al. 2012; Wan et al. 2010). I found delayed ES also promoted remyelination of the focally demyelinated peripheral nerve using the same stimulation parameters employed in the two regeneration studies (a single bout of ES delivered for 1 hour at 20 Hz). However, the timing of nerve ES relative to induction of the pathological state differed. In my studies, the ES was delivered in a more clinically relevant delayed fashion once the focal demyelination had occurred (5d post-LPC), as opposed to being applied immediately at the time of nerve injection with the demyelinating agent, which would have been akin to the timing employed in the aforementioned regeneration studies. This supports that even delayed, nerve stimulation is beneficial and reparative for axon remyelination. The exact time frame post-injury

of when delayed ES will have its maximal positive impact remains unknown. An important point to consider is that the greater the delay between injury to ES treatment, the greater the chance for degenerative axon loss that could potentially result in permanent disability. Furthermore, it is unlikely that a single set of ES parameters will result in favorable outcomes for all peripheral nervous system pathologies, as regional differences in the response to ES have been noted (Gibson et al. 2014), as well as differences in the response of sensory vs. motor axons to varying durations of stimulation (Al-Majed et al. 2000a; Geremia et al. 2007). The current study also does not give insight into whether ES therapy is able to mitigate the demyelinating insult if administered concurrently with the demyelinating agent, such as was seen for the administration of methylprednisolone in LPC-induced demyelination of central axons (Pavelko et al. 1998). Finally, the invasive nature of the current paradigm makes it unlikely to be employed for clinical purposes in the same manner as in this study. Instead alternative strategies to enhance neuronal activity such as specific motor exercises will have to be developed, tested, and refined before becoming part of the clinician's toolbox (Sampaio-Baptista et al. 2013; Scholz et al. 2009).

4.2.2 Increased BDNF in the zone of demyelination coincides with remyelination.

The link between brief ES and remyelination in nerve regeneration models may be attributable to the observed ES-induced elevation in neuronal BDNF expression. In these studies this extra BDNF would presumably be released from the growing axon tips (Singh et al. 2012; Verderio et al. 2007; Wan et al. 2010), with one study implicating BDNF in the remyelination of the regenerated axons (Wan et al. 2010) and another demonstrating the contribution of macrophage-derived BDNF to axonal regeneration (Bouhy et al. 2006). The present study revealed an ES-induced increase in BDNF levels that was most apparent in axons within the demyelination zone, at times coincident with the onset of remyelination. Further, the elevated BDNF expression was sustained, evident at least as long as the last time point examined (12d post-LPC). It is conceivable that this BDNF could be released directly from the focally demyelinated axons and/or by the infiltrating macrophages (Wong et al. 2010). In sensory neurons, BDNF is normally co-packaged with neuropeptide transmitters in large dense core

vesicles (Michael et al. 1997) which have been shown to be released from both the unmyelinated axons, as well as at the axon terminals (Bernardini et al. 2004; Sauer et al. 1999). The axons within the zone affected by the injection of LPC are a population of both normally myelinated as well as unmyelinated nerve fibers. Following demyelination additional axonal surface area of the normally myelin ensheathed axons is revealed. The stimulation procedure employed in this study has been well documented to promote increased production of BDNF in both sensory and motor neuronal cell bodies (Al-Majed et al. 2000a; Geremia et al. 2007). Rather than being released at the terminals of the myelinated axons, the anterogradely transported BDNF can potentially be released right at the zone of demyelination through the denuded axons, as occurs normally in the unmyelinated fibers (Bernardini et al. 2004; Sauer et al. 1999). This would provide an additional source of the trophic factor important for the initiation of peripheral nerve myelination right at the location where it is needed. The critical work by Ng and colleagues (Ng et al. 2007) demonstrating that BDNF synthesized by sensory neurons could be released by the axons and participate in critical axon/glial communications required for effective remyelination further bolsters our position that the ES-enhanced production of BDNF by sensory neuron likely participates in the remyelination process following LPC. The requirement for BDNF to be synthesized at the level of the cell body and subsequently transported anterogradely along the length of the axon to the zone of demyelination, is probably one of critical events that factor into the observed delay of three days before the beneficial effects of the stimulation procedure on remyelination are observed. Thus, it is conceivable that the ES-associated elevation in axonal- and/or macrophage-derived BDNF in the present study are causally linked to the enhanced remyelination observed. In support of this, studies that either modulate BDNF availability or utilize small trkB agonists in either wild type mice or mice where Schwann cell BDNF has been conditionally knocked out, have shown that BDNF or activation of its receptor to be critically linked to more effective nerve repair and myelination during development or nerve regeneration (English et al. 2013; Tolwani et al. 2004; Zhang et al. 2000).

My observed presence of elevated BDNF at the site of demyelination *in vivo* would serve as an important cue for initiation of the myelination process. This finding is in agreement with an *in vitro* in Schwann cell/DRG neuron co-culture myelination study that employed identical stimulation parameters to those used in my studies and also found increased BDNF production in response to ES (Wan et al. 2010). It also matters what form the BDNF is in. The mature/processed form of BDNF has been demonstrated to aid in the maturation of Schwann cells to a myelinating phenotype and in their functional polarization, via BDNF's association and activation of the pan neurotrophin receptor $p75^{NTR}$ (Cosgaya 2002). It is encouraging that the strategy we employed to mitigate demyelinating lesions, namely ES, has been shown to promote extracellular cleavage of pro-BDNF to its neuroprotective mature form (Nagappan et al. 2009) in cultured hippocampal cells. Beyond promoting apoptosis of a number of cell types via activation of $p75^{NTR}$ (Greenberg et al. 2009; Taylor et al. 2012), if left in its pro-form, BDNF can also impede infiltration of activated macrophages (Wong et al. 2010) an important cellular event for remyelination. My results showing that the ES-associated elevated levels of BDNF were in the mature processed form, provide evidence that it was in the correct form to promote the maturation of Schwann cells to the promyelinating phenotype and also favorably impact immune responses (see below). Additionally, elevated expression of the partitioning defective-3 (Par-3) protein and its asymmetric distribution to the inner surface of the Schwann cell membrane once axonal contact has been achieved, are important signals for initiation of myelination – an event dependent upon release of BDNF from the axon (Chan et al. 2006; Taveggia and Salzer 2007). Notably, in crush injured regenerating axons subjected to ES, increases this asymmetric distribution of the Par-3 protein were observed as the axons regenerated past the crush site, presumably creating the proper alignment between the Schwann cell and the axon needed for myelination (Wan et al. 2010). Collectively, these observations support that the elevated levels of BDNF observed in the stimulated focally demyelinated nerves analyzed in my *in vivo* studies, likely play a major role in the improved remyelination observed.

4.3 Delayed brief ES impacts axon-associated parameters

4.3.1 Brief ES promotes axon-protective neurofilament phosphorylation

The interactions between Schwann cells and the axons they associate with are critically important for proper neural function, and brief ES of the focally demyelinated nerve has a remarkable impact on axonal properties that affect this interaction. Axonal degeneration is widely observed in demyelinating neuropathies in which decreased neurofilament numbers and neurofilament phosphorylation have been noted (Dyck et al. 1989; Trapp et al. 1998; Yagihashi et al. 1990), consistent with my observations. Maintaining electrical activity in axons helps to preserve axon health and conduction properties, while a lack or decreased expression of neurofilament proteins results in reduced sciatic nerve conduction velocity (Sakaguchi et al. 1993). Neurofilament proteins play an important role in the determination of axon caliber (Friede and Samorajski 1970; Hoffman et al. 1987), which along with electrical activity (Demerens et al. 1996) are important factors in determining whether an axon will be myelinated and when the axon is ready for ensheathment (Colello et al. 1995).

In addition to promoting early remyelination of axons, I found that stimulating the demyelinated nerve promoted these key determinants of axonal health. When axonal neurofilaments are in a phosphorylated state, this appears to protect neurofilaments from proteolysis and also increases axon diameter/caliber (Goldstein et al. 1987; Greenwood et al. 1993; Hoffman et al. 1987). Thus, a more rapid return to this state is likely beneficial for both restoring axonal health and perhaps more importantly for maintaining axon numbers. In the stimulated nerves, I observed a marked positive effect on both neurofilament expression and the return of neurofilaments to the axon protective phosphorylated state. This was evident at the first time point post-ES examined (8d post-LPC; 3d post-ES) and coincided with the onset of remyelination and reorganization of the paranodal and juxtaparanodal regions. Whether the ES-induced increase in BDNF expression is linked to this observed increase in neurofilament phosphorylation is not known, but this relationship has been shown for cortical neurons (Tokuoka et al. 2000) and may prove to be another way by which the overall process of

myelination is controlled by this neurotrophin.

The increased NF- and phosphorylated NF SMI-31-immunoreactivity in the stimulated nerves remained present throughout all time points examined, revealing a tremendous impact of a single bout of ES on this axis. Nerves not subjected to brief ES also displayed only a slight increase in NF and SMI-31 immunoreactivity that was apparent only at later time points (10-12 d post-LPC), and was much less robust than that of the ES nerves. My results suggest that the stimulation procedure is successfully protecting the axons by promoting their return to a competent state amenable to myelination. Communication between competent axons and their associated Schwann cells is essential for the initiation of the myelination program and for ongoing maintenance of the myelin sheath (Camara et al. 2009; Chan et al. 2004; Weinberg and Spencer 1976). Thus, in addition to promoting axonal survival, it is possible that ES also enhances the communication between the axons and the associated Schwann cells in order to affect a more rapid repair process.

4.3.2 Brief ES promotes node of Ranvier re-assembly

While ES-associated increases in neurofilament expression and positive LFB staining are not definitive proof that remyelination has occurred, when taken together with the observed recapitulation of a discrete distribution of the paranodal and juxtaparanodal markers, Caspr and Kv1.2 as part of essential nodal architecture, they support that remyelination has most likely occurred. Demyelinated axons no longer have the axon-Schwann cell interactions critical for the clustering of nodal, paranodal and juxtaparanodal proteins (Arroyo et al. 2004; Karimi-Abdolrezaee et al. 2004) thus, the normally highly localized pattern of nodal, paranodal and juxtaparanodal proteins takes on a more diffuse appearance consistent with what was observed 5d post-LPC. Myelin formation provides a potent instructional signal to the proteins associated with the node of Ranvier, resulting in the distinctive clustering of ion channels only occurring once contact with a Schwann cell membrane expressing myelin proteins (such as MAG) has occurred (Vabnick et al. 1996; Wiley-Livingston and Ellisman 1980).

It has been shown that the highly localized appearance of Caspr is one of the first

indications axons are being ensheathed by mature, compact myelin (Einheber et al. 1997). The re-appearance of this restricted staining pattern in my studies, along with quantitative differences in the number of visible nodes per field of view observed at earlier time points in the nerves treated with delayed brief ES, support that remyelination was indeed taking place. Axonal expression of Caspr helps to stabilize and maintain the restriction of sodium channels to the nodal region that begins following Schwann cell-axon contact (Einheber et al. 1997; Rosenbluth 1983). Interestingly, BDNF has also been shown to promote the clustering of Caspr and sodium channels in oligodendrocyte progenitor cell/sensory neuron co-cultures (Cui et al. 2010), which yet again emphasizes the potential role of BDNF as a master regulatory factor in controlling processes related to myelination.

4.4 Impact of delayed brief ES on the neuro-immune axis

4.4.1 Demyelination-associated immune responses resolve more quickly with ES

Beyond enhancing remyelination, ES also attenuated and/or accelerated the inflammatory immune response that accompanies the generation and resolution of these demyelinating insults. In electrically stimulated animals, beginning at 10d post-LPC (5d post-ES), macrophages that had infiltrated the lesion site transitioned from being distributed throughout the nerve to being more concentrated near the periphery, with many macrophages now also devoid of myelin debris. It is known that the majority of macrophages responsible for the phagocytosis of myelin debris following a demyelinating insult are derived from the peripheral circulation, with the resident macrophages of the peripheral nerve making only a minor contribution (Kiefer et al. 2001). Once the process of phagocytosis has been completed, these peripheral blood-derived macrophages may undergo apoptosis at the lesion site (Kuhlmann et al. 2001) or exit the lesion site and eventually return to the circulation via the SC basal lamina (Kuhlmann et al. 2001; Martini et al. 2008). Because at earlier time points (6d and 8d post-LPC) both stimulated and non-stimulated nerves displayed similar levels and distribution of macrophages as identified using histological stains or ED-1/CD68 immunofluorescence, the differences observed between the two groups beginning 10d post-injection (5d post-ES) are unlikely the result of impairment in

the initial infiltration of the nerve by the peripheral blood-derived macrophages. Rather, my findings are consistent with an ES-enhanced resolution of inflammation associated with the focal demyelination. This supports the idea that brief ES heightens macrophage activity, as those animals receiving brief ES displayed signs consistent with macrophage egress or macrophages that have undergone apoptosis sooner than their non-stimulated counterparts.

This more rapid resolution of inflammation may also be an indirect factor promoting axonal preservation and health. As the nerve becomes inflamed following the focal injection of LPC, changes in vessel permeability are necessary in order to allow accumulation of immune cells at the site of demyelination. This leads to inter-, and potentially intra-fascicular edema, with the increased pressure due to swelling placing the axons at increased risk for damage (Rydevik and Lundborg 1977). Examination of nerve cross sections showed that the stimulated nerves have reduced space between the fascicles, compared to their non-stimulated counterparts. The reduced swelling and edema noted in these nerves may serve a neuroprotective function, as the decreased stress on the nerve fibers will reduce the risk of further damage, and help keep the axons in a state that is amenable for the remyelination process to occur. The precise mechanism behind the enhanced clearance of the macrophages from within the stimulated nerves remains unknown. It could be due to either increased metabolic activity of the macrophages and/or, upregulation of a signaling pathway that effects early clearance of the phagocytic cells from the lesion site. While the signals that direct this cellular egress are not fully understood, evidence implicates the Nogo family of receptors (NgRs). Macrophages express NgRs on their surface that upon interaction with ligands (such as MAG) present in myelin are capable of initiating repulsive migration (Fry et al. 2007). ES may affect expression of these receptors and/or their ligands, which might underlie the observed enhanced clearance of macrophages and will serve as a target for future studies.

4.4.2 Delayed ES shifts macrophage polarization towards a pro-repair phenotype

The role of macrophages and their CNS counterpart, microglia, in repair of the nervous system is still a contentious issue, especially in MS where macrophages are implicated in both

the demyelination and remyelination phases of the disease (Kroner et al. 2014) While on one hand microglia and macrophages contribute to autoimmune disease through the release of toxins and via antigen presentation to cytotoxic lymphocytes (Banati et al. 1993; Myers et al. 1993), they are also beneficial in their ability to phagocytose myelin debris and through the secretion of growth factors. Their existence in a continuum of activation states makes them highly dynamic cells, polarizing into pro-inflammatory "classically activated " M1 macrophages with the "alternatively activated pro-repair M2 phenotype representing the opposite end of the spectrum. How this might impact peripheral demyelinating disease has not been elucidated. In Guillain-Barré syndrome, macrophages produce elevated levels of the M1 marker TNF-α that combined with direct phagocytosis of myelin, likely contributes the demyelination process (De La Hoz et al. 2010; Shin et al. 2013). The data presented within this study indicate that the ES procedure has a remarkable impact, not only on the resolution of the inflammatory response, but also on the nature of the inflammatory response. Macrophages, with their high degree of phenotypic plasticity, are able to shift between the classically activated M1 (pro-inflammatory) phenotype and the alternatively activated (pro-repair) M2 phenotype depending on the nature of the local microenvironment (Gratchev et al. 2006; Stout et al. 2005; Stout and Suttles 2004). This current study did not determine what state the macrophages were in when they first infiltrated the nerve in the LPC injection zone. But by the 5 days post-LPC injection, the majority are polarized toward the M1 phenotype, and expressed markers (i.e. iNOS and TNF-α) that are associated with this polarization state. It is likely that the presence of myelin debris in the zone played a role in this response. Past studies have shown that exposure to myelin debris and myelin phagocytosis can polarize M2 macrophages toward an M1 phenotype (Wang et al. 2015).

The application of a single episode of brief ES appears to be sufficient to alter the local chemical milieu so that the balance of macrophage polarity becomes shifted towards the pro-repair state with the majority of the macrophages present expressing markers (i.e. Arg1 and C206) associated with the M2 phenotype. There is a sustained decrease detected at both 8 and 10d post-LPC in the number of cells visibly expressing iNOS and TNF-α, as well as a reduction

in the total detectable amounts of these proteins. Conversely, at the same time points the incidence of cells expressing M2-associated markers and the total amount of CD206 and Arg1 protein detected increased. Other notable changes were a more rapid disappearance of myelin debris in the zone of demyelination and a paucity of myelin debris laden/foamy macrophages in the ES animals at the later 10 and 12 days post-LPC time points examined. It is plausible that the shift in polarization states may contribute to the observed more rapid clearance of myelin debris as past studies have shown that human M2 polarized macrophages can phagocytose significantly more myelin than M1 macrophages (Durafourt et al. 2012). This shift towards the pro-repair phenotype occurred at a time concurrent with the other noted beneficial effects of the ES procedure. The ability to polarize the macrophages toward a pro-repair phenotype appears to be dependent on axonal activity, as blocking action potential conduction at the time of stimulation blocked the phenotype transition from taking place. The implication here is that the electrically active axons are providing an instructive signal to the macrophages, much as they appear to do for the Schwann cells which are responsible for the remyelination observed following ES. However, it cannot be ruled out that the stimulation procedure is having some as of yet unknown direct effect on the macrophages themselves, with elucidation of the precise mechanism of how ES-induces this shift in polarity a target for future investigation.

The work presented within this thesis represents one of the first studies examining the link between axonal activity and its impact on macrophage polarity and the repair of peripheral myelin following a focal demyelinating insult. It has been demonstrated that during wound healing of cutaneous or cardiac tissues a shift in the polarity of the infiltrated macrophages from the M1 to the M2 phenotype occurs, and is necessary for proper resolution of the injury (Deonarine et al. 2007; Nahrendorf et al. 2007). Within the CNS there is ongoing communication between the neurons and the resident microglia, which modulates both neuronal connections and provides ongoing feedback to the microglia regarding the current homeostatic conditions within the brain (Hung et al. 2010). Further, biasing the microenvironment towards one favoring M2 polarization by impregnating scaffolding with IL-4 improves axonal

regeneration when compared to a bias towards an M1 phenotype using IFN-γ (Mokarram et al. 2012).

My observed shift in macrophage polarity induced by ES may also be a key factor in previously reported studies linking electrical stimulation with the regeneration of both motor and sensory axons (Al-Majed et al. 2000a; Geremia et al. 2007; Singh et al. 2012). Macrophage polarity and the associated cytokines play an important role in demyelination of CNS axons in the EAE model of experimental demyelination. Blocking of the pro-inflammatory (M1) cytokine TNF-α mitigates the extent of the demyelinating insult associated with the injection of LPC (Ousman and David 2001). As the induction of an M2 dominant state following CNS injury is typically of a transient nature, prolonging the M2 dominant phase of the inflammatory response has been shown to promote a neuroprotective response following spinal cord injury (Ma et al. 2015). Furthermore, when exogenous M2 polarized cells are introduced into the peripheral circulation, they appear to promote the induction of a recovery/repair response and an active suppression of the induced EAE (Mikita et al. 2011). These M2 polarized macrophages have also been shown to aid in the differentiation and maturation of oligodendrocytes (Miron et al. 2013), thus demonstrating their important role in the remyelination process. The results presented within the current study correlate with these CNS studies, and support that the shift in macrophage polarization towards the pro-repair macrophage phenotype affected by ES is also important for peripheral nerve remyelination.

4.5 Implications of thesis findings

4.5.1 Translation into clinical practice

The ultimate goal for many biomedical research studies is to convert the basic science knowledge that has been acquired into a tangible solution to a "real world" clinical problem. Conventional therapeutic approaches for the treatment of demyelinating disorders tend to focus on modulation of the immune response believed responsible for the generation of the demyelinated lesions (Clerico et al. 2008; Nakahara et al. 2009). While this may help to the reduce relapse rate and delay progression of the disorder, immune system modulation does not

tackle the fundamental problem of remyelination of these damaged areas of the nervous system and preservation of the demyelinated axon. The LPC-mediated focal demyelination model employed in the current study, while not a perfect recapitulation of the immune-associated demyelination observed with disorders such as GBS, does elicit a similar inflammatory pathology (Kuwabara 2004) and therefore may serve as a good proxy for early stage development and evaluation of novel therapeutic interventions. Furthermore, the intervention of interest here, namely *delayed* brief ES mimics the usual course of patient management, with treatment occurring only once the damage has occurred and the patient becomes symptomatic.

The current study revealed that delayed brief ES of focally demyelinated nerves has a tremendous impact on many of the cellular determinants associated with axon protection and effective remyelination. Whether these are all causally linked to the observed increases in BDNF expression is not currently known. Regardless, these results are encouraging as they indicate that it is indeed possible to significantly enhance the existing intrinsic remyelination processes in the peripheral nervous system *in vivo* by increasing neuronal activity, giving hope for the more debilitating demyelinating disorders of the central nervous system as well as the demyelination that occurs secondary to spinal cord injury.

The electrical stimulation paradigm employed in the current study has begun to make the bench to bedside transition. Electrical stimulation improves neuromuscular function in patients with both partial as well as complete spinal cord injuries (Crameri et al. 2002; Field-Fote 2001), demonstrating the ability of the damaged nervous system to respond to, and benefit from stimulation. Furthermore, a pilot study evaluating the efficacy of this paradigm in the management of nerve damage associated with carpal tunnel syndrome has yielded promising results, with ES accelerating both the regeneration of the axons and the innervation of their end targets (Gordon et al. 2010). One major limitation of the ES paradigm as employed in the current study is its invasive nature. It is relatively simple to add the stimulation procedure to standard nerve repair surgeries, as the site will be fully exposed and the electrodes can be applied directly to the nerve. This is simply not feasible for extending this work into the management of

demyelinating disorders, especially those that affect the CNS. Rather, the goal moving forward will be to develop non-invasive means to elicit the same response observed with direct ES of the nerve. The elucidation of the molecular pathways activated by the stimulation procedure will be an important part of this process. From the data obtained in this and other studies it appears that BDNF is a key molecule involved in the beneficial response to ES. Identifying alternative means to activate this pathway may be the key to translation of the knowledge obtained in the current study to the treatment of demyelinating disorders. It has been documented that physical activity is able to increase the expression of BDNF (Gomez-Pinilla et al. 2001; Neeper et al. 1996; Neeper et al. 1995). More specifically, treadmill training effected an increase in BDNF within the dendrites of the neurons found within the lumbar enlargement of the spinal cord, and also enhanced the expression of the BDNF receptor TrkB receptor in oligodendrocytes, particularly those within the grey matter (Skup et al. 2002). Additionally, physical activity also affects the cells of the immune system, as acute exercise increases not only the mature BDNF content in cells of the monocyte lineage, but also the expression of the $p75^{NTR}$ neurotrophin receptor (Brunelli et al. 2012).

4.5.2 Future Directions

The work presented within this thesis represents an exciting proof of principle for the successful application of delayed brief electrical stimulation to the repair of focally demyelinated peripheral axons. The data presented has led to the generation of a number of additional experimental questions, which while outside the bounds of the present work, represent rich potential for future study. One such avenue is the determination of the precise molecular mechanism(s) responsible for the beneficial effects of ES. As many of the facets examined point to a critical role for BDNF, it would be pertinent to confirm the master regulatory role for this molecule and to examine the downstream pathways activated by its signaling. Perturbation of the expression of BDNF via the introduction of siRNA and/or a function-blocking antibody (Geremia et al. 2010) along with administration of the ES procedure will allow for the examination of the effects of ES in an environment lacking this neurotrophin. I speculate that

this will likely lead to an inhibition of the stimulation procedure to produce a beneficial response leading to enhanced remyelination. Furthermore, it would be interesting to examine the effects of providing additional exogenous BDNF (Lang et al. 2008) or small molecule TrkB agonists (English et al. 2013) to see if an even more rapid repair response can be elicited following delayed brief ES. An important factor to bear in mind during these future experiments is the complex relationship between the various members of the neurotrophin family. For example, expression of BDNF can upregulated in sensory neurons by NGF in a paracrine manner (Apfel et al. 1996), which raises the question of whether the stimulation is increasing BDNF expression on its own, or whether this is occurring as a downstream consequence of increased NGF expression. Evidence also exists supporting a role for NGF in the myelination of DRG neurons whose initial survival is dependent upon NGF. *In vitro* studies have shown that the addition of NGF to co-cultures of DRG neurons and Schwann cells enhances the amount of myelin that is able to be formed (Chan et al. 2004), however, it is unknown if this response is due to a potential redundancy/convergence of the neurotrophin signaling pathways as the Schwann cell expresses and uses the common $p75^{NTR}$ receptor to mediate myelination (Tomita et al. 2007) or whether it is a consequence of NGF's ability to effect increased BDNF expression within neurons expressing the NGF receptor TrkA (Karchewski et al. 2002).

Given the apparent ability of the employed electrical stimulation procedure to impact the polarization of macrophages toward an M2 pro-repair phenotype, an important line of investigation will be to explore what the underlying mechanism might be. Because lidocaine-mediated blockade of action potential conduction at the time of ES appears to prevent the shift in the environment from an M1 to an M2 dominant phenotype suggesting that an axon-derived signal is likely at play. While the nature of this signal is currently unknown, examining the changes in axonal gene expression following ES via microarray analysis may provide some important clues as to which protein(s) are mediating this axon-macrophage or axon-Schwann cell-macrophage cross talk. Additionally, while the macrophage is not considered to be one of the classically defined electrically active cell types (e.g. neurons), based on the parameters of the

current study it cannot be entirely ruled out that there is some direct effect of the stimulation procedure on the macrophages as there is a high presence of macrophages in the nerve at the time of stimulation (although they are not concentrated at the site of stimulation). To assess this possibility, *in vitro* studies examining the result of electrically stimulating (Ishibashi et al. 2006; Wake et al. 2011) isolated macrophages that have been polarized toward an M1 phenotype by treatment of the culture with cytokines such as IFN-γ (Gratchev et al. 2006) before replacement with a "phenotype neutral" medium can be performed. It also remains unknown at this time whether the shift from an M1 to an M2 macrophage dominated environment is necessary for the enhanced remyelination observed following the delivery of delayed ES. In order to address the necessity of the presence of M2 polarized macrophages the effect of preventing this transition from occurring should be examined. The pharmaceutical compound doxycycline is a potent inhibitor of the transition from an M1 to an M2 polarization state (He and Marneros 2014), and can be used both in an *in vitro* and *in vivo* setting combined with the ES paradigm to examine the subsequent effect on myelination.

Once the precise nature of the mechanisms behind the beneficial effects of brief ES have been elucidated, an important extension of the knowledge gained will be to examine the effect of the delayed electrical stimulation paradigm on experimental demyelination of axons of the CNS. The myelin sheath elaborated by the oligodendrocytes is a major target and source of the pathology associated with multiple sclerosis (MS), with therapies that target repair of the associated myelin loss currently lacking. It has recently been demonstrated that increasing the activity of CNS neurons *in vivo* is linked to increased proliferation of myelinating precursor cells as well as an increase in the thickness of the myelin sheath surrounding the axons of the stimulated neurons (Gibson et al. 2014). This indicates that the potential exists for the adaptation of the paradigm employed within the current study in order to address the repair of demyelinated axons of the CNS. The LPC model of demyelination can be used to create focal lesions of the dorsal columns of the spinal cord (Hall 1972), at the level where the afferents from the L4/L5 dorsal root ganglia enter the spinal cord, and delayed brief ES of the sciatic nerve can be

performed according to the established parameters used in the present study. Assessment of the effects of ES on remyelination of the CNS axons will largely consist of examining the same markers and cellular events employed in the current study examining peripheral nerve remyelination (e.g. myelin protein expression, glial reactivity, immune cell phenotype, etc.). As both BDNF and NT-3 are involved in the myelination of CNS axons (Jean et al. 2003), it would be prudent to examine the effects of the delayed stimulation procedure on the expression and activity of both of these trophic factors. Examination of the affect of delayed brief ES on the remyelination of central axons will provide important insights that can be exploited in developing of novel therapies to address MS pathologies.

In conclusion, the findings of this thesis have revealed that increasing axonal activity is a very promising therapeutic strategy for future remyelination efforts in peripheral nerve.

LIST OF REFERENCES

Al-Majed AA, Brushart TM, Gordon T. 2000a. Electrical stimulation accelerates and increases expression of BDNF and trkB mRNA in regenerating rat femoral motoneurons. European Journal of Neuroscience 12:4381-4390.

Al-Majed AA, Neumann CM, Brushart TM, Gordon T. 2000b. Brief electrical stimulation promotes the speed and accuracy of motor axonal regeneration. The Journal of Neuroscience 20(7):2602-2608.

Allavena P, Sica A, Solinas G, Porta C, Mantovani A. 2008. The inflammatory micro-environment in tumor progression: the role of tumor-associated macrophages. Critical reviews in oncology/hematology 66(1):1-9.

Allt G, Ghabriel MN, Sikri K. 1988. Lysophosphatidyl choline-induced demyelination a freeze-fracture study. Acta Neuropathologica 75:456-464.

Altevogt BM, Kleopa KA, Postma FR, Scherer SS, Paul DL. 2002. Connexin29 is uniquely distributed within myelinating glial cells of the central and peripheral nervous systems. The Journal of Neuroscience 22(15):6458-6470.

Ambarus CA, Krausz S, van Eijk M, Hamann J, Radstake TR, Reedquist KA, Tak PP, Baeten DL. 2012. Systematic validation of specific phenotypic markers for in vitro polarized human macrophages. Journal of Immunological Methods 375(1-2):196-206.

Apfel SC, Wright DE, Wiideman AM, Dormia C, Snider WD, Kessler JA. 1996. Nerve growth factor regulates the expression of brain-derived neurotrophic factor mRNA in the peripheral nervous system. Molecular and Cellular Neuroscience 7:134-142.

Arroyo EJ, Sirkowski EE, Chitale R, Scherer SS. 2004. Acute demyelination disrupts the molecular organization of peripheral nervous system nodes. The Journal of Comparative Neurology 479(4):424-434.

Asbury AK, Arnason BG, Adams RD. 1969. The inflammatory lesion in idiopathic polyneuritis. Medicine 48(3):173-215.

Back SA, Tuohy TM, Chen H, Wallingford N, Craig A, Struve J, Luo NL, Banine F, Liu Y, Chang A and others. 2005. Hyaluronan accumulates in demyelinated lesions and inhibits oligodendrocyte progenitor maturation. Nature Medicine 11(9):966-972.

Banati RB, Gehrmann J, Schubert P, Kreutzberg GW. 1993. Cytotoxicity of microglia. Glia 7(1):111-118.

Baranes D, Lederfein D, Huang Y-Y, Chen M, Bailey CH, Kandel ER. 1998. Tissue plasminogen activator contributes to the late phase of LTP and to synaptic growth in the hippocampal mossy fiber pathway. Neuron 21:813-825.

Barouch R, Appel E, Kazimirsky G, Brodie C. 2001. Macrophages express neurotrophins and neurotrophin receptors: Regulation of nitric oxide production by NT-3. Journal of Neuroimmunology 112:72-77.

Bear MF, Connors BW, Paradiso MA. 2007. Neuroscience: Exploring the brain. Baltimore: Lippincott Williams & Wilkins.

Bernardini N, Neuhuber W, Reeh PW, Sauer SK. 2004. Morphological evidence for functional capsaicin receptor expression and calcitonin gene-related peptide exocytosis in isolated peripheral nerve axons of the mouse. Neuroscience 126(3):585-590.

Biswas SK, Mantovani A. 2010. Macrophage plasticity and interaction with lymphocyte subsets: cancer as a paradigm. Nature immunology 11(10):889-96.

Boron WF, Boulpaep EL. 2005. Organization of the nervous system. Medical Physiology. Philadelphia: Elsevier Saunders. p 257-279.
Boucher JL, Moali C, Tenu JP. 1999. Nitric oxide biosynthesis, nitric oxide synthase inhibitors and arginase competition for L-arginine utilization. Cellular and Molecular Life Sciences 55:1015-1028.
Bouhy D, Malgrange B, Multon S, Poirrier AL, Scholtes F, Schoenen J, Franzen R. 2006. Delayed GM-CSF treatment stimulates axonal regeneration and functional recovery in paraplegic rats via an increased BDNF expression by endogenous macrophages. The FASEB Journal 20(8):1239-41.
Bronte V, Zanovello P. 2005. Regulation of immune responses by L-arginine metabolism. Nature Reviews Immunology 5(8):641-54.
Bruck W. 1997. The role of macrophages in Wallerian degeneration. Brain Pathology 7:741-752.
Brunelli A, Dimauro I, Sgro P, Emerenziani GP, Magi F, Baldari C, Guidetti L, Luigi LD, Parisi P, Caporossi D. 2012. Acute exercise modulates BDNF and pro-BDNF protein content in immune cells. Medicine and Science in Sports and Exercise 44(10):1871-80.
Brushart TM, Jari R, Verge V, Rohde C, Gordon T. 2005. Electrical stimulation restores the specificity of sensory axon regeneration. Experimental Neurology 194(1):221-229.
Burns TM. 2008. Guillain-Barre syndrome. Seminars in Neurology 28(2):152-67.
Camara J, Wang Z, Nunes-Fonseca C, Friedman HC, Grove M, Sherman DL, Komiyama NH, Grant SG, Brophy PJ, Peterson A and others. 2009. Integrin-mediated axoglial interactions initiate myelination in the central nervous system. The Journal of Cell Biology 185(4):699-712.
Campbell WW. 2008. Evaluation and management of peripheral nerve injury. Clinical Neurophysiology 119(9):1951-65.
Chan JR. 2001. Inaugural Article: Neurotrophins are key mediators of the myelination program in the peripheral nervous system. Proceedings of the National Academy of Sciences USA 98(25):14661-14668.
Chan JR, Jolicoeur C, Yamauchi J, Elliott J, Fawcett JP, Ng BK, Cayouette M. 2006. The polarity protein Par-3 directly interacts with p75NTR to regulate myelination. Science 314(5800):832-6.
Chan JR, Watkins TA, Cosgaya JM, Zhang C, Chen L, Reichardt LF, Shooter EM, Barres BA. 2004. NGF controls axonal receptivity to myelination by Schwann cells or oligodendrocytes. Neuron 43(2):183-191.
Chao MV, Bothwell M. 2002. Neurotrophins: To cleave or not to cleave. Neuron 33:9-12.
Chaudhry V, Glass JD, Griffin JW. 1992. Wallerian degeneration in peripheral nerve disease. Neurologic Clinics 10(3):613-627.
Chen ZY, Patel PD, Sant G, Meng CX, Teng KK, Hempstead BL, Lee FS. 2004. Variant brain-derived neurotrophic factor (BDNF) (Met66) alters the intracellular trafficking and activity-dependent secretion of wild-type BDNF in neurosecretory cells and cortical neurons. The Journal of Neuroscience 24(18):4401-11.
Cheng C, Zochodne DW. 2002. In vivo proliferation, migration and phenotypic changes of schwann cells in the presence of myelinated fibers. Neuroscience 115(1):321-329.
Chio A, Cocito D, Leone M, Giordana MT, Mora G, Mutani R. 2003. Guillain-Barre syndrome a prospective, population-based incidence and outcome survey. Neurology 60:1146-1150.

Chiu SY, Ritchie JM. 1984. On the physiological role of internodal potassium channels and the security of conduction in myelinated nerve fibres. Proceedings of the Royal Society London 220:415-422.
Chomarat P, Banchereau J, Davoust J, Palucka AK. 2000. IL-6 switches the differentiation of monocytes from dendritic cells to macrophages. Nature Immunology 1(6):510-516.
Clerico M, Rivoiro C, Contessa G, Viglietti D, Durelli L. 2008. The therapy of multiple sclerosis with immune-modulating or immunosuppressive drug. Clinical Neurology and Neurosurgery 110(9):878-885.
Colello RJ, Devey LR, Imperato E, Pott U. 1995. The chronology of oligodendrocyte differentiation in the rat optic nerve: Evidence for a signaling step initiating myelination in the CNS. The Journal of Neuroscience 15(11):7665-7672.
Cosgaya JM. 2002. The Neurotrophin Receptor p75NTR as a Positive Modulator of Myelination. Science 298(5596):1245-1248.
Crameri RM, Weston A, Climstein M, Davis GM, Sutton JR. 2002. Effects of electrical stimulation-induced leg training on skeletal muscle adaptability in spinal cord injury. Scandinavian Journal of Medicine and Science in Sports 12(5):316-322.
Cui QL, Fragoso G, Miron VE, Darlington PJ, Mushynski WE, Antel JP, Almazan G. 2010. Response of human oligodendrocyte progenitors to growth factors and axon signals. Journal of Neuropathology and Experimental Neurology 69(9):930-944.
Dailey AT, Avellino AM, Benthem L, Silver J, Kliot M. 1998. Compelement depletion reduces macrophage infiltration and activation during Wallerian degeneration and axonal regeneration. The Journal of Neuroscience 18(17):6713-6722.
Damoiseaux JGMC, Dopp EA, Calame W, Chao D, MacPherson GG. 1994. Rat macrophage lysosomal membrane antigen recognized by monoclonal antibody ED1. Immunology 83:149-147.
Dashiell SM, Tanner SL, Pant H, C., Quarles RH. 2002. Myelin-associated glycoprotein modulates expression and phosphorylation of neuronal cytoskeletal elements and their associated kinases. Journal of Neurochemistry 81:1263-1272.
De La Hoz CL, Castro FR, Santos LM, Langone F. 2010. Distribution of inducible nitric oxide synthase and tumor necrosis factor-alpha in the peripheral nervous system of Lewis rats during ascending paresis and spontaneous recovery from experimental autoimmune neuritis. Neuroimmunomodulation 17(1):56-66.
de Waegh S, M., Lee VM-Y, Brady ST. 1992. Local modulation of neurofilament phosphorylation, axonal caliber, and slow axonal transport by myelinating schwann cells. Cell 68:451-463.
Delneste Y, Charbonnier P, Herbault N, Magistrelli G, Caron G, Bonnefoy JY, Jeannin P. 2003. Interferon-gamma switches monocyte differentiation from dendritic cells to macrophages. Blood 101(1):143-50.
Demerens C, Stankoff B, Logak M, Anglade P, Allinquant B, Couraud F, Zalc B, Lubetzki C. 1996. Induction of myelination in the central nervous system by electrical activity. Proceedings of the National Academy of Sciences USA 93:9887-9892.
Deonarine K, Panelli M, Stashower M, Jin P, Smith KD, Slade H, al. e. 2007. Gene expression profiling of cutaneous wound healing. Journal of Translational Medicine 5:11-22.
Detering NK, Wells MA. 1976. The non-synchronous synthesis of myelin components during early stages of myelination in the rat optic nerve. Journal of Neurochemistry 26:253-257.

Dougherty KD, Dreyfus CF, Black IB. 2000. Brain-derived neurotrophic factor in astrocytes, oligodendrocytes, and microglia/macrophages after spinal cord injury. Neurobiology of Disease 7(6):574-585.
Drenthen J, Jacobs BC, Maathuis EM, van Doorn PA, Visser GH, Blok JH. 2013. Residual fatigue in Guillain-Barre syndrome is related to axonal loss. Neurology 81:1827-1831.
Durafourt BA, Moore CS, Zammit DA, Johnson TA, Zagula F, Guiot M-C, Bar-Or A, Antel JP. 2012. Comparison of polarization properties of human adult microglia and blood-derived macrphages. Glia 60:717-727.
Dyck PJ, Karnes JL, Lambert EH. 1989. Longitudinal study of neuropathic deficits and nerve conduction abnormalities in hereditary motor and sensory neuropathy type 1. Neurology 39:1302-1308.
Eaton SL, Roche SL, Llavero Hurtado M, Oldknow KJ, Farquharson C, Gillingwater TH, Wishart TM. 2013. Total protein analysis as a reliable loading control for quantitative fluorescent Western blotting. PLoS ONE 8(8):e72457.
Egan MF, Kojima M, Callicott JH, Goldberg TE, Kolachana BS, Bertolino A, Zaitsev E, Gold B, Goldman D, Dean M and others. 2003. The BDNF val66met polymorphism affects activity-dependen secretion of BDNF and human memory and hippocampal fuction. Cell 112:257-269.
Einheber S, Zanazzi G, Ching W, Scherer SS, Milner TA, Peles E, Salzer JL. 1997. The axonal membrane protein Caspr, a homologue of neurexin IV, is a component of the septate-like paranodal junctions that assemble during myelination. The Journal of Cell Biology 139(6):1495-1506.
Elhanany E, Jaffe H, Link WT, Sheeley DM, Gainer H, Pant H, C. 1994. Identification of endogenously phosphorylated KSP sites in the high-molecular-weight rat neurofilament protein. Journal of Neurochemistry 63:2324-2335.
English AW, Liu K, Nicolini JM, Mulligan AM, Ye K. 2013. Small-molecule trkB agonists promote axon regeneration in cut peripheral nerves. Proceedings of the National Academy of Sciences USA 110(40):16217-22.
English AW, Schwartz G, Meador W, Sabatier MJ, Mulligan A. 2006. Electrical stimulation promotes peripheral axon regeneration by enhanced neuronal neurotrophin signaling. Developmental Neurobiology 67(2):158-172.
Fearon DT, Locksley RM. 1996. The instructive role of innate immunity in the acquired immune response. Science 272:50-54.
Field-Fote EC. 2001. Combined use of body weight support, functional electric stimulation, and treadmill training to improve walking ability in individuals with chronic incomplete spinal cord injury. Archives of physical medicine and rehabilitation 82(6):818-24.
Filbin MT. 1995. Myelin-associated glycoprotein: a role in myelination and in the inhibition of axonal regeneration? Current Opinion in Neurobiology 5:588-595.
Fitzgerald M. 1987. Spontaneous and evoked activity of fetal primary afferents in vivo. Nature 326:603-605.
Friede RL, Samorajski T. 1970. Axon caliber related to neurofilaments and microtubules in sciatic nerve fibers of rats and mice. Anatomical Record 167:379-388.
Fry EJ, Ho C, David S. 2007. A role for Nogo receptor in macrophage clearance from injured peripheral nerve. Neuron 53(5):649-662.
Garbay B, Heape AM, Sargueil F, Cassagne C. 2000. Myelin synthesis in the peripheral nervous system. Progress in Neurobiology 61:267-304.

Geisler N, Kaufmann E, Fischer S, Plessman U, Weber K. 1983. Neurofilament architecture combines structural principles of intermediate filaments with carboxy-terminal extensions increasing in size between triplet proteins. The Journal of Embryology 2(8):1295-1302.
Geissmann F, Gordon S, Hume DA, Mowat AM, Randolph GJ. 2010. Unravelling mononuclear phagocyte heterogeneity. Nature Reviews Immunology 10(6):453-60.
Georgiou J, Tropak MB, Roder JC. 2004. Myelin-associated glycoprotein gene. In: Lazzarini RA, editor. Myelin Biology and Disorders. San Diego: Elsevier Academic Press. p 421-467.
Geremia NM, Gordon T, Brushart TM, Al-Majed AA, Verge VMK. 2007. Electrical stimulation promotes sensory neuron regeneration and growth-associated gene expression. Experimental Neurology 205(2):347-359.
Geremia NM, Pettersson LME, Hasmatali JC, Hryciw T, Danielsen N, Schreyer DJ, Verge VMK. 2010. Endogenous BDNF regulates induction of intrinsic neuronal growth programs in injured sensory neurons. Experimental Neurology 223(1):128-142.
Giasson BI, Mushynski WE. 1997. Study of proline-directed protein kinases involved in phophorylation of the heavy neurofilament subunit. The Journal of Neuroscience 17(24):9466-9472.
Gibson EM, Purger D, Mount CW, Goldstein AK, Lin GL, Wood LS, Inema I, Miller SE, Bieri G, Zuchero JB and others. 2014. Neuronal activity promotes oligodendrogenesis and adaptive myelination in the mammalian brain. Science 344(6183):1252304.
Gold R, Hartung H-P, Toyka KV. 2000. Animal models for autoimmune demyelinating disorders of the nervous sustem. Molecular Medicine Today 6:88-91.
Goldstein ME, Sternberger NH, Sternberger LA. 1987. Phosphorylation protects neurofilaments against proteolysis. Journal of Neuroimmunology 14:149-160.
Gomez-Pinilla F, Ying Z, Opazo P, Roy RR, Edgerton VR. 2001. Differential regulation by exercise of BDNF and NT-3 in rat spinal cord and skeletal muscle. European Journal of Neuroscience 13:1078-1084.
Gordon S, Taylor PR. 2005. Monocyte and macrophage heterogeneity. Nature Reviews Immunology 5(12):953-64.
Gordon T, Amirjani N, Edwards DC, Chan KM. 2010. Brief post-surgical electrical stimulation accelerates axon regeneration and muscle reinnervation without affecting the functional measures in carpal tunnel syndrome patients. Experimental Neurology 223(1):192-202.
Gratchev A, Kzhyshkowska J, Kothe K, Muller-Molinet I, Kannookadan S, Utikal J, Goerdt S. 2006. Mphi1 and Mphi2 can be re-polarized by Th2 or Th1 cytokines, respectively, and respond to exogenous danger signals. Immunobiology 211(6-8):473-86.
Greenberg ME, Xu B, Lu B, Hempstead BL. 2009. New insights in the biology of BDNF synthesis and release: implications in CNS function. The Journal of neuroscience : the official journal of the Society for Neuroscience 29(41):12764-7.
Greenwood JA, Troncoso JC, Costello AC, Johnson GVW. 1993. Phosphorylation modulates calpain-mediated proteolysis and calmodulin binding of the 200-kDA and 160-kDa neurofilament proteins. Journal of Neurochemistry 61:191-199.
Griffin JW, George R, Ho T. 1993. Macrophage systems in peripheral nerves. A review. Journal of Neuropathology and Experimental Neurology 52(6):553-560.
Griffin JW, Stocks EA, Fahnestock K, Van Praagh A, Trapp BD. 1990. Schwann cell proliferation following lysolecithin-induced demyelination. Journal of Neurocytology 19:367-384.

Hall SM. 1972. The effect of injections of lysophosphatidyl choline into white matter of the adult mouse spinal cord. Journal of Cell Science 10:535-546.
Hall SM. 1973. Some aspects of remyelination after demyelination produced by the intraneural injection of lysophosphatidyl choline. Journal of Cell Science 13(461-477).
Hall SM, Gregson NA. 1971. The in vivo and ultrastructural effects of injection of lysophosphatidyl choline into myelinated peripheral nerve fibres of the adult mouse. Journal of Cell Science 9:769-789.
He L, Marneros AG. 2014. Doxycycline inhibits polarization of macrophages to the proangiogenic M2-type and subsequent neovascularization. The Journal of Biological Chemistry 289(12):8019-28.
Hesse M, Modolell M, La Flamme AC, Schito M, Fuentes JM, Cheever AW, Pearce EJ, Wynn TA. 2001. Differential Regulation of Nitric Oxide Synthase-2 and Arginase-1 by Type 1/Type 2 Cytokines In Vivo: Granulomatous Pathology Is Shaped by the Pattern of L-Arginine Metabolism. The Journal of Immunology 167(11):6533-6544.
Hiraga A, Kuwabara S, Ogawara K, Misawa S, Kanesaka T, Koga M, Yuki N, Hattori T, Mori M. 2005. Patterns and serial changes in electrodiagnostic abnormalities of axonal Guillain–Barré syndrome. Neurology 64:856-860.
Hirokawa N, Glicksman MA, Willard MB. 1984. Organization of mammalian neurofilament polypeptides within the neuronal cytoskeleton. The Journal of Cell Biology 98:1523-1536.
Hoffman PN, Cleveland DW, Griffin JW, Landes PW, Cowan NJ, Price DL. 1987. Neurofilament gene expression: A major determinant of axonal caliber. Proceedings of the National Academy of Sciences USA 84:3472-3476.
Hsieh S-T, Kidd G, J., Crawford TO, Xu Z, Lin W-M, Trapp BD, Cleveland DW, Griffin JW. 1994. Regional modulation of neurofilament organization by myelination in normal axons. The Journal of Neuroscience 14(11):6392-6401.
Hughes RAC, Cornblath DR. 2005. Guillain Barre syndrome. Lancet 366:1653-1656.
Hung J, Chansard M, Ousman SS, Nguyen MD, Colicos MA. 2010. Activation of microglia by neuronal activity: results from a new in vitro paradigm based on neuronal-silicon interfacing technology. Brain, Behavior, and Immunity 24(1):31-40.
Ishibashi T, Dakin KA, Stevens B, Lee PR, Kozlov SV, Stewart CL, Fields RD. 2006. Astrocytes Promote Myelination in Response to Electrical Impulses. Neuron 49(6):823-832.
Jaffe H, Veeranna, Pant H, C. 1998a. Charaterization of serine and threonine phosphorylation sites in b-elimination/ethanethiol addition-modified proteins by electrospray tandem mass spectrometry and database searching. Biochemistry 37:16211-16224.
Jaffe H, Veeranna, Shetty KT, Pant H, C. 1998b. Charaterization of the phosphorylation sites of human high molecular weight neurofilament protein by electrospray ionization tandem mass spectrometry and database searching. Biochemistry 37:3931-3940.
Je HS, Yang F, Ji Y, Nagappan G, Hempstead BL, Lu B. 2012. Role of pro-brain-derived neurotrophic factor (proBDNF) to mature BDNF conversion in activity-dependent competition at developing neuromuscular synapses. Proceedings of the National Academy of Sciences USA 109(39):15924-15929.
Jean I, Lavialle C, Barthelaix-Pouplard A, Fressinaud C. 2003. Neurotrophin-3 specifically increases mature oligodendrocyte population and enhances remyelination after chemical demyelination of adult rat CNS. Brain Research 972(1-2):110-118.

Jessen KR, Morgan L, Stewart HJS, Mirsky R. 1990. Three markers of adult non-myelin-forming Schwann cells, 217c(Ran-1), A5E3 and GFAP: Development and regulation by neuron-Schwann cell interactions. Development 109:91-103.
Jessen KR, Rhona M. 1992. Schwann cells: Early lineage, regulation of proliferation and control of myelin formation. Current Opinion in Neurobiology 2:575-581.
Ji RC. 2012. Macrophages are important mediators of either tumor- or inflammation-induced lymphangiogenesis. Cellular and Molecular Life Sciences 69(6):897-914.
Kamakura K, ishiura S, Sugita H, Toyokura Y. 1983. Identification of Ca2+-activated neutral protease in the peripheral nerve and its effects on neurofilament degeneration. Journal of Neurochemistry 40(4):908-913.
Karchewski LA, Gratto KA, Wetmore C, Verge VMK. 2002. Dynamic patterns of BDNF expression in injured sensory neurons: Differential modulation by NGF and NT-3. European Journal of Neuroscience 16:1449-1462.
Karimi-Abdolrezaee S, Eftekharpour E, Fehlings MG. 2004. Temporal and spatial patters of Kv1.1 and Kv1.2 protein and gene expression in spinal cord white matter after acute and chronic spinal cord injury in rats: implications for axonal pathophysiology after neurotrauma. European Journal of Neuroscience 19:577-589.
Kiefer R, Kieseier BC, Stoll G, Hartung H-P. 2001. The role of macrophages in immune-mediated damage to the peripheral nervous system. Progress in Neurobiology 64:109-127.
Kirkpatrick LL, Brady ST. 1999. Cytoskeleton of neurons and glia. In: Siegel GJ, Agranoff BW, Albers RW, Fisher SK, Uhler MD, editors. Basic Neurochemistry: Molecular cellular and medical aspects. Philadelphia: Lippincott-Raven. p 155-174.
Kirshner DA, Wrabetz L, Feltri ML. 2004. The P0 Gene. In: Lazzarini RA, editor. Myelin Biology and Disorders. San Diego: Elsevier Academic Press. p 523-545.
Kotter MR. 2006. Myelin Impairs CNS Remyelination by Inhibiting Oligodendrocyte Precursor Cell Differentiation. The Journal of Neuroscience 26(1):328-332.
Kotter MR, Setzu A, Sim FJ, Van Rooijen N, Franklin RJ. 2001. Macrophage depletion impairs oligodendrocyte remyelination following lysolecithin-induced demyelination. Glia 35(3):204-12.
Kotter MR, Zhao C, van Rooijen N, Franklin RJ. 2005. Macrophage-depletion induced impairment of experimental CNS remyelination is associated with a reduced oligodendrocyte progenitor cell response and altered growth factor expression. Neurobiology of Disease 18(1):166-75.
Kroner A, Greenhalgh AD, Zarruk JG, Passos Dos Santos R, Gaestel M, David S. 2014. TNF and increased intracellular iron alter macrophage polarization to a detrimental M1 phenotype in the injured spinal cord. Neuron 83(5):1098-116.
Kuhlmann T, Bitsch A, Stadelmann C, Siebert H, Bruck W. 2001. Macrophages are eliminated from the injured peripheral nerve via local apoptosis and circulation to regional lymph nodes and the spleen. The Journal of Neuroscience 21(10):3401-3408.
Kuwabara S. 2004. Guillain Barre Syndrom: Epidemiology, pathophysiology and management. Drugs 64(5):1-14.
Lang EM, Schlegel N, Reiners K, Hofman GO, Sendtner M, Asan E. 2008. Single-dose application of CNTF and BDNF improves remyelination of regenerating nerve fibers after C7 ventral root avulsion and replantation. Journal of Neurotrauma 25:384-400.

Lee VM, Carden MJ, Schlaepfer WW, Trojanowski JQ. 1987. Monoclonal antibodies distinguish several differentially phosphorylated states of the two largest rat neurofilament subunits (NF-H and NF-M) and demonstrate their existence in the normal nervous system of adult rats. The Journal of Neuroscience 7(11):3474-88.

Lemke G, Chao MV. 1988. Axons regulate Schwann cell expression of the major myelin and NGF receptor genes. Development 102:499-504.

Li X, Lynn BD, Olson C, Meier C, Davidson KGV, Yasumura T, Rash JE, Nagy JI. 2002. Connexin29 expression, immunocytochemistry and freeze-fracture replica immunogold labelling (FRIL) in sciatic nerve. European Journal of Neuroscience 16:795-806.

Liem RKH, Yen S-H, D. SG, Shelanski ML. 1978. Intermediate filaments in nervous tissues. The Journal of Cell Biology 79:637-645.

Lu B, Pang PT, Woo NH. 2005. The yin and yang of neurotrophin action. Nature Reviews Neuroscience 6(8):603-14.

Ma SF, Chen YJ, Zhang JX, Shen L, Wang R, Zhou JS, Hu JG, Lu HZ. 2015. Adoptive transfer of M2 macrophages promotes locomotor recovery in adult rats after spinal cord injury. Brain, behavior, and immunity 45:157-70.

Mannion RJ, Costigan M, Decosterd I, Amaya F, Ma Q-P, Holstege JC, Ji R-R, Acheson A, Lindsay RM, Wilkinson GA and others. 1999. Neurotrophins: Peripherally and centrally acting modulators of tactile stimulus-induced infalmmatory pain hypersensitivity. Proceedings of the National Academy of Sciences USA 96:9385-9390.

Mantovani A, Garlanda C, Locati M. 2009. Macrophage diversity and polarization in atherosclerosis: a question of balance. Arteriosclerosis, Thrombosis, and Vascular Biology 29(10):1419-23.

Martinez FO, Gordon S. 2014. The M1 and M2 paradigm of macrophage activation: time for reassessment. F1000prime reports 6:13.

Martini R, Fischer S, López-Vales R, David S. 2008. Interactions between Schwann cells and macrophages in injury and inherited demyelinating disease. Glia 56(14):1566-1577.

Mata M, Kupina N, Fink DJ. 1992. Phosphorylation-dependent neurofilament epitopes are reduced at the node of Ranvier. Journal of Neurocytology 21:199-210.

Matsushima GK, Morell P. 2001. The neurotoxicant, cuprizone, as a model to study demyelination and remyelination in the central nervous system. Brain Pathology 11:107-116.

McTigue DM, Horner PJ, Stokes BT, Gage FH. 1998. Neurotrophin-3 and brain-derived neurotrophic factor induce oligodendrocyte proliferation and myelination of regenerating axons in the contused adult rat spinal cord. The Journal of Neuroscience 18(14):5354-5365.

Mendell JR, Whitaker JN. 1978. Immunocytochemical localization studies of myelin basic protein. The Journal of Cell Biology 76:502-511.

Menetrier-Caux C, Montmain G, Dieu MC, Bain C, Favrot MC, Caux C, Blay JY. 1998. Inhibition of the differentiation of dendritic cells from CD34+ progenitors by tumor cells: Role of interleukin-6 and macrophage colony-stimulating factor. Blood 92(12):4778-4791.

Merrill JE, Ignarro LJ, Sherman MP, Melinek J, Lane TE. 1993. Microglial cell cytotoxicity of oligodendrocytes is mediated through nitric oxide. The Journal of Immunology 151(4):2132-2141.

Meyer M, Matsuoka I, Wetmore C, Olson L, Thoenen H. 1992. Enhanced synthesis of brain-derived neurotrophic factor in the lesioned peripheral nerve: Different mechanisms are responsible for the regulation of BDNF and NGF mRNA. The Journal of Cell Biology 119(1):45-54.

Michael GJ, Averill S, Nitkunan A, Rattray M, Bennett DLH, Yan Q, Priestly JV. 1997. Nerve growth factor treatment increases brain-derived neurotrophic factor selectively in TrkA-expressing dorsal root ganglion cells and in their central terminations within the spinal cord. The Journal of Neuroscience 17:8476-8490.

Michailov GV, Sereda MW, Brinkmann BG, Fischer TM, Haug B, Birchmeier C, Role L, Lai C, Schwab MH, Nave K-A. 2004. Axonal neuregulin-1 regulates myelin sheath thickness. Science 304:700-703.

Mikita J, Dubourdieu-Cassagno N, Deloire MS, Vekris A, Biran M, Raffard G, Brochet B, Canron MH, Franconi JM, Boiziau C and others. 2011. Altered M1/M2 activation patterns of monocytes in severe relapsing experimental rat model of multiple sclerosis. Amelioration of clinical status by M2 activated monocyte administration. Multiple Sclerosis 17(1):2-15.

Miron VE, Boyd A, Zhao JW, Yuen TJ, Ruckh JM, Shadrach JL, van Wijngaarden P, Wagers AJ, Williams A, Franklin RJ and others. 2013. M2 microglia and macrophages drive oligodendrocyte differentiation during CNS remyelination. Nature Neuroscience 16(9):1211-8.

Miron VE, Franklin RJ. 2014. Macrophages and CNS remyelination. Journal of Neurochemistry 130(2):165-71.

Mirsky R, Jessen KR. 1996. Schwann cell development, differentiation and myelination. Current Opinion in Neurobiology 6:89-96.

Mirsky R, Jessen KR. 1999. The neurobiology of Schwann cells. Brain Pathology 9:293-311.

Mokarram N, Merchant A, Mukhatyar V, Patel G, Bellamkonda RV. 2012. Effect of modulating macrophage phenotype on peripheral nerve repair. Biomaterials 33(34):8793-801.

Myers KJ, Dougherty JP, Ron Y. 1993. In vivo antigen presentation by both brain parenchymal cells and hematopoietically derived cells during the induction of experimental autoimmune encephalomyelitis. The Journal of Immunology 151(4):2252-2260.

Nagappan G, Zaitsev E, Senatorov VV, Yang J, Hempstead BL, Lu B. 2009. Control of extracellular cleavage of ProBDNF by high frequency neuronal activity. Proceedings of the National Academy of Sciences USA 106(4):1267-1272.

Nahrendorf M, Swirski FK, Aikawa E, Stangenberg L, Wurdinger T, Figueiredo JL, al. e. 2007. The healing myocardium sequentially mobilizes two monocyte subsets with divergent and complementary functions. Journal of Experimental Medicine 204:3037-3047.

Nakahara J, Aiso S, Suzuki N. 2009. Factors that retard remyelination in multiple sclerosis with a focus on TIP30: a novel therapeutic target. Expert Opinion on Therapeutic Targets 13(12):1375-1386.

Nathan C, Ding A. 2010. Nonresolving inflammation. Cell 140(6):871-82.

Neeper SA, Gomez-Pinilla F, Choi J, Cotman CW. 1996. Physical activity increases mRNA for brain-derived neurotrophic factor and nerve growth factor in rat brain. Brain Research 726:49-56.

Neeper SA, Gomez-Pinilla F, Choi JY, Cotman C. 1995. Exercise and brain neurotrophins. Nature 373:109.

Newswanger DL, Warren CR. 2004. Guillain Barre Syndrome. American Family Physician 69:2405-2410.
Ng BK, Chen L, Mandemakers W, Cosgaya JM, Chan JR. 2007. Anterograde transport and secretion of brain-derived neurotrophic factor along sensory axons promote Schwann cell myelination. The Journal of Neuroscience 27(28):7597-7603.
Notterpek L, Snipes GJ, Shooter EM. 1999. Temporal expression pattern of peripheral myelin protein 22 during in vivo and in vitro myelination. Glia 25:358-369.
Nussbaum JL, Neskovic N, Mandel P. 1969. A study of lipid components in brain of the 'Jimpy' mouse, a mutant with myelin deficiency. Journal of Neurochemistry 16:927-934.
Okuda Y, Nakatsuji Y, Fujimura H, Esumi H, Ogura T, Yanagihara T, Sakoda S. 1995. Expression of the inducible isoform of nitric oxide synthase in the central nervous system of mice correlates with the severity of actively induced experimental allergic encephalomyelitis. Journal of Neuroimmunology 62:103-112.
Olsson Y. 1968. Topographical differences in the vascular permeability of the peripheral nervous system. Acta Neuropathologica 10:26-33.
Omlin FX, Webster HD, Palkovits CG, Cohen SR. 1982. Immunocytochemical localization of basic protein in major dense line regions of central and peripheral myelin. The Journal of Cell Biology 95:242-248.
Ousman SS, David S. 2001. MIP-1a, MCP-1, GM-CSF, and TNF-a control the immune cell response that mediates rapid phagocytosis of myelin from the adult mouse spinal cord. The Journal of Neuroscience 21(13):4649-4645.
Pang PT, Teng HK, Zaitsev E, Woo NT, Sakata K, Zhen S, Teng KK, Yung WH, Hempstead BL, Lu B. 2004. Cleavage of proBDNF by tPA/plasmin is essential for long-term hippocampal plasticity. Science 306(5695):487-91.
Pant H, C. 1988. Dephosphorylation of neurofilament proteins enhances their susceptibility to degradation by calpain. Journal of Biochemistry 256:665-668.
Park KJ, Grosso CA, Aubert I, Kaplan DR, Miller FD. 2010. p75NTR-dependent, myelin-mediated axonal degeneration regulates neural connectivity in the adult brain. Nature Neuroscience 13(5):559-566.
Pavelko KD, van Engelen BGM, Rodriguez M. 1998. Acceleration in the rate of CNS remyelination in lysolecithin-induced demyelination. The Journal of Neuroscience 18(7):2498-2505.
Paz Soldan MM, Pirko I. 2012. Biogenesis and significance of central nervous system myelin. Seminars in Neurology 32(1):9-14.
Perry VH, Brown MC. 1992a. Macrophages and nerve regeneration. Current Opinion in Neurobiology 2:679-682.
Perry VH, Brown MC. 1992b. Role of macrophages in peripheral nerve degeneration and repair. BioEssays 14:401-406.
Porcheray F, Viaud S, Rimaniol AC, Leone C, Samah B, Dereuddre-Bosquet N, Dormont D, Gras G. 2005. Macrophage activation switching: an asset for the resolution of inflammation. Clinical and Experimental Immunology 142(3):481-9.
Qiao J, Huang F, Naikawadi RP, Kim KS, Said T, Lum H. 2006. Lysophosphatidylcholine impairs endothelial barrier function through the G protein-coupled receptor GPR4. American journal of physiology Lung cellular and molecular physiology 291(1):L91-101.
Quarles RH. 2002. Myelin sheaths: glycoproteins involved in their formation, maintenance and degeneration. Cellular and Molecular Life Sciences 59:1851-1871.

Quarles RH, Macklin WB, Morell P. 2006. Myelin formation, structure and biochemistry: Elsevier Inc.
Quinn MT, Parthasarathy S, Steinberg D. 1988. Lysophosphatidylcholine: A chemotactic factor for human monocytes and its potential role in atherogenesis. Proceedings of the National Academy of Sciences USA 85:2805-2809.
Rasband MN, Trimmer JS, Schwarz TL, Levinson SR, Ellisman MH, Schachner M, Shrager P. 1998. Potassium Channel Distribution, Clustering, and Function in Remyelinating Rat Axons. The Journal of Neuroscience 18(1):36-47.
Rawji KS, Yong VW. 2013. The benefits and detriments of macrophages/microglia in models of multiple sclerosis. Clinical & Developmental Immunology 2013:948976.
Reles A, Friede RL. 1991. Axonal cytoskeleton at the nodes of Ranvier. Journal of Neurocytology 20:450-458.
Robinson LR. 2000. Traumatic injury to peripheral nerves. Muscle & Nerve 23:863-873.
Rosenberg SS, Ng BK, Chan JR. 2006. The quest for remyelination: a new role for neurotrophins and their receptors. Brain Pathology 16:288-294.
Rosenbluth J. 1983. Structure of the node of Ranvier. In: Chang DC, Tasaki I, Adelman JWJ, Leuchtag HR, editors. Structure and function in excitable cells. New York: Plenum Press. p 25-52.
Rubinstein CT, Shrager P. 1990. Remyelination of nerve fibres in the transected frog sciatic nerve. Brain Research 524:303-312.
Ruckh JM, Zhao JW, Shadrach JL, van Wijngaarden P, Rao TN, Wagers AJ, Franklin RJ. 2012. Rejuvenation of regeneration in the aging central nervous system. Cell Stem Cell 10(1):96-103.
Rydevik B, Lundborg G. 1977. Permeability of intraneural microvessels and perineurium following acute, graded experimental nerve compression. Scandinavian Journal of Plastic and Reconstructive Surgery 11:179-187.
Sakaguchi T, Okada M, Kitamura T, Kawasaki K. 1993. Reduced diameter and conduction velocity of myelinated fibers in the sciatic nerve of a nerofilament-deficient mutant quail. Neuroscience Letters 153:65-68.
Sampaio-Baptista C, Khrapitchev AA, Foxley S, Schlagheck T, Scholz J, Jbabdi S, DeLuca GC, Miller KL, Taylor A, Thomas N and others. 2013. Motor skill learning induces changes in white matter microstructure and myelination. The Journal of Neuroscience 33(50):19499-503.
Sauer SK, Bove GM, Averbeck B, Reeh PW. 1999. Rat peripheral nerve components release calcitonin gene-related peptide and prostaglandin E2 in response to noxious stimuli: Evidence that nervi nervorum are nociceptors. Neuroscience 92(1):319-325.
Schafer DP, Custer AW, Shrager P, Rasband MN. 2006. Early events in node of Ranvier formation during myelination and remyelination in the PNS. Neuron Glia Biology 2(02):69.
Scherer SS, Salzer JL. 2001. Axon–Schwann cell interactions during peripheral nerve degeneration and regeneration. In: Jessen KR, Richardson WD, editors. Glial Cell Development. Oxford: Oxford University Press.
Schlaepfer WW. 1974. Calcium-induced degeneration of axoplasm in isolated segments of rat peripheral nerve. Brain Research 69:203-215.
Schlaepfer WW. 1987. Neurofilaments: Structure, metabolism and implications in disease. Journal of Neuropathology and Experimental Neurology 46(2):117-129.

Scholz J, Klein MC, Behrens TE, Johansen-Berg H. 2009. Training induces changes in white-matter architecture. Nature Neuroscience 12(11):1370-1.
Serbina NV, Jia T, Hohl TM, Pamer EG. 2008. Monocyte-mediated defense against microbial pathogens. Annual Review of Immunology 26:421-52.
Shaughnessy LM, Swanson JA. 2010. The role of the activated macrophage in clearing Listeria monocytogenes infection. Frontiers in Bioscience 12:2683-2692.
Shin T, Ahn M, Matsumoto Y, Moon C. 2013. Mechanism of experimental autoimmune neuritis in Lewis rats: The dual role of macrophages. Histology and Histopathology 28:679-684.
Silber E, Sharief MK. 1999. Axonal degeneration in the pathogenesis of multiple sclerosis. Journal of the Neurological Sciences 170:11-18.
Singh B, Xu Q-G, Franz CK, Zhang R, Dalton C, Gordon T, Verge VMK, Midha R, Zochodne DW. 2012. Accelerated axon outgrowth, guidance, and target reinnervation across nerve transection gaps following a brief electrical stimulation paradigm. Journal of Neurosurgery 116(3):498-512.
Skup M, Dwornik A, Macias M, Sulejczak D, Wiater M, Czarkowska-Bauch J. 2002. Long-Term Locomotor Training Up-Regulates TrkBFL Receptor-like Proteins, Brain-Derived Neurotrophic Factor, and Neurotrophin 4 with Different Topographies of Expression in Oligodendroglia and Neurons in the Spinal Cord. Experimental Neurology 176(2):289-307.
Starr R, Attema B, DeVries GH, Monteiro MJ. 1996. Neurofilament phosphorylation is modulated by myelination. Journal of Neuroscience Research 44:328-337.
Stein M, Keshav S, Harris N, Gordon S. 1992. Interleukin 4 potently enhances murine macrophage mannose receptor activity: A marker of alternative immunologic macrophage activation. Journal of Experimental Medicine 176:287-292.
Sternberger NH, Quarles RH, Itoyama Y, Webster HD. 1979. Myelin-associated glycoprotein demonstrated immunocytochemically in myelin and myelin-forming cells of developing rat. Proceedings of the National Academy of Sciences USA 76(3):1510-1514.
Stevens B. 2000. Response of Schwann Cells to Action Potentials in Development. Science 287(5461):2267-2271.
Stevens B, Tanner SL, Fields RD. 1998. Control of myelination by specific patterns of neural impulses. The Journal of Neuroscience 18(22):9303-9311.
Stout RD, Jiang C, Matta B, Tietzel I, Watkins SK, Suttles J. 2005. Macrophages sequentially change their functional phenotype in resonse to changes in microenvironmental influences. The Journal of Immunology 175:342-349.
Stout RD, Suttles J. 2004. Functional plasticity of macrophages: reversible adaptation to changing microenvironments. Journal of Leukocyte Biology 76(3):509-13.
Sun Y, Lim Y, Li F, Liu S, Lu JJ, Haberberger R, Zhong JH, Zhou XF. 2012. ProBDNF collapses neurite outgrowth of primary neurons by activating RhoA. PLoS ONE 7(4):e35883.
Sunderland S. 1978. Nerves and nerve injuries. New York: Churchill Livingstone. p 133-138.
Sunderland S. 1990. The anatomy and physiology of nerve injury. Muscle & Nerve 13(9):771-784.
Suter U, Welcher AA, Snipes GJ. 1993. Progress in the molecular understanding of hereditary peripheral neuropathies reveals new insights into the biology of the peripheral nervous system. Trends in Neurosciences 16(2):50-56.

Taveggia C, Salzer JL. 2007. PARsing the events of remyelination. Nature Neuroscience 10(1):17-18.
Taylor AR, Gifondorwa DJ, Robinson MB, Strupe JL, Prevette D, Johnson JE, Hempstead B, Oppenheim RW, Milligan CE. 2012. Motoneuron programmed cell death in response to proBDNF. Developmental Neurobiology 72(5):699-712.
Teng HK, Teng KK, Lee R, Wright S, Tevar S, Almeida RD, Kermani P, Torkin R, Chen ZY, Lee FS and others. 2005. ProBDNF induces neuronal apoptosis via activation of a receptor complex of p75NTR and sortilin. The Journal of Neuroscience 25(22):5455-63.
Tokuoka H, Saito T, Yorifuji H, Wei F-Y, Kishimoto T, Hisanaga S-i. 2000. Brain-derived neurotrophic factor-induced phosphorylaton of neurofilament-H subunit in primary cultures of embryo rat cortical neurons. Journal of Cell Science 113:1059-1068.
Tolwani RJ, Cosgaya JM, Varma S, Jacob R, Kuo LE, Shooter EM. 2004. BDNF overexpression produces a long-term increase in myelin formation in the peripheral nervous system. Journal of Neuroscience Research 77(5):662-9.
Tomita K, Kubo T, Matsuda K, Fujiwara T, Yano K, Winograd JM, Tohyama M, Hosokawa K. 2007. The neurotrophin receptor p75NTR in Schwann cells is implicated in remyelination and motor recovery after peripheral nerve injury. Glia 55(11):1199-208.
Tonra JR, Curtis R, Wong V, Cliffer KD, Park JS, Timmes A, Nguyen T, Lindsay RM, Acheson A, DiStefano PS. 1998. Axotomy upregulates the anterograde transport and expression of brain-derived neurotrophic factor by sensory neurons. The Journal of Neuroscience 18(11):4374-4383.
Topilko P, Schneider-Maunoury S, Levi G, Baron-Van Evercooren A, Chennoufl ABY, Seitanidou T, Babinet C, Charnay P. 1994. Krox-20 controls myelination in the peripheral nervous system. Nature 371:796-799.
Trapp BD, Andrews SB, Cootauco C, Quarles RH. 1989. The myelin-associated glycoprotein is enriched in multivesicular bodies and periaxonal membranes of actively myelinating oligodendrocytes. The Journal of Cell Biology 109:2417-2426.
Trapp BD, Peterson J, Ransohoff RM, Rudick R, Mork S, Bo L. 1998. Axonal transection in the lesions of multiple sclerosis. The New England Journal of Medicine 338:278-285.
Uutela M, Wirzenius M, Paavonen K, Rajantie I, He Y, Karpanen T, Lohela M, Wiig H, Salven P, Pajusola K and others. 2004. PDGF-D induces macrophage recruitment, increased interstitial pressure, and blood vessel maturation during angiogenesis. Blood 104(10):3198-204.
Vabnick i, Novakovic SD, Levinson SR, Schachner M, Shrager P. 1996. The clustering of axonal sodium channels during development of the peripheral nervous system. The Journal of Neuroscience 16(16):4914-4922.
Vabnick i, Trimmer JS, Schwarz TL, Levinson SR, Risal D, Shrager P. 1999. Dynamic potassium channel distributions during axonal development prevent aberrant firing patterns. The Journal of Neuroscience 19(2):747-758.
Veeranna, Niranjana AD, Ahn NG, Jaffe H, Winters CA, Grant P, Pant H, C. 1998. Mitogen-activated protein kinases (Erk1,2) phosphorylate lys-ser-pro (KSP) repeats in neurofilament proteins NF-H and NF-M. The Journal of Neuroscience 18(11):4008-4021.
Verderio C, Bianco F, Blanchard MP, Bergami M, Canossa M, Scarfone E, Matteoli M. 2007. Cross talk between vestibular neurons and Schwann cells mediates BDNF release and neuronal regeneration. Brain Cell Biology 35(2-3):187-201.

Vucic S, Kiernan MC, Cornblath DR. 2009. Guillain-Barré syndrome: An update. Journal of Clinical Neuroscience 16(6):733-741.
Wake H, Lee PR, Fields RD. 2011. Control of local protein synthesis and initial events in myelination by action potentials. Science 333(6049):1647-1651.
Wan L, Zhang S, Xia R, Ding W. 2010. Short-term low-frequency electrical stimulation enhanced remyelination of injured peripheral nerves by inducing the promyelination effect of brain-derived neurotrophic factor on Schwann cell polarization. Journal of Neuroscience Research 88:2578-2587.
Wang J, Zhang P, Wang Y, Kou Y, Zhang H, Jiang B. 2010. The observation of phenotypic changes of Schwann cells after rat sciatic nerve injury. Artificial Cells, Blood Substitutes and Biotechnology 38(1):24-28.
Wang X, Cao K, Sun X, Chen Y, Duan Z, Sun L, Guo L, Bai P, Sun D, Fan J and others. 2015. Macrophages in spinal cord injury: phenotypic and functional change from exposure to myelin debris. Glia 63(4):635-51.
Webster HD. 1971. The geometry of peripheral myelin sheaths during their formation and growth in rat sciatic nerves. The Journal of Cell Biology 48:348-367.
Weinberg HJ, Spencer PS. 1976. Studies on the control of myelinogenesis II: Evidence for neuronal regulation of myelin production. Brain Research 113:363-378.
Wiley-Livingston C, Ellisman MH. 1980. Development of axonal membrane specializations defines nodes of Ranvier and precedes Schwann cell myelin elaboration. Developmental Biology 79:334–355.
Willard M, Simon C. 1983. Modulations of neurofilament axonal transport during the development of rabbit retinal ganglion cells. Cell 35:551-559.
Willison HJ. 2005. The immunobiology of Guillain-Barre syndromes. Journal of the Peripheral Nervous System 10:94-112.
Winer JB, Hughes AC, Osmond C. 1988. A prospective study of acute idiopathic neuropathy. I. Clinical features and their prognostic value. Journal of Neurology, Neurosurgery & Psychiatry 51:605-612.
Wong I, Liao H, Bai X, Zaknic A, Zhong J, Guan Y, Li HY, Wang YJ, Zhou XF. 2010. ProBDNF inhibits infiltration of ED1+ macrophages after spinal cord injury. Brain, Behavior, and Immunity 24(4):585-97.
Wu GF, Dandekar AA, Pewe L, Perlman S. 2000. CD4 and CD8 T Cells Have Redundant But Not Identical Roles in Virus-Induced Demyelination. The Journal of Immunology 165(4):2278-2286.
Wynn TA, Barron L. 2010. Macrophages: master regulators of inflammation and fibrosis. Seminars in Liver Disease 30(3):245-57.
Yagihashi S, Kamijo M, Watanabe K. 1990. Reduced myelinated fiber size correlates with loss of axonal neurofilaments in peripheral nerve of chronically streptozotocin diabetic rats. The American Journal of Pathology 136:1365-1373.
Yamauchi J, Chan JR, Shooter EM. 2004. Neurotrophins regulate Schwann cell migration by activating divergent signaling pathways dependent on Rho GTPases. Proceedings of the National Academy of Sciences USA 101(23):8774-9.
Ydens E, Cauwels A, Asselbergh B, Goethals S, Peeraer L, Lornet G, Almeida-Souza L, Van Ginderachter JA, Timmerman V, Janssens S. 2012. Acute injury in the peripheral nervous system triggers an alternative macrophage response. Journal of Neuroinflammation 9:176.

Yuki N, Hartung H-P. 2012. Guillain-Barre syndrome. The New England Journal of Medicine 366:2294-2304.
Zhang J-Y, Luo X-G, Xian CJ, Liu Z-H, Zhou X-F. 2000. Endogenous BDNF is required for myelination and regeneration of injured sciatic nerve in rodents. European Journal of Neuroscience 12:4171-4180.
Zhou X-F, Chie ET, Deng Y-S, Zhong J-H, Xue Q, Rush RA, Xian CJ. 1999. Injured primary sensory neurons switch phenotype for brain-derived neurotrophic factor in the rat. Neuroscience 92(3):841-853.
Zhou X-F, Rush RA. 1996. Endogenous brain-derived neurotrophic factor is anterogradely transported in primary sensory neurons. Neuroscience 74(4):945-951.
Zorick TS, Lemke G. 1996. Schwann cell differentiation. Current Opinion in Cell Biology 8:870-876.

APPENDIX A
PERMISSIONS FOR FIGURE USE

FIGURE 1:

Dear Nikki McLean
We hereby grant you permission to reproduce the material detailed below at no charge **in your thesis, in print and eCommons at University Of Saskatchewan** subject to the following conditions:

1. If any part of the material to be used (for example, figures) has appeared in our publication with credit or acknowledgement to another source, permission must also be sought from that source. If such permission is not obtained then that material may not be included in your publication/copies.

2. Suitable acknowledgment to the source must be made, either as a footnote or in a reference list at the end of your publication, as follows:

   "This article was published in Publication title, Vol number, Author(s), Title of article, Page Nos, Copyright Elsevier (or appropriate Society name) (Year)."

3. Your thesis may be submitted to your institution in either print or electronic form.

4. Reproduction of this material is confined to the purpose for which permission is hereby given.

5. This permission is granted for non-exclusive world **English** rights only. For other languages please reapply separately for each one required. Permission excludes use in an electronic form other than as specified above. Should you have a specific electronic project in mind please reapply for permission.

6. This includes permission for the Library and Archives of Canada to supply single copies, on demand, of the complete thesis. Should your thesis be published commercially, please reapply for permission.

Yours sincerely

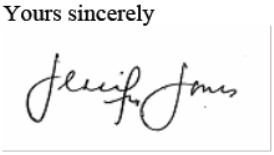

Jennifer Jones
Permissions Specialist

Elsevier Limited, a company registered in England and Wales with company number 1982084, whose registered office is The Boulevard, Langford Lane, Kidlington, Oxford, OX5 1GB, United Kingdom.

FIGURE 2:

ELSEVIER LICENSE
TERMS AND CONDITIONS

Jul 16, 2015

This is a License Agreement between Nikki A McLean ("You") and Elsevier ("Elsevier") provided by Copyright Clearance Center ("CCC"). The license consists of your order details, the terms and conditions provided by Elsevier, and the payment terms and conditions.

All payments must be made in full to CCC. For payment instructions, please see information listed at the bottom of this form.

Supplier	Elsevier Limited The Boulevard,Langford Lane Kidlington,Oxford,OX5 1GB,UK
Registered Company Number	1982084
Customer name	Nikki A McLean
Customer address	612 Coppermine Bay Saskatoon, SK S7K4M1
License number	3670960619336
License date	Jul 16, 2015
Licensed content publisher	Elsevier
Licensed content publication	Trends in Neurosciences
Licensed content title	Progress in the molecular understanding of hereditary peripheral neuropathies reveals new insights into the biology of the peripheral nervous system
Licensed content author	Ueli Suter,Andrew A. Welcher,G. Jackson Snipes
Licensed content date	February 1993
Licensed content volume number	16
Licensed content issue number	2
Number of pages	7
Start Page	50
End Page	56
Type of Use	reuse in a thesis/dissertation
Portion	figures/tables/illustrations
Number of figures/tables/illustrations	1
Format	both print and electronic
Are you the author of this	No

Elsevier article?	
Will you be translating?	No
Original figure numbers	Figure 1
Title of your thesis/dissertation	Stimulating Remyelination
Expected completion date	Oct 2015
Estimated size (number of pages)	150
Elsevier VAT number	GB 494 6272 12
Permissions price	0.00 USD
VAT/Local Sales Tax	0.00 USD / 0.00 GBP
Total	0.00 USD